

NASA  
TP  
2119  
c.1

**NASA  
Technical  
Paper  
2119**

February 1983

# Effect of Thrust Vectoring and Wing Maneuver Devices on Transonic Aeropropulsive Characteristics of a Supersonic Fighter Aircraft

TECH LIBRARY KAFB, NM  
0134993  
E699ETD

Francis J. Capone  
and David E. Reubush

LOAN COPY: RETURN TO  
AFWL TECHNICAL LIBRARY  
KIRTLAND AFB, N.M.



**NASA  
Technical  
Paper  
2119**

1983

TECH LIBRARY KAFB, NM



0134993

# Effect of Thrust Vectoring and Wing Maneuver Devices on Transonic Aeropropulsive Characteristics of a Supersonic Fighter Aircraft

Francis J. Capone  
and David E. Reubush  
*Langley Research Center  
Hampton, Virginia*

**NASA**

National Aeronautics  
and Space Administration

Scientific and Technical  
Information Branch

## SUMMARY

The aeropropulsive characteristics of an advanced fighter designed for supersonic cruise have been determined in the Langley 16-Foot Transonic Tunnel. The objectives of this investigation were to evaluate the interactive effects of thrust vectoring and wing maneuver devices on lift and drag and to determine trim characteristics. The wing maneuver devices consisted of a drooped leading edge and a trailing-edge flap. Thrust vectoring was accomplished with two-dimensional (nonaxisymmetric) convergent-divergent nozzles located below the wing in two single-engine podded nacelles. A canard was utilized for trim. Thrust vector angles of 0°, 15°, and 30° were tested in combination with a drooped wing leading edge and with wing trailing-edge flap deflections up to 30°. This investigation was conducted at Mach numbers from 0.60 to 1.20, at angles of attack from 0° to 20°, and at nozzle pressure ratios from about 1 (jet off) to 10. Reynolds number based on mean aerodynamic chord varied from  $9.24 \times 10^6$  to  $10.56 \times 10^6$ .

As expected, deployment of the drooped wing leading edge resulted in a lift loss, an increase in zero-lift drag, and a decrease in drag-due-to-lift. Deflection of the wing trailing-edge flap produced a lift increase and a decrease in drag-due-to-lift. The mutual interference effect of deployment of the drooped leading edge in conjunction with thrust vectoring was beneficial to untrimmed drag-minus-thrust polars because an additional drag reduction was obtained that was greater than the sum of the individual drag reductions due separately to either the drooped leading edge or vectoring. However, deflection of the trailing-edge flap in combination with the drooped leading edge and thrust vectoring caused an unexpected increase in incremental interference drag. The configuration with 15° thrust vectoring, the drooped wing leading edge, and 7° wing trailing-edge flap deflection had the best drag-minus-thrust performance at trimmed maneuver conditions. At 30° wing trailing-edge flap deflection, large trim drag increments degraded the performance of this configuration although it had the best untrimmed drag-minus-thrust performance.

## INTRODUCTION

The mission requirements for the next generation fighter aircraft may dictate a highly versatile vehicle capable of operating over a wide range of flight conditions. This aircraft will most likely be designed for high maneuverability and agility, operate in a highly hostile environment, and possess STOL characteristics to operate from bomb-damaged airfields. An aircraft designed primarily for supersonic cruise may be required to maximize attack options and minimize exposure to hostile action. To achieve this truly multimission capability, new technologies such as thrust vectoring, thrust reversing, vortex flow control, and favorable canard-wing interaction must be considered in the design of fighter aircraft. As a result, NASA has devoted considerable research effort to developing these technologies for application to the next generation of fighter aircraft. (See refs. 1-5.)

Thrust vectoring and reversing on high-performance aircraft configurations have received considerable attention in the past several years and have been shown to provide improved maneuverability and shorter take-off and landing distances. (See refs. 5-8.) Taking full advantage of thrust vectoring technology will require incorporation of auxiliary trimming devices such as canard surfaces or nose jets. Further

aerodynamic improvement can be achieved through the use of wing maneuver devices such as leading- and trailing-edge flaps (refs. 9 and 10). Care must be exercised, however, when integrating these technologies since interactions between them can negate any individual performance gains. This paper will present results from a wind tunnel study of an advanced tactical fighter designed for supersonic cruise.

The objectives of this investigation were to evaluate the interactive effects of thrust vectoring and wing maneuver devices on lift and drag and to determine trim characteristics. The wing maneuver devices consisted of a drooped leading edge and a trailing-edge flap. Thrust vectoring was accomplished with two-dimensional (non-axisymmetric) convergent-divergent nozzles located below the wing in two single-engine podded nacelles. A canard was utilized for trim. The aeropropulsive characteristics of this configuration with various nonaxisymmetric nozzles installed were reported in reference 11.

This investigation was conducted in the Langley 16-Foot Transonic Tunnel at Mach numbers from 0.60 to 1.20. Angle of attack was varied from 0° to about 20°, and nozzle pressure ratio was varied from about 1 (jet off) to 10, depending on Mach number.

#### SYMBOLS

Model forces and moments are referred to the stability-axis system with the model moment reference center located at fuselage station 174.82 cm, which corresponds to 0.28 $\bar{c}$ . The symbols used in the computer-generated tables are given in parentheses in the second column. A discussion of the data-reduction procedure and definitions of the aerodynamic force and moment terms and the propulsion relationships used herein are presented in the "Data Reduction" section.

$C_D$	(CDAERO)	drag coefficient, $\frac{\text{Drag}}{q_\infty S}$
$\Delta C_{D,int}$		incremental interference drag coefficient (see fig. 22)
$C_{(D-F)}$	(C(D-F))	drag-minus-thrust coefficient, $C_{(D-F)} \equiv C_D$ at NPR = 1.0 (jet off)
$C_{F,jet}$	(CFJET)	thrust coefficient along stability axis, $\frac{\text{Thrust}}{q_\infty S}$
$C_L$	(CL)	total lift coefficient including thrust component, $\frac{\text{Lift}}{q_\infty S}$
$C_{L,a}$	(CLAERO)	aerodynamic (thrust component removed) lift coefficient, $C_{L,a} \equiv C_L$ at NPR = 1.0 (jet off)
$C_{L,jet}$	(CLJET)	jet-lift coefficient
$C_m$	(CM)	pitching moment coefficient including thrust component, $\frac{\text{Pitching moment}}{q_\infty S \bar{c}}$
	(CMJET)	jet pitching moment coefficient
	(CT)	nozzle gross thrust coefficient, $\sqrt{C_{F,jet}^2 + C_{L,jet}^2}$

$\bar{c}$		mean geometric chord, 80.46 cm
$F_g$		gross thrust, N
M	(MACH)	free-stream Mach number
NPR	(NPR)	nozzle pressure ratio, $p_{t,j}/p_\infty$
$p_{t,j}$		average jet total pressure, Pa
$p_\infty$		free-stream static pressure, Pa
$q_\infty$		free-stream dynamic pressure, Pa
S		wing area, 6043.1 cm <sup>2</sup>
$\alpha$	(ALPHA)	angle of attack, deg
$\beta$		nozzle boattail angle, deg
$\Delta$		increment
$\delta_c$	(CANALP)	canard incidence angle, positive leading edge up, deg
$\delta_{te}$		trailing-edge flap deflection, positive trailing edge down, deg
$\delta_v$		nozzle geometric turning angle, positive direction deflects jet flow downward, measured with respect to thrust axis, deg

Abbreviations:

C-D	convergent-divergent
c.g.	center of gravity
FS	fuselage station
LE	leading edge
NRP	nozzle reference plane
STOL	short-field take-off and landing
trim	trimmed
2-D	two-dimensional
WBL	wing butt line, cm
WL	water line, cm

## MODEL

This investigation was conducted with a 10.5 percent scale model of a twin-engine fighter aircraft designed to cruise at supersonic speeds. A sketch showing the general arrangement of the model and support system is presented in figure 1. A photograph of the model is shown in figure 2. The high-performance model featured a cambered and twisted wing and canard and two single-engine podded nacelles mounted under the wing.

### Wing/Canard/Fuselage Design

The configuration with the basic wing was designed for self-trimming (unloaded canard) at a cruise speed of Mach 2 and a design lift coefficient of 0.10. The trim condition for the vehicle was established from the criteria that the vehicle be 5 percent unstable subsonically, which resulted in the vehicle being 4 percent stable for the supersonic design case.

The aerodynamic design of the lifting surfaces was accomplished by the use of the FLEXSTAB code (ref. 12). This code uses the aerodynamic influence coefficient method and includes the effects of nonplanar surfaces such as a canard above the wing plane. The method is based upon linearized potential flow theory with constant pressure panels. The twist and camber of both the canard and the wing surfaces are determined simultaneously such that the induced drag is minimized. Figure 3 illustrates the modeling of the vehicle from the FLEXSTAB code and the resulting wing and canard design. In addition, an alternate drooped leading edge was designed for attached flow in the transonic maneuver regime. Wing cross sections with the drooped leading edge are also shown in figure 3.

The planform geometry of the wing is shown in figure 4. The wing had a leading-edge sweep of  $68^\circ$ , an aspect ratio of 1.53, a reference area of  $6043.1 \text{ cm}^2$ , and a wing mean geometric chord of 80.46 cm. A wing trailing-edge flap, also shown in figure 4, was tested at deflection angles of  $0^\circ$ ,  $7^\circ$  (typical for maneuver), and  $30^\circ$  (typical for landing). Photographs of the wing showing both the drooped leading edge and deflected trailing-edge flap are shown in figure 5. The planform geometry of the canard is shown in figure 6. The canard incidence angle was remotely controlled about the hinge axis located at FS 117.29. The canard also had  $10^\circ$  dihedral (fig. 6).

### Nacelle/Nozzle Installation

The nacelle with the 2-D C-D nozzle, shown in figure 7, was located inboard and under the wing. This is the baseline nacelle position of reference 11. The nacelle, which was toed in  $2^\circ$ , had a faired over inlet. Details of the 2-D C-D nozzle are presented in figure 8. This nozzle had a nozzle duct aspect ratio of 1 and was tested in an afterburner power setting at  $\delta_v = 0^\circ, 15^\circ, \text{ and } 30^\circ$ .

The 2-D C-D nozzle full-scale design allows independent actuation of the throat area control flaps and the divergent flaps. The nozzle area ratio can therefore be set, within mechanical limits, independently from the nozzle throat area for good internal performance over a wide variety of flight conditions.

The length of the divergent flaps was selected to provide good internal nozzle performance at the supersonic design point. The flap actuators are integral to the

flaps to reduce sidewall thickness. For thrust vectoring, the divergent flaps are differentially actuated. Since the nozzle flow is turned at a relatively low Mach number, high internal performance is maintained during vectored operation.

## APPARATUS AND PROCEDURE

### Wind Tunnel and Support System

This investigation was conducted in the Langley 16-Foot Transonic Tunnel, which is a single-return, atmospheric pressure tunnel with a slotted, octagonal test section and continuous air exchange. Test-section plenum suction is used for speeds above a Mach number of 1.10. A complete description of this facility and its operating characteristics can be found in reference 13.

The model was supported in the wind tunnel by a sting strut support system (figs. 1 and 2) in which the strut replaced the vertical tail. The strut had an NACA 0006 airfoil section with a 60° sweep and maximum thickness of 4.46 cm.

### Propulsion Simulation System and Instrumentation

An external high-pressure air system provided a continuous source of clean, dry air at a controlled temperature of about 294 K at the nozzles. The air was brought to a plenum mounted within the wind tunnel support system ahead of the sting. Here, the flow was divided into two separate flows and passed through remote-controlled flow valves to two critical flow venturis, which were used to determine mass flow rate of the individual nozzles. The air was then routed through the sting/strut and forward through the fuselage from the bottom of the strut, as shown in figure 9. Three bellows were installed in each air line to provide a three-axis, flexible air line bridge across the main balance and model. The air was then routed out through each wing to the respective nacelles and nozzles.

At the end of the round-to-rectangular transition section, a choke plate and two screens were installed to regulate and smooth the flow prior to entry to the nozzle instrumentation or charging station. (See fig. 7.) The transition sections were made to interface with the flow supply pipe on the right and left ducts. Nine total pressure probes, arranged in an equal area weighted, cruciform fashion, were used to determine average nozzle total pressure in each duct. The 18 total pressure probes (left- and right-hand sides) were averaged to give overall nozzle total pressure. Two total temperature probes in each duct measured stagnation temperature of the exhaust flow.

Thrust and external aerodynamic forces and moments on the entire model were measured by a six-component force balance which attached directly to the bottom of the strut (fig. 9). A gap between the metric model forebody and nonmetric vertical tail support strut prevented grounding of the force balance. Additional instrumentation was used to measure pressure and temperature of the airflow through the venturis and internal tare static pressures.

### Data Reduction

All data were recorded simultaneously on magnetic tape. Twenty-four frames of data, taken at the approximate rate of one frame per second, were used for each data

point. Average values of the recorded data were used to compute standard force and moment coefficients based on wing area and mean geometric chord for reference area and length, respectively.

Axial force of the main balance was corrected for a tare force that resulted from pressurizing the air supply lines and bellows. This tare force was determined by capping off the air supply system at the wings and recording balance data as the lines were pressurized. No corrections due to pressurization were found to be necessary for the other balance components. Normal force and pitching moment of the force balance were also adjusted to the condition of the free-stream static pressure acting across the gap (metric break) around the support strut. Note that no pressure-area correction to axial force is required for this type support system.

The adjusted forces and moments measured by the balance were transferred from the body axis (WL 26.67) to the stability axis. Angle of attack  $\alpha$  was obtained by applying deflection terms, caused by model support and balance bending under aerodynamic loads, and a flow angularity term to the angle of the model support system. The flow angularity adjustment of  $0.1^\circ$ , which is the average tunnel upflow angle measured in the Langley 16-Foot Transonic Tunnel, was applied.

Thrust-removed aerodynamic force and moment coefficients are obtained by determining the components of thrust in axial force, normal force, and pitching moment and subtracting these values from the measured total (aerodynamic plus thrust) forces and moments. These thrust components at forward speeds were determined from measured static data and were a function of the free-stream static and dynamic pressure. Forces and moments were measured at static conditions by the main force balance for each nozzle/vector angle combination tested. Thrust-removed aerodynamic coefficients are

$$C_{L,a} = C_L - C_{L,jet}$$

$$C_D = C_{(D-F)} + C_{F,jet}$$

#### Tests

This investigation was conducted at Mach numbers from 0.60 to 1.20. Angle of attack was varied from  $0^\circ$  to  $20^\circ$ . Nozzle pressure ratio was varied from about 1 (jet off) to 10, depending on Mach number. Canard incidence was held at about  $0^\circ$  for all configurations. Some configurations were also tested at a canard incidence of about  $5^\circ$ . Nozzle thrust vector angles of  $0^\circ$ ,  $15^\circ$ , and  $30^\circ$  in combination with the basic and drooped wing leading edge and with the wing trailing-edge flap at  $0^\circ$ ,  $7^\circ$ , and  $30^\circ$  were tested. Reynolds number based on mean aerodynamic chord varied from  $9.24 \times 10^6$  to  $10.56 \times 10^6$ . All tests were conducted with 0.20-cm-wide boundary layer transition strips consisting of No. 100 silicon carbide grit sparsely distributed in a thin film of lacquer. These strips were located 5.08 cm from the tip of the forebody nose and nacelle and on both the upper and lower surfaces of the wings and canard at 0.51 cm normal to the leading edges.



## PRESENTATION OF RESULTS

The results of this investigation are presented in both tabular and plotted form. Table 1 is an index to the tabular results contained in tables 2 to 12. The computer symbols appearing in these tables are defined in the "Symbols" section of the paper with their corresponding mathematical symbols. The basic results for selected conditions at  $\delta = 0^\circ$  are presented in figures 10 to 19, and summary data are given in figures 20 to 29 as follows:

	Figure
<b>Basic data:</b>	
Effect of drooped leading edge, $\delta_v = 15^\circ$ , $\delta_{te} = 0^\circ$ on	
Total aerodynamic characteristics $\dot{v}$ .....	10
Thrust-removed aerodynamic characteristics .....	11
Effect of trailing-edge flap deflection, basic LE, $\delta_v = 15^\circ$ on	
Total aerodynamic characteristics .....	12
Thrust-removed aerodynamic characteristics .....	13
Effect of trailing-edge flap deflection, drooped LE, $\delta_v = 15^\circ$ on	
Total aerodynamic characteristics $\dot{v}$ .....	14
Thrust-removed aerodynamic characteristics .....	15
Effect of thrust vectoring, basic LE, $\delta_{te} = 0^\circ$ on	
Total aerodynamic characteristics $\dot{v}$ .....	16
Thrust-removed aerodynamic characteristics .....	17
Effect of thrust vectoring, drooped LE, $\delta_{te} = 30^\circ$ on	
Total aerodynamic characteristics $\dot{v}$ .....	18
Thrust-removed aerodynamic characteristics .....	19
<b>Summary data:</b>	
Incremental lift and drag coefficients due to	
drooped leading edge .....	20
Incremental lift and drag coefficients due to	
trailing-edge flap deflection .....	21
Definition of $\Delta C_{D,int}$ .....	22
Effect of drooped leading edge on $\Delta C_{D,int}$ .....	23
Effect of trailing-edge flap deflection on $\Delta C_{D,int}$ .....	24
Vehicle force diagram .....	25
Typical effect of wing maneuver devices on untrimmed drag polars .....	26
Effect of wing maneuver devices on trimmed powered polars .....	27
Canard deflection required for trim, $\Delta C_{D,trim}$ , and $\Delta C_{L,trim}$ .....	28
Trimmed powered and optimum polars .....	29

## DISCUSSION

### Effect of Drooped Leading Edge

The effect of the drooped leading edge on total and thrust-removed aerodynamic characteristics at  $\delta_v = 15^\circ$  is shown in figures 10 and 11, respectively. Incremental lift and drag coefficients are summarized in figure 20. As expected, use of the drooped leading edge resulted in a loss in lift at all Mach numbers over the angle of attack range tested. This loss in lift occurs because the configuration with the drooped leading edge operates at a lower local angle of attack than the configuration with the basic leading edge. The effect of deploying the drooped leading edge on either the powered or thrust-removed polars shows typical camber effects of an increase in drag at zero lift and lower drag-due-to-lift. (See fig. 11

or fig. 20.) The effect of Mach number ( $M = 0.6$  and  $0.87$ ) on the incremental lift and drag coefficient variation with angle of attack is generally small up to  $\alpha = 16^\circ$  (fig. 20). However, as shown in the lower part of figure 20, improvement to the drag polars (here shown as drag increment versus lift coefficient) was similar at all three Mach numbers tested. The effects of nozzle pressure ratio on either incremental lift or drag are small (compare, for example, fig. 11(a) with fig. 11(b)).

#### Effect of Trailing-Edge Flap Deflection

The effect of trailing-edge flap deflection on total and thrust-removed aerodynamic characteristics at  $\delta_v = 15^\circ$  is shown in figures 12 and 13 for the configuration with the basic leading edge and in figures 14 and 15 for the configuration with the drooped leading edge. Incremental lift and drag coefficients are summarized in figure 21. These results also show expected trends. Deflection of the trailing-edge flap resulted in an increase in lift, which was nearly independent of angle of attack at Mach numbers from  $0.60$  to  $1.20$ . There was a decrease in drag-due-to-lift only at  $M = 0.60$  and  $0.87$ . (See, for example, figs. 13(a), 15(a), 21(a), and 21(b).) Deploying the drooped leading edge had a small effect on drag-due-to-lift at all the Mach numbers tested.

#### Effect of Thrust Vectoring

The effect of thrust vectoring on the total and thrust-removed aerodynamic characteristics is presented in figures 16 and 17 for the configuration with the basic leading edge,  $\delta_{te} = 0^\circ$  and in figures 18 and 19 for the drooped leading edge,  $\delta_{te} = 30^\circ$ . At supersonic Mach numbers, as thrust vector angle increases, there is the typical "crossover" of the individual drag-minus-thrust polars, with the crossovers occurring at successively higher lift coefficients. The results generally show that for  $\delta_v = 0^\circ$  and  $15^\circ$ , the thrust or jet-induced effects are generally beneficial to both lift and drag. (That is, jet operation increases lift and decreases drag. Compare, for example, figs. 17(a) and 17(b) or 17(e) and 17(f).)

#### Combined Effect of Wing Maneuver Devices and Thrust Vectoring

As stated earlier, one of the objectives of this investigation was to evaluate the interactive effects of thrust vectoring and wing maneuver devices on lift and drag. One means of accomplishing this is to determine interference effects on powered polars. First, however, it is necessary to define an incremental interference drag term  $\Delta C_{D,int}$ . Figure 22 shows a sketch of four typical thrust-removed drag polars with the baseline polar being the configuration with  $\delta_{te} = 7^\circ$  and  $NPR = 1.0$ . The other curves are typical polars for various combinations of  $\delta_{te}$  and  $NPR$ . Although the conditions  $\delta_{te} = 7^\circ$  and  $NPR = 3.0$  are used for the example shown in figure 22, the analysis for other trailing-edge flap deflections, nozzle pressure ratios, or for the drooped leading edge would be similar.

The first increment shown  $(\Delta C_D)_{\delta_{te}}$  is simply the jet-off trailing-edge flap effect shown previously in figure 21. The second increment  $(\Delta C_D)_{NPR}$  is the jet effect for  $\delta_v = 0^\circ$  and  $\delta_{te} = 0^\circ$ . The third increment, which results from the combined effects of jet operation and trailing-edge flap deflection, contains the first two increments plus any mutual interference effects. Thus the incremental

interference drag term at a constant flap deflection is simply the difference between the third increment and the first and second increments or

$$\Delta C_{D,int} = (\Delta C_{D'})_{\delta_{te}} - (\Delta C_{D'})_{\delta_{te}} - (\Delta C_{D'})_{NPR}$$

This term is evaluated for the configuration with either the basic or drooped leading edge.

As shown in figure 23, use of the drooped leading edge with thrust vectoring had a beneficial effect (negative values of  $\Delta C_{D,int}$ ) at  $M = 0.60$  except at  $C_{L,a} \approx 0.70$ . That is, an additional drag reduction was obtained that was greater than the sum of the individual drag reductions due separately to either the drooped leading edge or vectoring. At  $M = 0.87$ , improved powered polars occurred at  $C_{L,a} > 0.50$ , which is typical of maneuver lift coefficients. Figure 24 shows that deflection of the trailing-edge flap to  $7^\circ$  at  $M = 0.60$  with the wing with the basic leading edge produced additional drag; whereas, at  $\delta_{te} = 30^\circ$ , a decrease in drag was noted. There was little effect of deflecting the trailing-edge flap to  $7^\circ$  at  $M = 0.87$ . However, use of the drooped leading edge with the trailing-edge flaps for this configuration was generally detrimental, which was unexpected because the drooped leading edge was found to be beneficial with  $\delta_{te} = 0^\circ$ .

The preceding analysis of powered drag polars indicated both beneficial and detrimental mutual interference effects of thrust vectoring when combined with wing maneuver devices. More than likely, these effects are configuration-dependent for this type vehicle in which vectorable nozzles are located near the wing trailing edge.

A similar analysis was done to determine the incremental interference lift coefficient over the angle of attack range tested. Most of the incremental values of interference lift were less than  $\pm 0.003$ , which indicates little or no interference effects of thrust vectoring.

#### Trimmed Aerodynamic Characteristics

The previous discussions of the effects of wing maneuver devices and thrust vectoring dealt only with untrimmed, powered drag-minus-thrust polars. The lift and drag increments associated with trimming the induced lift and drag increments resulting from use of the above items can negate any benefits that may accrue.

In order to understand the trim characteristics of this model, it is helpful to review the resulting moment contributions from various force inputs (fig. 25). Typical untrimmed longitudinal aerodynamic characteristics with various wing maneuver devices deployed are presented in figure 26 for  $\delta_v = 15^\circ$  at  $M = 0.60$  and  $NPR = 3.0$ . The nozzle gross thrust at  $\delta_v = 0^\circ$  causes a nose-up pitching moment because the thrust axis is inclined downward and located below the c.g. For this c.g. location, there is a nose-up pitching moment with respect to  $\delta_v = 0^\circ$  for nozzle vector angles greater than  $4.8^\circ$ . The drooped wing leading edge induces nose-up pitching moment, and deflection of the wing trailing-edge flap results in a nose-down moment (fig. 26). It should be noted that an adjustment was made to the pitching moment data to account for the faired-over inlet. Addition of the nacelle with

the faired-over inlet caused a  $C_m$  shift at  $C_L = 0$  of about 0.046 (nose-up). In order to account for the faired-over inlet, an assumed value 0.02 was subtracted from the untrimmed pitching moment over the entire angle of attack range. The wing/body/canard data of reference 11 were used to trim the configuration.

Trimmed, powered maneuver polars are presented for the configurations of figure 26 in the lower portion of figure 27(a). These results indicate that although the configuration with  $\delta_{te} = 30^\circ$  shows untrimmed polar improvements above  $C_L = 0.60$  (fig. 26), no trimmed polar improvements occur over the angle of attack range tested because of large trim drag increments.

In order to show the effects of deployment of the wing maneuver devices on trimming the aircraft, canard incidence angles required for trim and resulting trim lift and drag increments are presented in figure 28 for  $\delta_v = 15^\circ$  at  $M = 0.60$ . It can be seen that drooping the wing leading edge compensates for a significant portion of the nose-down moment that results from deflecting the wing trailing-edge flap to  $7^\circ$ . The canard angles required for trim for the configurations shown in figure 28 except  $\delta_{te} = 30^\circ$  are those that generally result in minimum trim drag penalties (ref. 11). However, further deflection of the trailing-edge flap to  $30^\circ$  causes a large nose-down moment which requires large positive canard angles for trim. These canard deflections result in substantial trim drag penalties.

A similar set of trimmed, powered maneuver polars was also generated for those configurations that were not tested at  $\delta_v = 0^\circ$ . This was accomplished by first adding the increments of lift and drag (figs. 20 and 21) and pitching moment due to the drooped leading edge and deflected trailing-edge flap to the corresponding untrimmed aerodynamic parameters for the configuration with  $\delta_v = 0^\circ$ , basic leading edge, and  $\delta_{te} = 0^\circ$  found in table 2. The same wing/body/canard results of reference 11 previously used to trim the configuration with  $\delta_v = 15^\circ$  were used to trim the configuration with  $\delta_v = 0^\circ$ . These results, also shown in figure 27, do not contain any mutual interference drag increments that may exist for  $\delta_v = 0^\circ$  since these configurations were not tested.

An envelope polar can be drawn about the individual trimmed drag polars of figure 27 that represents deploying the drooped wing leading edge and varying wing trailing-edge flap deflection as a function of angle of attack at constant thrust vector angles of  $0^\circ$  and  $15^\circ$ . A comparison of trimmed envelope maneuver polars between the unvectored ( $\delta_v = 0^\circ$ ) and vectored ( $\delta_v = 15^\circ$ ) configurations at  $M = 0.60$  and  $0.87$  is presented in figure 29. The configuration with drooped leading edge and  $\delta_{te} = 7^\circ$  has better trimmed drag-minus-thrust performance with  $\delta_v = 15^\circ$  than with  $\delta_{te} = 0^\circ$ . As discussed in reference 11, canard deflections of  $-12^\circ$  to  $-14^\circ$  are required to trim the large nose-up moment for the configuration with  $\delta_v = 0^\circ$ ; whereas, only  $-4.5^\circ$  to  $-5.5^\circ$  canard deflection is necessary at  $\delta_v = 15^\circ$ . This results in smaller trim drag increments for the configuration with  $\delta_v = 15^\circ$ .

#### CONCLUSIONS

An investigation has been conducted in the Langley 16-Foot Transonic Tunnel to determine the aeropropulsive characteristics of an advanced fighter designed for supersonic cruise. The objectives of this investigation were to evaluate the interactive effects of thrust vectoring and wing maneuver devices on lift and drag and to determine trim characteristics. A canard was utilized for trim. Thrust vector angles of  $0^\circ$ ,  $15^\circ$ , and  $30^\circ$  were tested in combination with a drooped wing leading edge and with wing trailing-edge flap deflections of  $0^\circ$ ,  $7^\circ$ , and  $30^\circ$ . This investi-

gation was conducted at Mach numbers from 0.60 to 1.20, at angles of attack from 0° to 20°, and at nozzle pressure ratios from about 1 (jet off) to 10. Reynolds number based on mean aerodynamic chord varied from  $9.24 \times 10^6$  to  $10.56 \times 10^6$ .

The results of this investigation indicate the following:

1. As expected, deployment of the drooped wing leading edge resulted in a lift loss, an increase in zero-lift drag, and a decrease in drag-due-to-lift. Deflection of the wing trailing-edge flap produced a lift increase and a decrease in drag-due-to-lift.

2. The mutual interference effect of deployment of the drooped leading edge in conjunction with thrust vectoring was beneficial to untrimmed drag-minus-thrust polars because an additional drag reduction was obtained that was greater than the sum of the individual drag reductions due separately to either the drooped leading edge or vectoring.

3. However, deflection of the trailing-edge flap in combination with the drooped leading edge and thrust vectoring caused an unexpected increase in incremental interference drag.

4. The configuration with 15° thrust vectoring, the drooped wing leading edge, and 7° wing trailing-edge flap deflection had the best drag-minus-thrust performance at trimmed maneuver conditions. At 30° wing trailing-edge flap deflection, large trim drag increments degraded the performance of this configuration although it had the best untrimmed drag-minus-thrust performance.

Langley Research Center  
National Aeronautics and Space Administration  
Hampton, VA 23665  
December 15, 1982

#### REFERENCES

1. Tactical Aircraft Research and Technology - Volume I. NASA CP-2162, 1981.
2. Henderson, William P.; and Leavitt, Laurence D.: Stability and Control Characteristics of a Three-Surface Advanced Fighter Configuration at Angles of Attack up to 45°. NASA TM-83171, 1981.
3. Gloss, Blair B.; and McKinney, Linwood W.: Canard-Wing Lift Interference Related to Maneuvering Aircraft at Subsonic Speeds. NASA TM X-2897, 1973.
4. Re, Richard J.; and Capone, Francis J.: Longitudinal Aerodynamic Characteristics of a Fighter Model With a Close-Coupled Canard at Mach Numbers From 0.40 to 1.20. NASA TP-1206, 1978.
5. Capone, Francis J.: The Nonaxisymmetric Nozzle - It Is for Real. AIAA Paper 79-1810, Aug. 1979.
6. Nelson, B. D.; and Nicolai, L. M.: Application of Multi-Function Nozzles to Advanced Fighters. AIAA-81-2618, Dec. 1981.
7. Miller, Eugene H.; and Protopapas, John: Nozzle Design and Integration in an Advanced Supersonic Fighter. AIAA Paper 79-1813, Aug. 1979.
8. Hiley, P. E.; and Bowers, D. L.: Advanced Nozzle Integration for Supersonic Strike Fighter Application. AIAA-81-1441, July 1981.
9. Ray, Edward J.; McKinney, Linwood W.; and Carmichael, Julian G.: Maneuver and Buffet Characteristics of Fighter Aircraft. NASA TN D-7131, 1973.
10. Capone, Francis J.: Effect of Various Wing High-Lift Devices on the Longitudinal Aerodynamic Characteristics of a Swept-Wing Fighter Model at Transonic Speeds. NASA TM X-3204, 1975.
11. Capone, Francis J.; and Reubush, David E.: Effect of Varying Podded Nacelle/Nozzle Installations on Transonic Aeropropulsive Characteristics of a Supersonic Fighter Aircraft. NASA TP-2120, 1983.
12. Tinoco, E. N.; and Mercer, J. E.: FLEXSTAB - A Summary of the Functions and Capabilities of the NASA Flexible Airplane Analysis Computer System. NASA CR-2564, 1975.
13. Peddrew, Kathryn H., compiler: A User's Guide to the Langley 16-Foot Transonic Tunnel. NASA TM-83186, 1981.

TABLE 1.- INDEX TO DATA TABLES

Table	$\delta_v$ , deg	$\delta_c$ , deg	Leading edge	$\delta_{te}$ , deg
2	0	0	Basic	0
3	15	↓	↓	↓
4	30	↓	↓	7
5	15	↓	↓	30
6	↓	0, 5	Drooped	0
7	↓	↓	↓	7
8	↓	↓	↓	30
9	↓	↓	↓	7
10	0	0	↓	30
11	0	0, 5	↓	30
12	30	0, 5	↓	30







TABLE 4.- AERODYNAMIC CHARACTERISTICS: BASIC LEADING EDGE,  
 $\delta_{te} = 0^\circ$ ,  $\delta_v = 30^\circ$

MACH	ALPHA	NPR	CANALP	CL	C(D-F)	CM	CLAERO	CDAERO	CLJET	CFJET	CMJET	CT
.87	.02	.82	-.07	-.0659	.0305	.0350	-.0659	.0305	0.0000	0.0000	0.0000	0.0000
.87	2.03	.82	-.09	.0208	.0288	.0313	.0208	.0288	0.0000	0.0000	0.0000	0.0000
.87	4.03	.81	-.16	.1051	.0322	.0310	.1051	.0322	0.0000	0.0000	0.0000	0.0000
.87	6.04	.81	-.23	.1905	.0405	.0356	.1905	.0405	0.0000	0.0000	0.0000	0.0000
.87	8.04	.82	-.31	.2912	.0583	.0364	.2912	.0583	0.0000	0.0000	0.0000	0.0000
.87	10.03	.81	-.37	.3997	.0863	.0361	.3997	.0863	0.0000	0.0000	0.0000	0.0000
.87	15.04	.79	-.45	.6810	.1955	.0277	.6810	.1955	0.0000	0.0000	0.0000	0.0000
.87	19.03	.76	-.53	.8890	.3188	.0257	.8890	.3188	0.0000	0.0000	0.0000	0.0000
.87	.04	2.40	-.02	-.0385	-.0100	.0231	-.0553	.0244	.0168	.0344	-.0099	.0383
.87	4.02	2.40	-.07	.1307	-.0064	.0198	.1116	.0266	.0191	.0330	-.0099	.0382
.87	10.06	2.40	-.20	.4309	.0515	.0244	.4084	.0824	.0225	.0308	-.0099	.0381
.87	19.03	2.41	-.38	.9246	.2889	.0132	.8974	.3159	.0272	.0271	-.0099	.0384
.87	.03	3.91	-.08	-.0111	-.0418	.0058	-.0468	.0267	.0357	.0686	-.0218	.0773
.87	2.02	3.91	-.09	.0761	-.0418	.0024	.0380	.0256	.0381	.0674	-.0218	.0774
.87	4.03	3.91	-.11	.1606	-.0363	.0024	.1203	.0296	.0403	.0658	-.0217	.0772
.87	6.02	3.91	-.17	.2493	-.0255	.0063	.2067	.0389	.0426	.0644	-.0217	.0772
.87	8.05	3.91	-.23	.3526	-.0058	.0065	.3076	.0572	.0450	.0630	-.0218	.0774
.87	10.02	3.91	-.27	.4645	.0243	.0059	.4175	.0857	.0470	.0613	-.0218	.0773
.87	15.02	3.92	-.36	.7509	.1391	-.0028	.6984	.1963	.0524	.0572	-.0218	.0776
.87	18.99	3.92	-.45	.9619	.2670	-.0069	.9058	.3203	.0561	.0533	-.0218	.0774
.87	.03	5.41	.07	.0122	-.0765	-.0060	-.0401	.0278	.0523	.1043	-.0316	.1167
.87	4.04	5.40	.02	.1873	-.0693	-.0097	.1279	.0310	.0594	.1003	-.0316	.1166
.87	10.03	5.39	-.12	.4951	-.0051	-.0070	.4255	.0885	.0696	.0936	-.0316	.1166
.87	16.03	5.40	-.24	.8391	.1427	.0160	.7601	.2286	.0791	.0859	-.0317	.1167
.87	4.02	7.93	-.03	.2273	-.1271	-.0309	.1354	.0337	.0920	.1607	-.0484	.1852
.87	4.02	5.41	-.03	.2007	-.0884	-.0186	.1303	.0306	.0704	.1189	-.0374	.1382
.60	.03	.90	.04	-.0429	.0276	.0261	-.0429	.0276	0.0000	0.0000	0.0000	0.0000
.60	2.03	.90	.03	.0349	.0268	.0254	.0349	.0268	0.0000	0.0000	0.0000	0.0000
.60	4.03	.90	.02	.1080	.0301	.0272	.1080	.0301	0.0000	0.0000	0.0000	0.0000
.60	6.04	.90	.00	.1878	.0383	.0325	.1878	.0383	0.0000	0.0000	0.0000	0.0000
.60	8.02	.90	-.02	.2790	.0546	.0353	.2790	.0546	0.0000	0.0000	0.0000	0.0000
.60	10.02	.90	-.04	.3790	.0799	.0378	.3790	.0799	0.0000	0.0000	0.0000	0.0000
.60	15.04	.89	-.09	.6415	.1799	.0474	.6415	.1799	0.0000	0.0000	0.0000	0.0000
.60	19.04	.89	-.11	.8471	.2981	.0578	.8471	.2981	0.0000	0.0000	0.0000	0.0000
.60	.04	2.33	.05	-.0014	-.0457	.0027	-.0347	.0227	.0333	.0684	-.0196	.0761
.60	4.03	2.30	.03	.1530	-.0380	.0046	.1161	.0263	.0369	.0643	-.0190	.0741
.60	10.04	2.27	-.03	.4355	.0186	.0143	.3927	.0779	.0428	.0593	-.0187	.0731
.60	19.02	2.31	-.10	.9115	.2435	.0330	.8589	.2964	.0526	.0529	-.0191	.0746
.60	.00	3.01	.07	.0235	-.0745	-.0134	-.0278	.0271	.0513	.1016	-.0306	.1138
.60	2.04	3.00	.06	.1066	-.0715	-.0140	.0523	.0271	.0543	.0986	-.0303	.1126
.60	4.02	3.00	.05	.1837	-.0665	-.0130	.1259	.0305	.0578	.0970	-.0304	.1129
.60	6.02	3.00	.04	.2656	-.0553	-.0080	.2046	.0394	.0610	.0946	-.0303	.1126
.60	8.02	3.00	.02	.3642	-.0358	-.0060	.2997	.0570	.0645	.0927	-.0304	.1130
.60	10.02	3.00	.00	.4691	-.0075	-.0043	.4014	.0830	.0677	.0905	-.0304	.1130
.60	15.04	3.00	-.05	.7417	.1021	.0044	.6666	.1861	.0752	.0840	-.0303	.1127
.60	19.03	3.00	-.08	.9543	.2267	.0145	.8734	.3054	.0809	.0786	-.0303	.1128
.60	.02	4.48	.08	.0684	-.1455	-.0370	-.0203	.0267	.0887	.1723	-.0539	.1938
.60	4.05	4.51	.06	.2337	-.1349	-.0373	.1331	.0310	.1006	.1659	-.0539	.1940
.60	10.04	4.52	.00	.5309	-.0698	-.0298	.4131	.0852	.1178	.1550	-.0541	.1947
.60	19.04	4.52	-.08	1.0250	.1741	-.0130	.8838	.3093	.1411	.1353	-.0543	.1955
.60	4.02	4.51	.03	.2327	-.1355	-.0374	.1319	.0308	.1008	.1663	-.0540	.1945
.60	4.02	5.44	.04	.2628	-.1793	-.0513	.1370	.0335	.1259	.2128	-.0670	.2473
.60	19.03	5.77	-.08	1.0860	.1300	-.0341	.8958	.3172	.1902	.1872	-.0718	.2669
.40	4.02	5.40	.06	.4244	-.4366	-.1314	.1431	.0389	.2814	.4754	-.1498	.5525
0.00	.02	1.00	.07	-.0002	.0001	.0000	-.0002	.0001	0.0000	0.0000	0.0000	0.0000
1.20	.03	.55	.12	-.0493	.0536	.0479	-.0493	.0536	0.0000	0.0000	0.0000	0.0000
1.20	2.03	.55	.09	.0304	.0527	.0437	.0304	.0527	0.0000	0.0000	0.0000	0.0000
1.20	4.03	.55	.05	.1129	.0563	.0398	.1129	.0563	0.0000	0.0000	0.0000	0.0000
1.20	4.03	.55	.04	.1132	.0562	.0399	.1132	.0562	0.0000	0.0000	0.0000	0.0000
1.20	6.03	.55	-.04	.2036	.0668	.0350	.2036	.0668	0.0000	0.0000	0.0000	0.0000
1.20	6.03	.55	-.04	.2040	.0670	.0350	.2040	.0670	0.0000	0.0000	0.0000	0.0000
1.20	8.01	.55	.10	.2975	.0851	.0297	.2975	.0851	0.0000	0.0000	0.0000	0.0000
1.20	8.00	.55	.10	.2971	.0850	.0297	.2971	.0850	0.0000	0.0000	0.0000	0.0000
1.20	10.02	.55	.08	.3955	.1114	.0228	.3955	.1114	0.0000	0.0000	0.0000	0.0000
1.20	10.02	.55	.08	.3962	.1114	.0225	.3962	.1114	0.0000	0.0000	0.0000	0.0000
1.20	15.02	.55	.01	.6202	.2040	.0075	.6202	.2040	0.0000	0.0000	0.0000	0.0000
1.20	15.01	.56	.01	.6194	.2036	.0075	.6194	.2036	0.0000	0.0000	0.0000	0.0000
1.20	16.05	.55	-.02	.6658	.2282	.0038	.6658	.2282	0.0000	0.0000	0.0000	0.0000
1.20	.10	3.82	.04	-.0281	.0119	.0371	-.0464	.0469	.0183	.0350	-.0112	.0395
1.20	.11	3.82	.04	-.0256	.0126	.0370	-.0439	.0476	.0183	.0350	-.0111	.0395

TABLE 5.- AERODYNAMIC CHARACTERISTICS: BASIC LEADING EDGE,  
 $\delta_{te} = 7^\circ$ ,  $\delta_v = 15^\circ$

MACH	ALPHA	NPR	CANALP	CL	C(D-F)	CM	CLAERD	CDAERD	CLJET	CFJET	CMJET	CT
.87	-.00	.95	-.01	-.0322	.0231	.0117	-.0322	.0231	0.0000	0.0000	0.0000	0.0000
.87	2.01	.95	-.08	.0513	.0221	.0098	.0513	.0221	0.0000	0.0000	0.0000	0.0000
.87	3.99	.94	-.06	.1346	.0269	.0114	.1346	.0269	0.0000	0.0000	0.0000	0.0000
.87	6.00	.94	-.08	.2197	.0360	.0145	.2197	.0360	0.0000	0.0000	0.0000	0.0000
.87	7.97	.94	-.13	.3202	.0545	.0144	.3202	.0545	0.0000	0.0000	0.0000	0.0000
.87	10.00	.93	-.08	.4310	.0841	.0153	.4310	.0841	0.0000	0.0000	0.0000	0.0000
.87	14.99	.92	-.12	.7066	.1957	.0120	.7066	.1957	0.0000	0.0000	0.0000	0.0000
.87	19.52	.91	-.18	.9335	.3377	.0128	.9335	.3377	0.0000	0.0000	0.0000	0.0000
.87	.00	2.41	.16	-.0237	-.0192	.0135	-.0293	.0191	.0056	.0383	-.0012	.0387
.87	4.00	2.41	-.03	.1421	-.0149	.0129	.1338	.0229	.0083	.0378	-.0012	.0386
.87	6.02	2.42	-.10	.2300	-.0052	.0161	.2204	.0323	.0096	.0375	-.0012	.0387
.87	9.99	2.41	-.22	.4398	.0427	.0169	.4277	.0794	.0122	.0367	-.0012	.0387
.86	19.48	2.40	-.16	.9525	.2979	.0145	.9344	.3322	.0181	.0343	-.0012	.0387
.87	-.00	3.90	.00	-.0090	-.0569	.0050	-.0259	.0192	.0169	.0760	-.0071	.0779
.87	1.99	3.91	-.02	.0766	-.0568	.0032	.0571	.0186	.0195	.0754	-.0071	.0779
.87	4.00	3.91	-.05	.1603	-.0515	.0043	.1382	.0232	.0222	.0747	-.0071	.0779
.87	6.00	3.91	-.08	.2493	-.0412	.0075	.2245	.0328	.0248	.0740	-.0071	.0780
.87	8.00	3.90	-.12	.3539	-.0217	.0072	.3265	.0515	.0274	.0731	-.0071	.0781
.87	10.01	3.91	-.19	.4651	.0090	.0075	.4352	.0810	.0299	.0720	-.0071	.0780
.87	14.99	3.91	-.10	.7497	.1243	.0036	.7136	.1936	.0361	.0693	-.0071	.0781
.87	19.23	3.91	-.19	.9710	.2601	.0021	.9298	.3267	.0412	.0666	-.0071	.0783
.87	.00	5.41	-.05	.0056	-.0970	-.0020	-.0222	.0173	.0278	.1144	-.0122	.1177
.87	3.99	5.42	-.13	.1781	-.0903	-.0025	.1425	.0215	.0356	.1117	-.0122	.1173
.87	6.00	5.42	-.04	.2689	-.0792	.0008	.2293	.0315	.0396	.1107	-.0122	.1176
.87	10.01	5.41	-.09	.4892	-.0272	.0003	.4420	.0806	.0473	.1078	-.0122	.1177
.87	19.11	5.42	-.09	.9934	.2243	-.0051	.9298	.3231	.0636	.0988	-.0122	.1176
.60	-.00	.97	-.00	-.0178	.0190	.0089	-.0178	.0190	0.0000	0.0000	0.0000	0.0000
.60	1.99	.97	-.01	.0563	.0192	.0093	.0563	.0192	0.0000	0.0000	0.0000	0.0000
.60	3.99	.97	-.02	.1314	.0229	.0117	.1314	.0229	0.0000	0.0000	0.0000	0.0000
.60	5.98	.96	-.03	.2082	.0316	.0163	.2082	.0316	0.0000	0.0000	0.0000	0.0000
.60	8.00	.96	-.04	.3058	.0497	.0178	.3058	.0497	0.0000	0.0000	0.0000	0.0000
.60	9.99	.96	-.04	.4087	.0762	.0183	.4087	.0762	0.0000	0.0000	0.0000	0.0000
.60	15.00	.96	-.05	.6715	.1783	.0274	.6715	.1783	0.0000	0.0000	0.0000	0.0000
.60	19.11	.96	-.08	.8816	.2999	.0371	.8816	.2999	0.0000	0.0000	0.0000	0.0000
.60	-.00	2.31	.02	-.0082	-.0577	.0065	-.0189	.0172	.0107	.0748	-.0022	.0756
.60	4.00	2.31	.01	.1464	-.0535	.0097	.1305	.0204	.0159	.0739	-.0022	.0756
.60	6.00	2.30	-.00	.2291	-.0445	.0141	.2106	.0291	.0185	.0736	-.0022	.0759
.60	9.99	2.31	-.02	.4337	.0016	.0170	.4102	.0732	.0235	.0716	-.0022	.0754
.60	17.17	2.30	-.04	.8204	.1680	.0313	.7880	.2364	.0324	.0684	-.0022	.0757
.60	.00	3.02	.04	.0045	-.0949	.0011	-.0156	.0173	.0201	.1122	-.0070	.1140
.60	2.00	3.02	.03	.0848	-.0944	.0014	.0608	.0176	.0240	.1119	-.0069	.1145
.60	3.99	3.02	.03	.1605	-.0901	.0034	.1325	.0210	.0280	.1111	-.0070	.1145
.60	6.00	3.02	.01	.2463	-.0802	.0080	.2144	.0299	.0319	.1101	-.0070	.1146
.60	8.00	3.02	-.00	.3501	-.0603	.0090	.3144	.0486	.0357	.1089	-.0070	.1146
.60	9.99	3.02	-.01	.4522	-.0333	.0097	.4126	.0744	.0396	.1077	-.0070	.1147
.60	14.99	3.01	-.02	.7253	.0744	.0186	.6771	.1773	.0482	.1029	-.0069	.1136
.60	19.15	3.02	-.05	.9513	.2030	.0277	.8956	.3025	.0557	.0995	-.0069	.1140
.60	-.00	4.51	.05	.0331	-.1764	-.0124	-.0117	.0154	.0447	.1918	-.0193	.1970
.60	4.00	4.50	.02	.1965	-.1690	-.0108	.1384	.0196	.0581	.1886	-.0193	.1974
.60	5.99	4.50	.01	.2806	-.1582	-.0070	.2159	.0284	.0647	.1866	-.0193	.1975
.60	10.00	4.50	-.01	.5007	-.1070	-.0056	.4232	.0745	.0775	.1814	-.0193	.1973
.60	19.16	4.50	-.05	1.0132	.1390	.0108	.9079	.3056	.1053	.1667	-.0193	.1971

TABLE 6.- AERODYNAMIC CHARACTERISTICS: BASIC LEADING EDGE,  
 $\delta_{te} = 30^\circ$ ;  $\delta_v = 15^\circ$

MACH	ALPHA	NPR	CANALP	CL	C(D-F)	CM	CLAERO	CDAERO	CLJET	CFJET	CMJET	CT
.60	-.00	.96	-.06	.0706	.0353	-.0427	.0706	.0353	0.0000	0.0000	0.0000	0.0000
.60	2.02	.96	-.08	.1504	.0392	-.0438	.1504	.0392	0.0000	0.0000	0.0000	0.0000
.60	4.02	.96	-.10	.2294	.0467	-.0430	.2294	.0467	0.0000	0.0000	0.0000	0.0000
.60	6.02	.96	-.12	.3155	.0604	-.0440	.3155	.0604	0.0000	0.0000	0.0000	0.0000
.60	8.07	.96	-.17	.4230	.0858	-.0481	.4230	.0858	0.0000	0.0000	0.0000	0.0000
.60	10.02	.95	-.20	.5259	.1189	-.0492	.5259	.1189	0.0000	0.0000	0.0000	0.0000
.60	15.04	.94	-.06	.7870	.2342	-.0348	.7870	.2342	0.0000	0.0000	0.0000	0.0000
.60	19.06	.94	-.09	.9742	.3576	-.0156	.9742	.3576	0.0000	0.0000	0.0000	0.0000
.60	.01	2.31	.06	.0882	-.0445	-.0451	.0774	.0305	.0108	.0750	-.0022	.0758
.60	4.05	2.31	.03	.2464	-.0314	-.0439	.2305	.0424	.0160	.0738	-.0022	.0755
.60	6.05	2.31	.01	.3401	-.0170	-.0447	.3214	.0569	.0187	.0738	-.0022	.0761
.60	10.02	2.31	-.02	.5606	.0455	-.0503	.5370	.1173	.0236	.0718	-.0022	.0755
.60	19.03	2.31	-.20	1.0192	.2865	-.0217	.9845	.3542	.0347	.0677	-.0022	.0761
.60	.04	3.00	-.09	.1007	-.0809	-.0499	.0807	.0309	.0200	.1118	-.0068	.1136
.60	2.02	3.02	-.12	.1817	-.0761	-.0512	.1577	.0352	.0239	.1113	-.0069	.1138
.60	4.06	3.06	-.15	.2612	-.0673	-.0494	.2335	.0427	.0277	.1100	-.0068	.1134
.60	6.02	3.00	-.16	.3536	-.0517	-.0509	.3221	.0573	.0315	.1090	-.0068	.1135
.60	8.03	3.00	-.18	.4658	-.0248	-.0552	.4305	.0829	.0352	.1077	-.0068	.1133
.60	10.01	3.00	-.20	.5793	.0108	-.0577	.5401	.1177	.0391	.1070	-.0068	.1139
.60	15.01	3.00	-.10	.8519	.1307	-.0480	.8038	.2335	.0481	.1028	-.0068	.1135
.60	19.03	3.00	-.12	1.0483	.2588	-.0280	.9929	.3584	.0554	.0995	-.0068	.1139
.60	.01	4.51	-.08	.1254	-.1637	-.0631	.0806	.0282	.0448	.1919	-.0193	.1971
.60	4.02	4.50	-.14	.2956	-.1471	-.0631	.2377	.0408	.0580	.1879	-.0192	.1966
.60	6.01	4.50	-.20	.3915	-.1307	-.0652	.3269	.0555	.0646	.1862	-.0193	.1970
.60	10.04	4.50	-.29	.6280	-.0632	-.0744	.5504	.1181	.0776	.1813	-.0193	.1972
.60	19.02	4.50	-.10	1.1031	.1925	-.0446	.9986	.3588	.1045	.1663	-.0192	.1964

TABLE 7.- AERODYNAMIC CHARACTERISTICS: DROOPED LEADING EDGE,  
 $\delta_{te} = 0^\circ, \delta_v = 15^\circ$

MACH	ALPHA	NPR	CANALP	CL	C(D-F)	CM	CLAERO	CDAERO	CLJET	CFJET	CMJET	CT
1.20	.05	.59	-.02	-.1004	.0640	.0673	-.1001	.0640	0.0000	0.0000	0.0000	0.0000
1.20	2.05	.60	-.05	-.0138	.0578	.0602	-.0138	.0578	0.0000	0.0000	0.0000	0.0000
1.20	4.05	.61	-.09	.0769	.0562	.0525	.0769	.0562	0.0000	0.0000	0.0000	0.0000
1.20	6.08	.61	-.13	.1671	.0603	.0467	.1671	.0603	0.0000	0.0000	0.0000	0.0000
1.20	8.05	.61	-.20	.2598	.0710	.0419	.2598	.0710	0.0000	0.0000	0.0000	0.0000
1.20	10.05	.62	-.28	.3542	.0890	.0373	.3542	.0890	0.0000	0.0000	0.0000	0.0000
1.20	15.02	.62	-.11	.5915	.1687	.0248	.5915	.1687	0.0000	0.0000	0.0000	0.0000
1.20	16.37	.63	-.12	.6574	.1982	.0185	.6574	.1982	0.0000	0.0000	0.0000	0.0000
1.20	.07	3.81	-.05	-.0860	.0171	.0642	-.0946	.0559	.0086	.0388	-.0035	.0398
1.20	4.06	3.80	-.12	.0885	.0112	.0501	.0774	.0489	.0111	.0377	-.0035	.0393
1.20	6.05	3.82	-.21	.1812	.0152	.0440	.1687	.0529	.0126	.0377	-.0035	.0398
1.20	10.07	3.81	-.05	.3725	.0461	.0366	.3575	.0826	.0150	.0365	-.0035	.0395
1.20	16.41	3.82	-.17	.6841	.1584	.0141	.6650	.1931	.0191	.0347	-.0035	.0396
1.20	.04	6.62	-.07	-.0773	-.0237	.0619	-.0964	.0522	.0191	.0759	-.0085	.0782
1.20	2.05	6.62	-.10	.0103	-.0288	.0552	-.3115	.0464	.0218	.0752	-.0085	.0783
1.20	4.05	6.59	-.14	.0990	-.0289	.0483	.0747	.0451	.0243	.0741	-.0085	.0779
1.20	6.05	6.59	-.23	.1942	-.0241	.0420	.1673	.0492	.0269	.0733	-.0085	.0781
1.20	8.04	6.60	-.29	.2888	-.0127	.0373	.2593	.0598	.0295	.0725	-.0085	.0783
1.20	10.04	6.60	-.06	.3844	.0069	.0348	.3525	.0782	.0320	.0713	-.0085	.0781
1.20	15.04	6.61	-.14	.6317	.0905	.0188	.5937	.1586	.0380	.0681	-.0085	.0780
1.20	16.15	6.60	-.16	.6870	.1153	.0136	.6476	.1828	.0394	.0675	-.0085	.0782
1.20	.05	9.31	-.08	-.0683	-.0624	.0590	-.0976	.0491	.0293	.1115	-.0132	.1153
1.20	4.05	9.31	-.31	.1100	-.0677	.0447	.0730	.0416	.0370	.1093	-.0132	.1154
1.20	6.06	9.32	-.06	.2090	-.0618	.0402	.1681	.0462	.0409	.1080	-.0133	.1155
1.20	10.06	9.33	-.15	.4010	-.0296	.0311	.3527	.0752	.0483	.1049	-.0133	.1155
1.20	11.99	9.30	-.19	.4986	-.0023	.0261	.4468	.1009	.0518	.1032	-.0133	.1155
.87	.07	.92	-.08	-.1391	.0413	.0672	-.1391	.0413	0.0000	0.0000	0.0000	0.0000
.87	2.04	.92	-.17	-.0459	.0329	.0611	-.0459	.0329	0.0000	0.0000	0.0000	0.0000
.87	4.03	.92	-.23	.0466	.0296	.0568	.0466	.0296	0.0000	0.0000	0.0000	0.0000
.87	6.06	.92	-.32	.1432	.0317	.0559	.1432	.0317	0.0000	0.0000	0.0000	0.0000
.87	8.08	.91	-.09	.2401	.0409	.0601	.2401	.0409	0.0000	0.0000	0.0000	0.0000
.87	10.05	.91	-.12	.3318	.0562	.0650	.3318	.0562	0.0000	0.0000	0.0000	0.0000
.87	15.05	.90	-.13	.5816	.1321	.0785	.5816	.1321	0.0000	0.0000	0.0000	0.0000
.87	19.03	.90	-.19	.8297	.2542	.0641	.8297	.2542	0.0000	0.0000	0.0000	0.0000
.87	.05	.92	-.03	-.1425	.0416	.0685	-.1425	.0416	0.0000	0.0000	0.0000	0.0000
.87	2.05	.92	-.07	-.0462	.0330	.0621	-.0462	.0330	0.0000	0.0000	0.0000	0.0000
.87	4.05	.92	-.14	.0460	.0297	.0579	.0460	.0297	0.0000	0.0000	0.0000	0.0000
.87	6.03	.92	-.22	.1414	.0322	.0569	.1414	.0322	0.0000	0.0000	0.0000	0.0000
.87	8.05	.91	-.29	.2366	.0405	.0589	.2366	.0405	0.0000	0.0000	0.0000	0.0000
.87	10.04	.91	-.34	.3283	.0554	.0641	.3283	.0554	0.0000	0.0000	0.0000	0.0000
.87	15.05	.90	-.13	.5818	.1326	.0785	.5818	.1326	0.0000	0.0000	0.0000	0.0000
.87	19.06	.90	-.19	.8252	.2528	.0650	.8252	.2528	0.0000	0.0000	0.0000	0.0000
.87	.04	2.42	.17	-.1325	-.0011	.0672	-.1382	.0372	.0057	.0383	-.0012	.0388
.87	4.02	2.42	.13	.0548	-.0123	.0581	.0465	.0257	.0083	.0380	-.0012	.0389
.87	6.03	2.42	-.12	.1512	-.0098	.0565	.1416	.0278	.0096	.0376	-.0012	.0388
.87	10.05	2.42	-.20	.3431	.0147	.0645	.3309	.0515	.0123	.0369	-.0012	.0388
.87	15.04	2.42	-.13	.5992	.0924	.0773	.5838	.1280	.0154	.0356	-.0012	.0388
.87	19.00	2.42	-.18	.8442	.2137	.0639	.8263	.2482	.0179	.0345	-.0012	.0389
.87	.06	3.90	.17	-.1143	-.0390	.0576	-.1313	.0370	.0170	.0760	-.0071	.0779
.87	2.04	3.90	-.06	-.0196	-.0467	.0509	-.0392	.0289	.0196	.0756	-.0071	.0781
.87	4.05	3.91	-.13	.0756	-.0489	.0473	.0533	.0257	.0222	.0746	-.0071	.0779
.87	6.03	3.92	-.23	.1743	-.0460	.0464	.1493	.0282	.0249	.0742	-.0071	.0783
.87	8.05	3.90	-.15	.2736	-.0358	.0496	.2462	.0373	.0274	.0731	-.0071	.0780
.87	10.04	3.91	-.15	.3672	-.0196	.0548	.3372	.0525	.0300	.0721	-.0071	.0781
.87	15.05	3.91	-.09	.6281	.0612	.0667	.5920	.1304	.0361	.0691	-.0071	.0780
.87	18.91	3.91	-.14	.8695	.1807	.0531	.8287	.2475	.0408	.0667	-.0071	.0782
.87	.05	5.42	-.05	-.1026	-.0794	.0497	-.1305	.0346	.0279	.1141	-.0122	.1174
.87	4.01	5.41	-.12	.0910	-.0881	.0409	.0554	.0237	.0356	.1118	-.0122	.1173
.87	6.05	5.42	-.14	.1941	-.0843	.0403	.1545	.0265	.0397	.1107	-.0122	.1176
.87	10.04	5.40	-.13	.3901	-.0562	.0478	.3428	.0516	.0473	.1078	-.0122	.1177
.87	15.05	5.42	-.21	.6531	.0259	.0580	.5966	.1289	.0564	.1030	-.0122	.1175
.87	.04	.92	4.94	-.1278	.0439	.0873	-.1278	.0439	0.0000	0.0000	0.0000	0.0000
.87	.06	3.88	4.94	-.1025	-.0379	.0755	-.1195	.0383	.0169	.0761	-.0071	.0780
.87	2.03	3.90	4.97	-.0647	-.0420	.0742	-.0240	.0327	.0194	.0747	-.0070	.0772
.87	4.03	3.87	4.94	.0959	-.0408	.0748	.0739	.0334	.0220	.0742	-.0070	.0774
.87	6.01	3.88	4.96	.1960	-.0334	.0777	.1714	.0400	.0245	.0734	-.0070	.0774

TABLE 7.- Concluded

MACH	ALPHA	NPR	CANALP	CL	C(D-F)	CM	CLAERO	COAERO	CLJET	CFJET	CMJET	CT
.87	8.07	3.89	4.93	.2983	-.0196	.0808	.2711	.0531	.0273	.0726	-.0070	.0776
.87	10.07	3.89	4.93	.3941	.0007	.0860	.3643	.0726	.0298	.0718	-.0070	.0778
.87	15.04	3.89	4.95	.6398	.0857	.0998	.6038	.1546	.0359	.0689	-.0070	.0777
.60	.05	.95	-.06	-.1204	.0374	.0514	-.1204	.0374	0.0000	0.0000	0.0000	0.0000
.60	2.05	.95	-.09	-.0317	.0312	.0499	-.0317	.0312	0.0000	0.0000	0.0000	0.0000
.60	4.08	.95	-.13	.0542	.0284	.0483	.0542	.0284	0.0000	0.0000	0.0000	0.0000
.60	6.05	.95	-.18	.1396	.0306	.0494	.1396	.0306	0.0000	0.0000	0.0000	0.0000
.60	8.06	.94	-.08	.2290	.0390	.0543	.2290	.0390	0.0000	0.0000	0.0000	0.0000
.60	10.06	.94	-.03	.3107	.0526	.0617	.3107	.0526	0.0000	0.0000	0.0000	0.0000
.60	15.04	.94	-.05	.5350	.1187	.0804	.5350	.1187	0.0000	0.0000	0.0000	0.0000
.60	19.04	.95	-.07	.7647	.2242	.0811	.7647	.2242	0.0000	0.0000	0.0000	0.0000
.60	.04	2.31	.09	-.1070	-.0420	.0497	-.1178	.0331	.0108	.0751	-.0022	.0759
.60	4.07	2.30	-.01	.0701	-.0495	.0461	.0542	.0240	.0159	.0735	-.0022	.0752
.60	6.06	2.30	-.03	.1624	-.0466	.0474	.1440	.0263	.0184	.0728	-.0022	.0751
.60	10.05	2.30	-.09	.3368	-.0238	.0584	.3134	.0476	.0234	.0714	-.0022	.0751
.60	19.07	2.30	-.13	.8100	.1561	.0778	.7756	.2230	.0344	.0668	-.0022	.0751
.60	.05	3.00	.07	-.0950	-.0783	.0432	-.1150	.0335	.0200	.1117	-.0068	.1135
.60	2.05	3.00	-.05	-.0049	-.0846	.0407	-.0289	.0269	.0239	.1114	-.0068	.1140
.60	4.05	3.01	-.06	.0854	-.0862	.0391	.0576	.0243	.0279	.1105	-.0069	.1140
.60	6.05	3.01	-.11	.1770	-.0831	.0403	.1452	.0267	.0318	.1098	-.0069	.1144
.60	8.06	3.01	-.14	.2698	-.0734	.0437	.2342	.0349	.0356	.1083	-.0069	.1140
.60	10.04	3.00	-.17	.3951	-.0583	.0507	.3161	.0482	.0390	.1064	-.0068	.1134
.60	15.03	3.01	-.15	.5936	.0122	.0698	.5451	.1155	.0485	.1033	-.0069	.1141
.60	19.05	3.00	-.14	.8360	.1253	.0700	.7807	.2246	.0553	.0993	-.0068	.1137
.60	.04	4.51	.04	-.0662	-.1605	.0288	-.1111	.0312	.0449	.1917	-.0193	.1969
.60	4.04	4.51	.01	.1214	-.1656	.0251	.0633	.0225	.0581	.1881	-.0193	.1969
.60	6.04	4.50	-.01	.2160	-.1608	.0262	.1512	.0254	.0647	.1863	-.0193	.1972
.60	10.04	4.51	-.04	.4017	-.1338	.0365	.3241	.0478	.0777	.1815	-.0193	.1975
.60	19.04	4.52	-.11	.8973	.0595	.0532	.7924	.2263	.1049	.1668	-.0193	.1970
.60	.06	.95	4.93	-.1105	.0394	.0692	-.1105	.0394	0.0000	0.0000	0.0000	0.0000
.60	.04	3.03	4.93	-.0838	-.0785	.0599	-.1043	.0350	.0205	.1135	-.0071	.1153
.60	2.05	3.02	4.91	.0086	-.0822	.0605	-.0157	.0300	.0243	.1121	-.0070	.1147
.60	4.05	2.99	4.88	.1030	-.0789	.0638	.0755	.0308	.0276	.1097	-.0067	.1131
.60	6.06	2.99	4.95	.1975	-.0715	.0688	.1662	.0372	.0314	.1086	-.0067	.1131
.60	8.04	2.99	4.94	.2907	-.0585	.0750	.2557	.0489	.0351	.1073	-.0067	.1129
.60	10.04	2.99	4.94	.3793	-.0396	.0827	.3405	.0664	.0388	.1060	-.0067	.1128
.60	15.05	2.99	4.92	.6128	.0389	.1060	.5648	.1413	.0479	.1024	-.0067	.1130
.60	19.07	2.99	4.94	.8472	.1553	.1075	.7922	.2540	.0550	.0987	-.0067	.1130



TABLE 9.- AERODYNAMIC CHARACTERISTICS: DROOPED LEADING EDGE,  
 $\delta_{te} = 30^\circ$ ,  $\delta_v = 15^\circ$

MACH	ALPHA	NPR	CANALP	CL	C(D-F)	CM	CLAERO	CDAERO	CLJET	CFJET	CMJET	CT
.60	-.01	.96	≈ 0.00	.0322	.0456	-.0350	.0322	.0456	0.0000	0.0000	0.0000	0.0000
.60	2.00	.95		.1108	.0445	-.0327	.1108	.0445	0.0000	0.0000	0.0000	0.0000
.60	3.99	.95		.1937	.0470	-.0310	.1937	.0470	0.0000	0.0000	0.0000	0.0000
.60	6.00	.95		.2753	.0541	-.0283	.2753	.0541	0.0000	0.0000	0.0000	0.0000
.60	8.00	.95		.3595	.0673	-.0244	.3595	.0673	0.0000	0.0000	0.0000	0.0000
.60	10.00	.95		.4489	.0874	-.0203	.4489	.0874	0.0000	0.0000	0.0000	0.0000
.60	15.00	.95		.6787	.1683	-.0055	.6787	.1683	0.0000	0.0000	0.0000	0.0000
.60	18.99	.94		.9123	.2921	-.0092	.9123	.2921	0.0000	0.0000	0.0000	0.0000
.60	-.02	2.34		.0485	-.0349	-.0380	.0374	.0419	.0111	.0768	-.0023	.0776
.60	3.97	2.34		.2134	-.0322	-.0341	.1971	.0431	.0163	.0753	-.0023	.0771
.60	6.00	2.31		.2996	-.0230	-.0311	.2810	.0506	.0186	.0737	-.0022	.0760
.60	9.99	2.32		.4771	.0115	-.0230	.4534	.0839	.0237	.0724	-.0022	.0762
.60	18.98	2.33		.9639	.2240	-.0161	.9288	.2923	.0351	.0684	-.0022	.0768
.60	-.02	2.98		.0589	-.0691	-.0427	.0393	.0418	.0196	.1109	-.0067	.1126
.60	1.99	2.99		.1427	-.0695	-.0408	.1191	.0410	.0236	.1105	-.0067	.1130
.60	3.99	2.99		.2269	-.0658	-.0393	.1995	.0437	.0274	.1095	-.0067	.1129
.60	5.98	2.98		.3148	-.0575	-.0366	.2836	.0511	.0312	.1086	-.0067	.1130
.60	7.99	2.98		.4029	-.0432	-.0327	.3680	.0642	.0350	.1074	-.0067	.1130
.60	9.97	2.99		.4961	-.0214	-.0289	.4573	.0849	.0388	.1063	-.0067	.1131
.60	14.99	2.99		.7467	.0674	-.0177	.6989	.1697	.0478	.1023	-.0067	.1130
.60	18.98	2.99		.9928	.1971	-.0219	.9379	.2962	.0550	.0991	-.0067	.1133
.60	.00	4.51		.0880	-.1543	-.0550	.0432	.0375	.0447	.1918	-.0193	.1969
.60	4.01	4.52		.2632	-.1474	-.0529	.2050	.0413	.0582	.1887	-.0194	.1975
.60	5.99	4.52		.3536	-.1375	-.0506	.2888	.0495	.0648	.1870	-.0194	.1979
.60	9.99	4.51		.5427	-.0985	-.0432	.4646	.0844	.0781	.1829	-.0195	.1988
.60	19.09	4.52		.0565	.1332	-.0385	.9512	.3004	.1054	.1672	-.0194	.1977
.60	-.01	.95	≈ 5.00	.0421	.0470	-.0163	.0421	.0470	0.0000	0.0000	0.0000	0.0000
.60	-.01	3.01		.0686	-.0689	-.0249	.0486	.0434	.0200	.1123	-.0069	.1141
.60	2.00	3.00		.1549	-.0670	-.0198	.1311	.0442	.0238	.1112	-.0068	.1137
.60	4.00	3.01		.2442	-.0608	-.0144	.2165	.0496	.0277	.1104	-.0069	.1138
.60	6.00	3.02		.3355	-.0483	-.0076	.3039	.0611	.0316	.1094	-.0069	.1139
.60	8.00	3.01		.4235	-.0301	-.0015	.3881	.0783	.0354	.1083	-.0069	.1140
.60	10.00	3.02		.5161	-.0043	.0039	.4769	.1026	.0391	.1068	-.0069	.1138
.60	14.99	3.00		.7544	.0886	.0228	.7061	.1918	.0483	.1032	-.0068	.1139
.60	19.13	3.00		.0026	.2280	.0182	.9471	.3273	.0555	.0993	-.0068	.1138



TABLE 10.- AERODYNAMIC CHARACTERISTICS: DROOPED LEADING EDGE,  
 $\delta_{te} = 7^\circ$ ,  $\delta_v = 0^\circ$

MACH	ALPHA	NPR	CANALP	CL	C(D-F)	CM	CLAERO	CDAERO	CLJET	CFJET	CMJET	CT
1.20	.04	.80	-.02	-.0969	.0595	.0641	-.0969	.0595	0.0000	0.0000	0.0000	0.0000
1.20	2.02	.81	-.05	-.0119	.0536	.0574	-.0119	.0536	0.0000	0.0000	0.0000	0.0000
1.20	4.04	.82	-.16	.0766	.0521	.0504	.0766	.0521	0.0000	0.0000	0.0000	0.0000
1.20	6.01	.82	-.22	.1654	.0557	.0444	.1654	.0557	0.0000	0.0000	0.0000	0.0000
1.20	8.03	.83	-.28	.2598	.0665	.0392	.2598	.0665	0.0000	0.0000	0.0000	0.0000
1.20	10.04	.83	-.33	.3549	.0849	.0348	.3549	.0849	0.0000	0.0000	0.0000	0.0000
1.20	15.03	.81	-.44	.5932	.1643	.0188	.5932	.1643	0.0000	0.0000	0.0000	0.0000
1.20	17.09	.80	-.51	.6966	.2119	.0081	.6966	.2119	0.0000	0.0000	0.0000	0.0000
1.20	.04	6.61	-.18	-.0944	-.0245	.0731	-.0874	.0527	-.0070	.0772	.0103	.0775
1.20	2.04	6.62	-.08	-.0076	-.0305	.0675	-.0033	.0471	-.0043	.0776	.0103	.0777
1.20	4.03	6.60	-.13	.0812	-.0319	.0612	.0829	.0460	-.0016	.0779	.0104	.0779
1.20	6.04	6.61	-.09	.1776	-.0277	.0558	.1765	.0504	.0011	.0781	.0104	.0781
1.20	8.04	6.60	-.12	.2720	-.0161	.0510	.2682	.0616	.0038	.0777	.0103	.0778
1.20	10.04	6.59	-.16	.3685	.0028	.0466	.3619	.0804	.0065	.0775	.0103	.0778
1.20	15.03	6.59	-.29	.6190	.0850	.0296	.6057	.1617	.0132	.0767	.0103	.0778
1.20	16.31	6.61	-.33	.6804	.1128	.0230	.6654	.1893	.0150	.0764	.0104	.0779
.87	.03	1.03	0.00	-.1251	.0357	.0563	-.1251	.0357	0.0000	0.0000	0.0000	0.0000
.87	2.04	1.03	-.03	-.0323	.0280	.0523	-.0323	.0280	0.0000	0.0000	0.0000	0.0000
.87	4.05	1.03	-.06	.0609	.0251	.0494	.0609	.0251	0.0000	0.0000	0.0000	0.0000
.87	6.05	1.03	-.08	.1550	.0282	.0497	.1550	.0282	0.0000	0.0000	0.0000	0.0000
.87	8.05	1.03	-.19	.2513	.0371	.0514	.2513	.0371	0.0000	0.0000	0.0000	0.0000
.87	10.01	1.03	-.23	.3409	.0526	.0569	.3409	.0526	0.0000	0.0000	0.0000	0.0000
.87	15.02	1.02	-.34	.5894	.1281	.0704	.5894	.1281	0.0000	0.0000	0.0000	0.0000
.87	18.69	1.01	-.08	.8126	.2405	.0633	.8126	.2405	0.0000	0.0000	0.0000	0.0000
.87	.01	2.40	.26	-.1265	-.0035	.0615	-.1231	.0341	-.0033	.0376	.0049	.0377
.87	4.04	2.41	.21	.0600	-.0138	.0559	.0607	.0240	-.0007	.0378	.0049	.0379
.87	6.04	2.41	.18	.1568	-.0113	.0559	.1562	.0269	.0006	.0381	.0050	.0382
.87	10.04	2.41	.10	.3477	.0145	.0640	.3444	.0523	.0033	.0378	.0049	.0379
.87	18.58	2.42	-.10	.8123	.1968	.0690	.8034	.2338	.0089	.0370	.0050	.0380
.87	.02	3.91	.21	-.1264	-.0425	.0661	-.1195	.0343	-.0069	.0769	.0101	.0772
.87	2.03	3.91	.19	-.0308	-.0500	.0623	-.0266	.0271	-.0042	.0771	.0101	.0772
.87	4.02	3.89	.17	.0608	-.0527	.0601	.0623	.0244	-.0016	.0771	.0101	.0771
.87	6.04	3.89	.13	.1613	-.0496	.0603	.1601	.0274	.0012	.0770	.0101	.0770
.87	8.03	3.91	.09	.2589	-.0404	.0627	.2551	.0368	.0038	.0773	.0102	.0773
.87	10.02	3.90	.05	.3534	-.0241	.0680	.3469	.0530	.0065	.0771	.0102	.0774
.87	15.02	3.89	-.05	.6112	.0543	.0802	.5980	.1303	.0132	.0760	.0101	.0771
.87	18.59	3.89	-.11	.8273	.1613	.0716	.8094	.2361	.0178	.0749	.0101	.0770
.87	.04	5.41	.19	-.1270	-.0827	.0709	-.1165	.0332	-.0105	.1159	.0154	.1164
.87	4.04	5.39	.15	.0641	-.0937	.0646	.0665	.0230	-.0024	.1167	.0155	.1167
.87	6.03	5.41	.11	.1622	-.0909	.0654	.1605	.0265	.0017	.1174	.0156	.1174
.87	10.03	5.40	.02	.3605	-.0642	.0732	.3507	.0523	.0098	.1165	.0155	.1169
.87	17.67	5.41	-.11	.7865	.0925	.0785	.7613	.2065	.0252	.1140	.0155	.1168
.60	.03	1.01	.19	-.1022	.0306	.0422	-.1022	.0306	0.0000	0.0000	0.0000	0.0000
.60	2.02	1.01	.18	-.0183	.0248	.0418	-.0183	.0248	0.0000	0.0000	0.0000	0.0000
.60	4.03	1.01	.17	.0662	.0228	.0419	.0662	.0228	0.0000	0.0000	0.0000	0.0000
.60	6.03	1.01	.16	.1528	.0262	.0444	.1528	.0262	0.0000	0.0000	0.0000	0.0000
.60	8.02	1.01	.16	.2389	.0344	.0485	.2389	.0344	0.0000	0.0000	0.0000	0.0000
.60	10.03	1.01	.15	.3242	.0492	.0553	.3242	.0492	0.0000	0.0000	0.0000	0.0000
.60	15.03	1.00	.11	.5464	.1160	.0746	.5464	.1160	0.0000	0.0000	0.0000	0.0000
.60	19.06	1.00	.11	.7852	.2276	.0726	.7852	.2276	0.0000	0.0000	0.0000	0.0000
.60	.03	2.31	.21	-.1100	-.0448	.0529	-.1034	.0295	-.0065	.0743	.0097	.0746
.60	4.04	2.32	.20	.0659	-.0526	.0521	.0673	.0219	-.0013	.0745	.0097	.0745
.60	6.03	2.30	.19	.1534	-.0489	.0544	.1521	.0248	.0012	.0737	.0096	.0737
.60	10.01	2.30	.17	.3308	-.0258	.0652	.3245	.0474	.0063	.0732	.0096	.0735
.60	19.09	2.30	.12	.8133	.1572	.0813	.7954	.2288	.0179	.0717	.0096	.0739
.60	.04	3.00	.23	-.1105	-.0819	.0577	-.1005	.0302	-.0100	.1121	.0147	.1126
.60	2.02	3.01	-.10	-.0238	-.0885	.0553	-.0177	.0243	-.0061	.1128	.0148	.1129
.60	4.05	3.01	-.16	.0658	-.0903	.0547	.0680	.0222	-.0021	.1125	.0146	.1125
.60	6.03	3.01	-.08	.1544	-.0872	.0571	.1526	.0253	.0018	.1126	.0146	.1126
.60	8.03	3.00	-.09	.2472	-.0788	.0615	.2415	.0336	.0057	.1124	.0147	.1126
.60	10.04	3.00	-.11	.3355	-.0645	.0680	.3259	.0478	.0096	.1123	.0147	.1127
.60	15.04	3.01	-.14	.5752	.0043	.0868	.5557	.1162	.0195	.1119	.0148	.1136
.60	19.05	3.00	-.09	.8213	.1184	.0839	.7941	.2280	.0272	.1097	.0148	.1130

TABLE 11.- AERODYNAMIC CHARACTERISTICS: DROOPED LEADING EDGE,  
 $\delta_{te} = 30^\circ$ ,  $\delta_v = 0^\circ$

MACH	ALPHA	NPR	CANALP	CL	C(D-F)	CM	CLAERD	CDAERD	CLJET	CFJET	CMJET	CT
.60	-.00	.95	.00	.0135	.0464	-.0254	.0135	.0464	0.0000	0.0000	0.0000	0.0000
.60	2.02	.95	.00	.0908	.0443	-.0217	.0908	.0443	0.0000	0.0000	0.0000	0.0000
.60	4.00	.95	.01	.1681	.0454	-.0193	.1681	.0454	0.0000	0.0000	0.0000	0.0000
.60	5.99	.95	.00	.2521	.0517	-.0160	.2521	.0517	0.0000	0.0000	0.0000	0.0000
.60	8.02	.95	-.01	.3295	.0622	-.0083	.3295	.0622	0.0000	0.0000	0.0000	0.0000
.60	10.02	.96	-.03	.4166	.0805	-.0033	.4166	.0805	0.0000	0.0000	0.0000	0.0000
.60	15.00	.96	-.09	.6436	.1563	.0133	.6436	.1563	0.0000	0.0000	0.0000	0.0000
.60	19.07	.96	-.07	.8815	.2788	.0107	.8815	.2788	0.0000	0.0000	0.0000	0.0000
.60	.02	2.30	.09	.0116	-.0327	-.0144	.0181	.0410	-.0065	.0737	.0096	.0740
.60	4.04	2.30	.08	.1764	-.0328	-.0107	.1778	.0409	-.0013	.0738	.0096	.0738
.60	10.01	2.30	.04	.4534	.0089	-.0052	.4440	.0823	.0064	.0734	.0096	.0737
.60	19.10	2.31	-.02	.9303	.2117	.0089	.9124	.2833	.0179	.0717	.0096	.0739
.60	.01	3.00	.07	.0072	-.0700	-.0097	.0173	.0418	-.0100	.1118	.0147	.1123
.60	2.01	3.00	.06	.0927	-.0732	-.0072	.0988	.0396	-.0062	.1128	.0148	.1130
.60	4.01	3.01	.05	.1769	-.0713	-.0060	.1791	.0414	-.0022	.1127	.0147	.1127
.60	5.98	3.01	.04	.2656	-.0645	-.0044	.2639	.0484	.0017	.1129	.0148	.1129
.60	8.01	3.01	.02	.3570	-.0513	-.0014	.3513	.0614	.0057	.1128	.0148	.1129
.60	10.01	3.01	.01	.4554	-.0297	-.0014	.4458	.0831	.0096	.1127	.0148	.1132
.60	15.00	3.01	-.04	.7008	.0505	.0129	.6814	.1621	.0194	.1117	.0147	.1133
.60	19.12	3.01	-.06	.9486	.1772	.0104	.9212	.2872	.0274	.1100	.0147	.1133
.60	-.00	4.49	.03	.0011	-.1548	.0013	.0189	.0401	-.0177	.1949	.0258	.1957
.60	4.03	4.51	.02	.1776	-.1561	.0047	.1817	.0404	-.0040	.1965	.0259	.1965
.60	6.01	4.52	.00	.2701	-.1480	.0060	.2673	.0470	.0028	.1950	.0257	.1950
.60	7.99	4.52	-.01	.3634	-.1354	.0091	.3539	.0601	.0095	.1955	.0258	.1958
.60	10.00	4.52	-.03	.4674	-.1130	.0084	.4509	.0828	.0164	.1958	.0259	.1965
.60	19.11	4.52	-.10	.9789	.0974	.0163	.9314	.2889	.0474	.1915	.0260	.1972
.60	.01	3.01	5.09	.0200	-.0690	.0068	.0301	.0436	-.0101	.1126	.0148	.1130
.60	2.00	3.01	5.00	.1047	-.0696	.0111	.1108	.0430	-.0062	.1126	.0147	.1128
.60	4.01	3.02	4.99	.1945	-.0658	.0161	.1968	.0476	-.0022	.1134	.0147	.1134
.60	5.99	3.02	4.97	.2895	-.0542	.0213	.2878	.0590	.0017	.1132	.0147	.1133
.60	8.04	3.01	4.95	.3787	-.0372	.0275	.3730	.0754	.0057	.1126	.0146	.1128
.60	10.00	3.02	4.93	.4771	-.0124	.0288	.4675	.1003	.0096	.1126	.0147	.1131
.60	15.02	3.02	4.88	.7250	.0774	.0419	.7055	.1893	.0195	.1119	.0148	.1136
.60	19.15	3.02	4.84	.9580	.2056	.0468	.9307	.3154	.0274	.1097	.0147	.1131

TABLE 12.- AERODYNAMIC CHARACTERISTICS: DROOPED LEADING EDGE,  
 $\delta_{te} = 30^\circ$ ,  $\delta_v = 30^\circ$

MACH	ALPHA	NPR	CANALP	CL	C(D-F)	CM	CLAERD	CDAERD	CLJET	CFJET	CMJET	CT
.60	.00	.93	.05	.0488	.0497	-.0454	.0488	.0497	0.0000	0.0000	0.0000	0.0000
.60	1.99	.93	.04	.1287	.0491	-.0435	.1287	.0491	0.0000	0.0000	0.0000	0.0000
.60	4.02	.93	.02	.2123	.0523	-.0425	.2123	.0523	0.0000	0.0000	0.0000	0.0000
.60	6.00	.93	.00	.2952	.0605	-.0407	.2952	.0605	0.0000	0.0000	0.0000	0.0000
.60	8.02	.93	-.03	.3817	.0746	-.0376	.3817	.0746	0.0000	0.0000	0.0000	0.0000
.60	10.00	.93	-.06	.4703	.0959	-.0349	.4703	.0959	0.0000	0.0000	0.0000	0.0000
.60	15.00	.93	-.06	.7030	.1794	-.0210	.7030	.1794	0.0000	0.0000	0.0000	0.0000
.60	19.08	.92	-.06	.9399	.3073	-.0228	.9399	.3073	0.0000	0.0000	0.0000	0.0000
.60	.01	2.31	.07	.0912	-.0230	-.0661	.0586	.0444	.0327	.0674	-.0192	.0749
.60	4.03	2.31	.05	.2614	-.0160	-.0643	.2244	.0486	.0371	.0646	-.0191	.0745
.60	10.00	2.31	-.00	.5280	.0340	-.0581	.4842	.0945	.0438	.0606	-.0192	.0747
.60	19.07	2.31	-.07	1.0179	.2590	-.0524	.9648	.3123	.0531	.0533	-.0193	.0752
.60	.00	3.00	.03	.1168	-.0520	-.0830	.0661	.0484	.0507	.1004	-.0302	.1124
.60	2.03	3.01	.02	.2056	-.0498	-.0825	.1512	.0490	.0544	.0988	-.0303	.1128
.60	4.02	3.00	.00	.2932	-.0432	-.0822	.2356	.0534	.0576	.0966	-.0303	.1125
.60	6.01	3.00	-.01	.3795	-.0324	-.0801	.3185	.0623	.0611	.0947	-.0303	.1127
.60	8.00	3.00	-.03	.4693	-.0150	-.0774	.4051	.0773	.0642	.0923	-.0302	.1124
.60	9.99	3.00	-.05	.5630	.0098	-.0762	.4954	.1003	.0676	.0905	-.0304	.1130
.60	15.01	3.00	-.09	.8066	.1028	-.0638	.7315	.1867	.0751	.0839	-.0303	.1126
.60	19.07	3.00	-.00	1.0567	.2422	-.0699	.9757	.3208	.0809	.0785	-.0303	.1128
.60	.01	3.01	5.07	.1322	-.0504	-.0665	.0812	.0505	.0510	.1008	-.0304	.1130
.60	2.03	3.01	5.05	.2191	-.0461	-.0632	.1648	.0526	.0544	.0987	-.0303	.1127
.60	4.00	3.01	5.01	.3089	-.0378	-.0592	.2508	.0596	.0581	.0975	-.0305	.1135
.60	5.99	3.01	5.04	.3973	-.0226	-.0531	.3363	.0722	.0611	.0948	-.0303	.1127
.60	8.00	3.01	5.02	.4904	-.0018	-.0473	.4258	.0912	.0646	.0930	-.0305	.1132
.60	10.03	3.01	5.02	.5830	.0263	-.0430	.5150	.1172	.0680	.0909	-.0305	.1135
.60	15.00	3.01	5.04	.8166	.1249	-.0248	.7409	.2095	.0757	.0846	-.0306	.1136
.60	19.10	3.01	5.02	1.0613	.2687	-.0300	.9797	.3478	.0816	.0791	-.0306	.1137

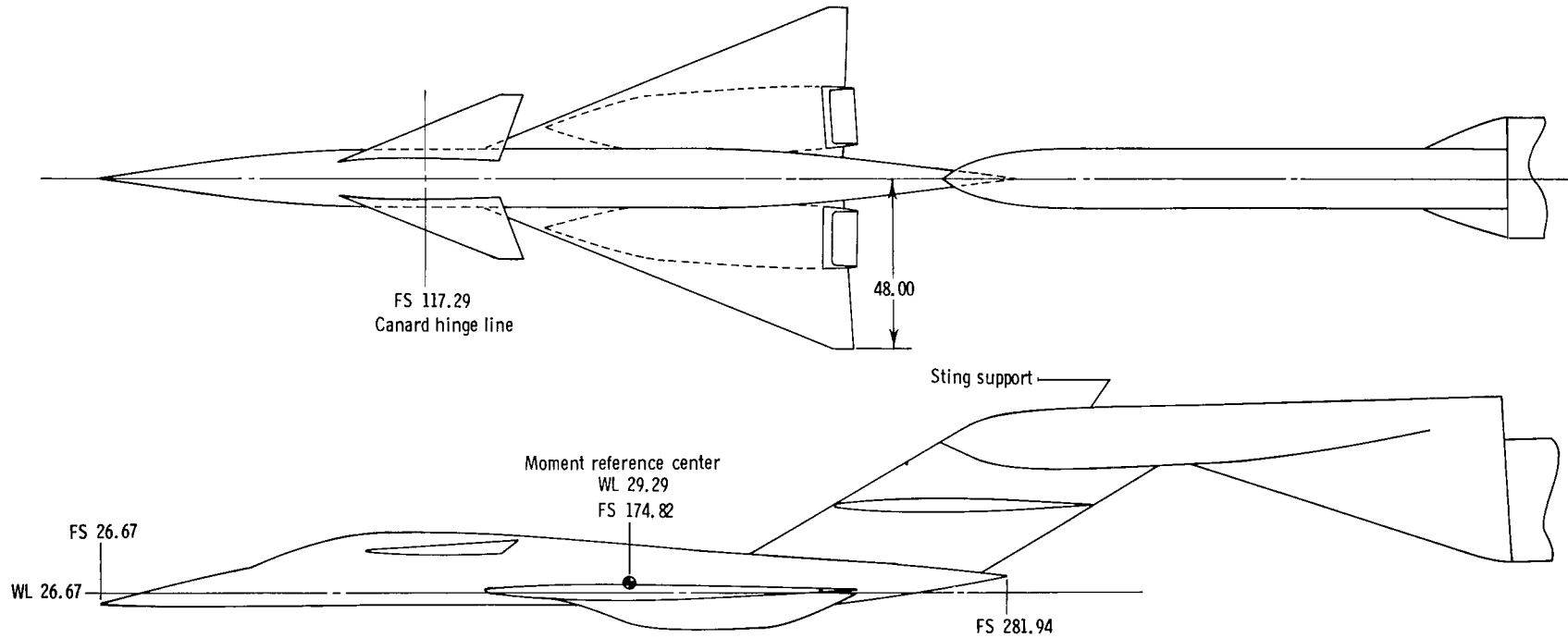
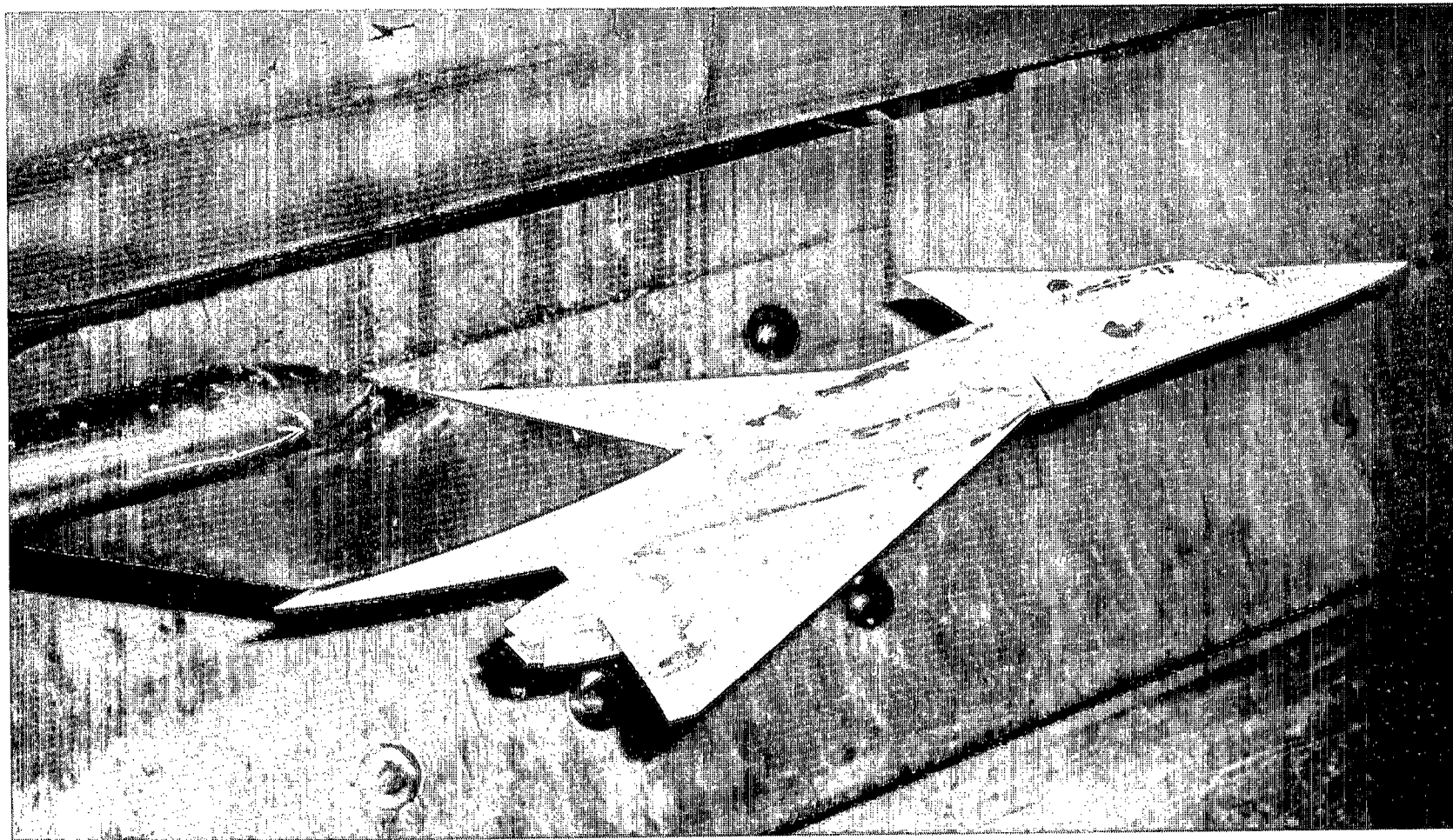
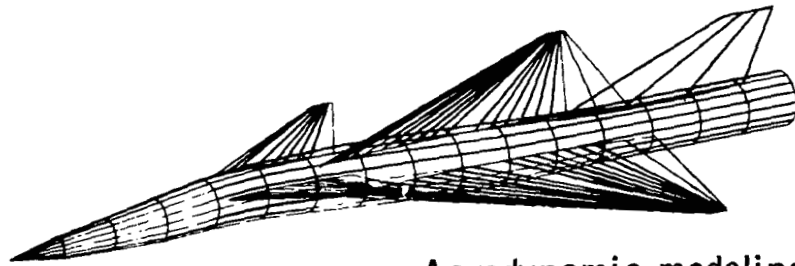


Figure 1.- Sketch showing general arrangement of model and support system. All dimensions are in centimeters unless otherwise noted.



L-80-1228

Figure 2.- Photograph of model.



Aerodynamic modeling  
(Nacelles removed)

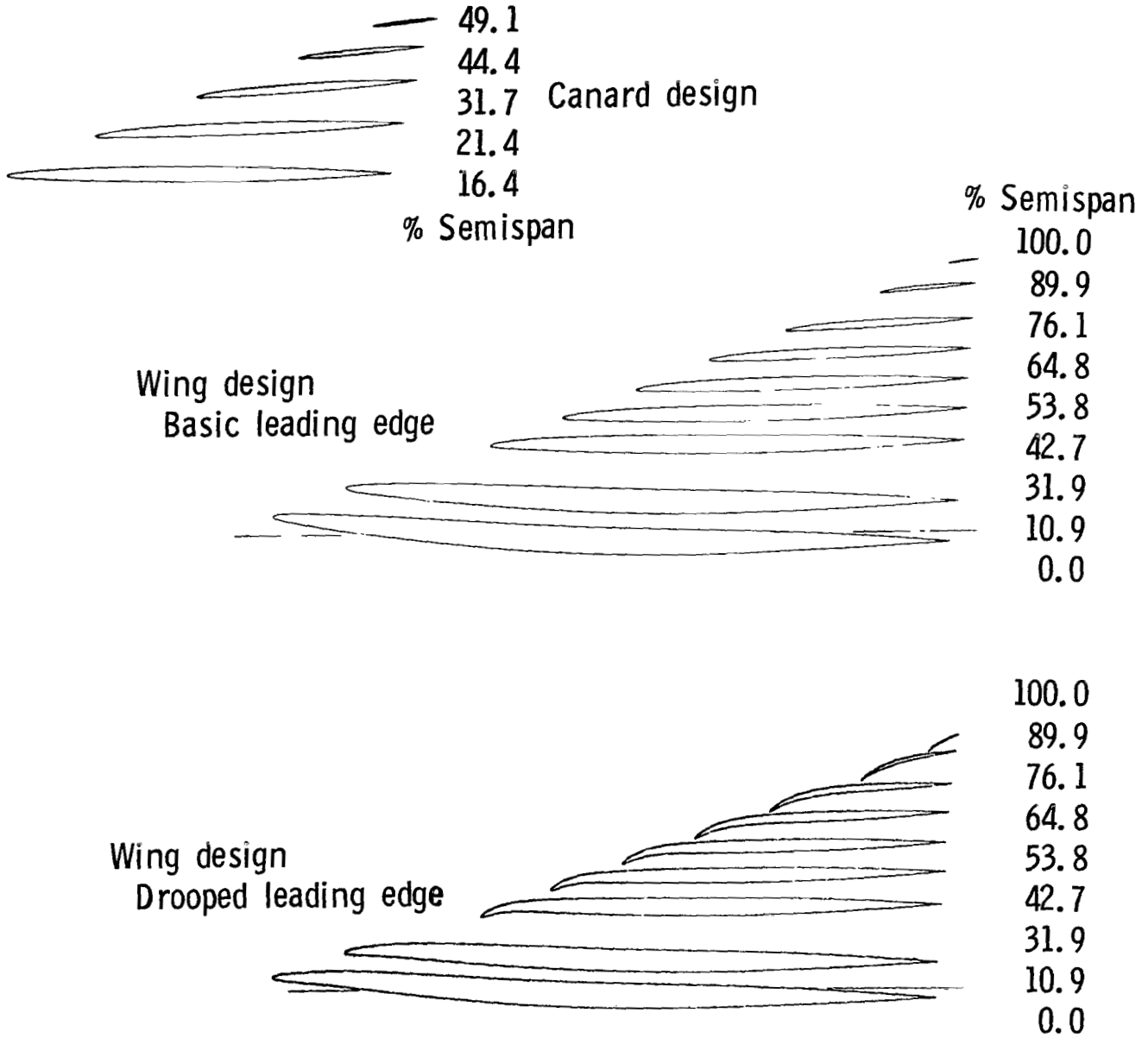


Figure 3.- Wing-canard design characteristics.

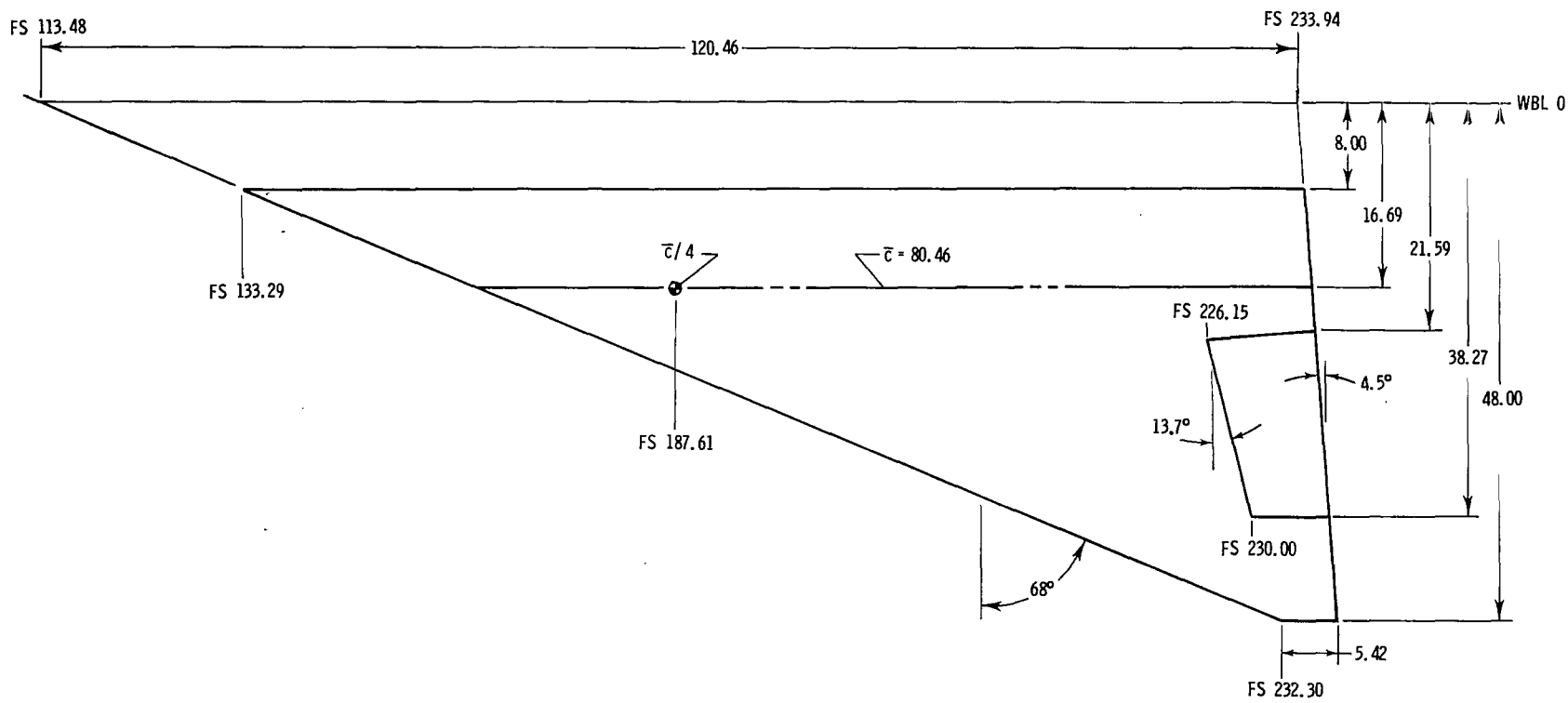
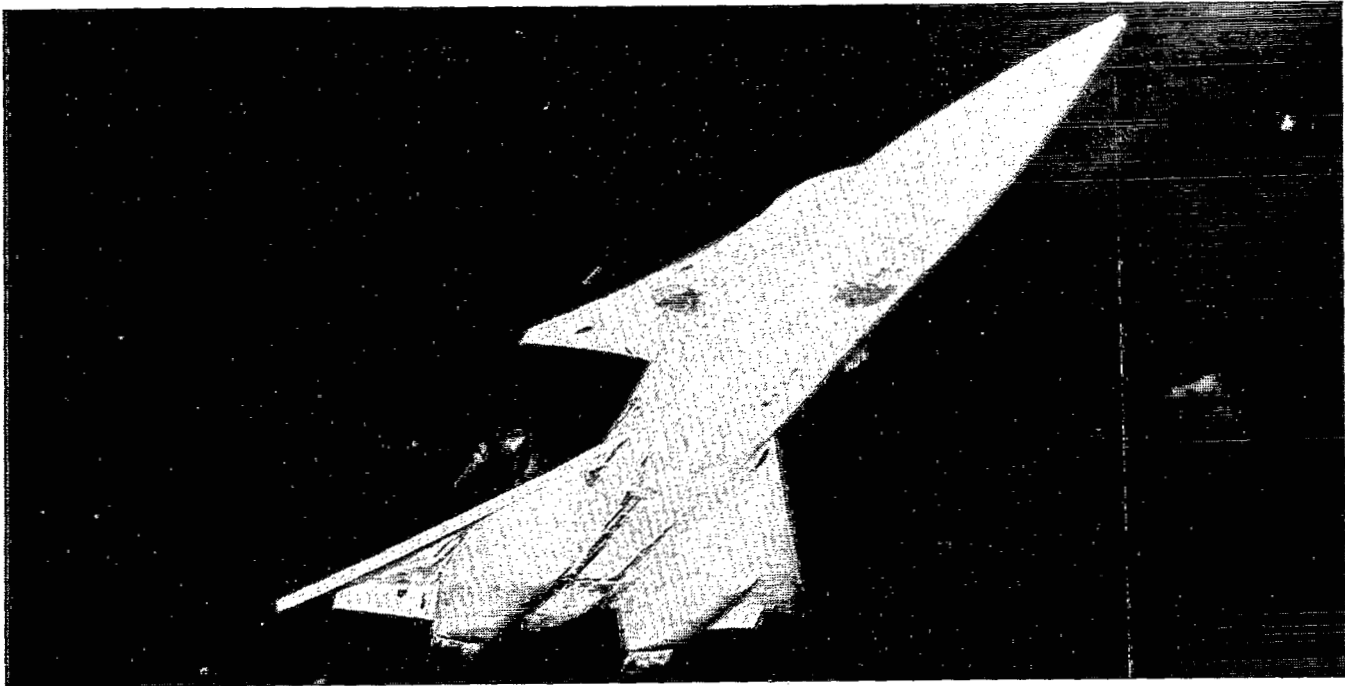
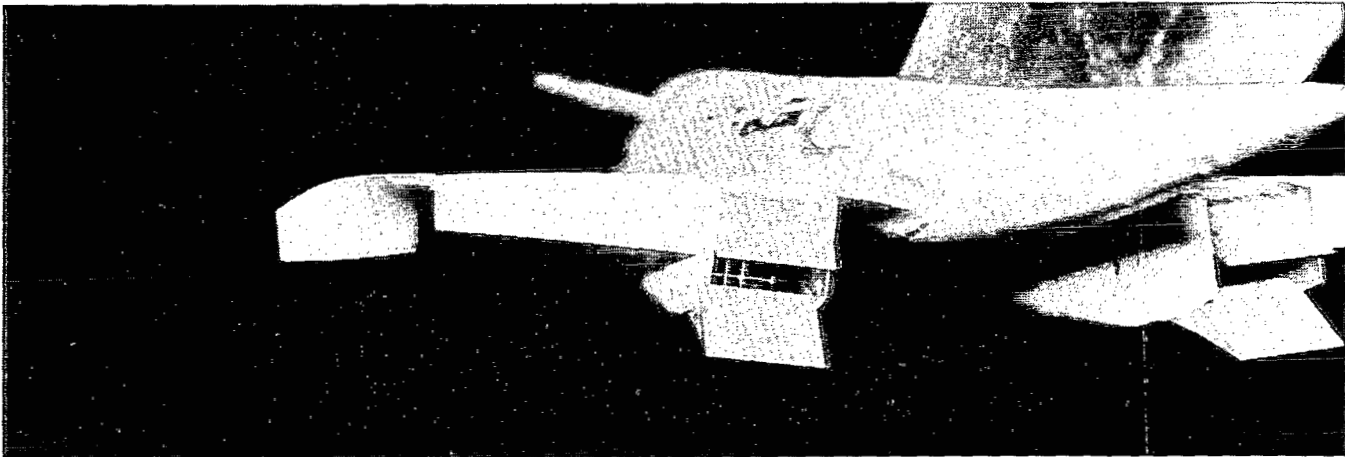


Figure 4.- Sketch showing geometry of wing. All dimensions are in centimeters unless otherwise noted.



L-80-1130



L-80-1127

Figure 5.- Photographs showing wing maneuver devices and vectored nozzles, drooped leading edge.  $\delta_{te} = 30^\circ$ ;  $\delta_v = 30^\circ$ .



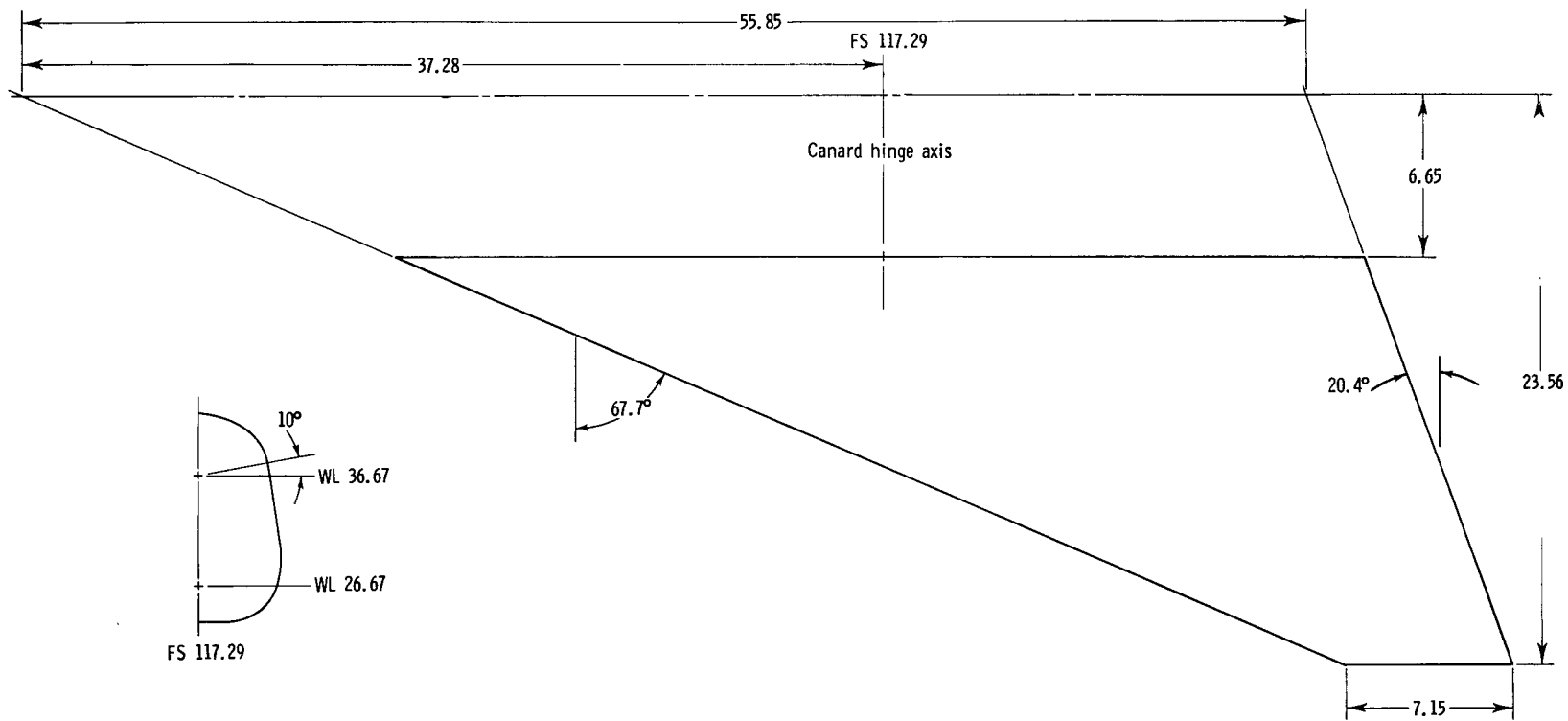
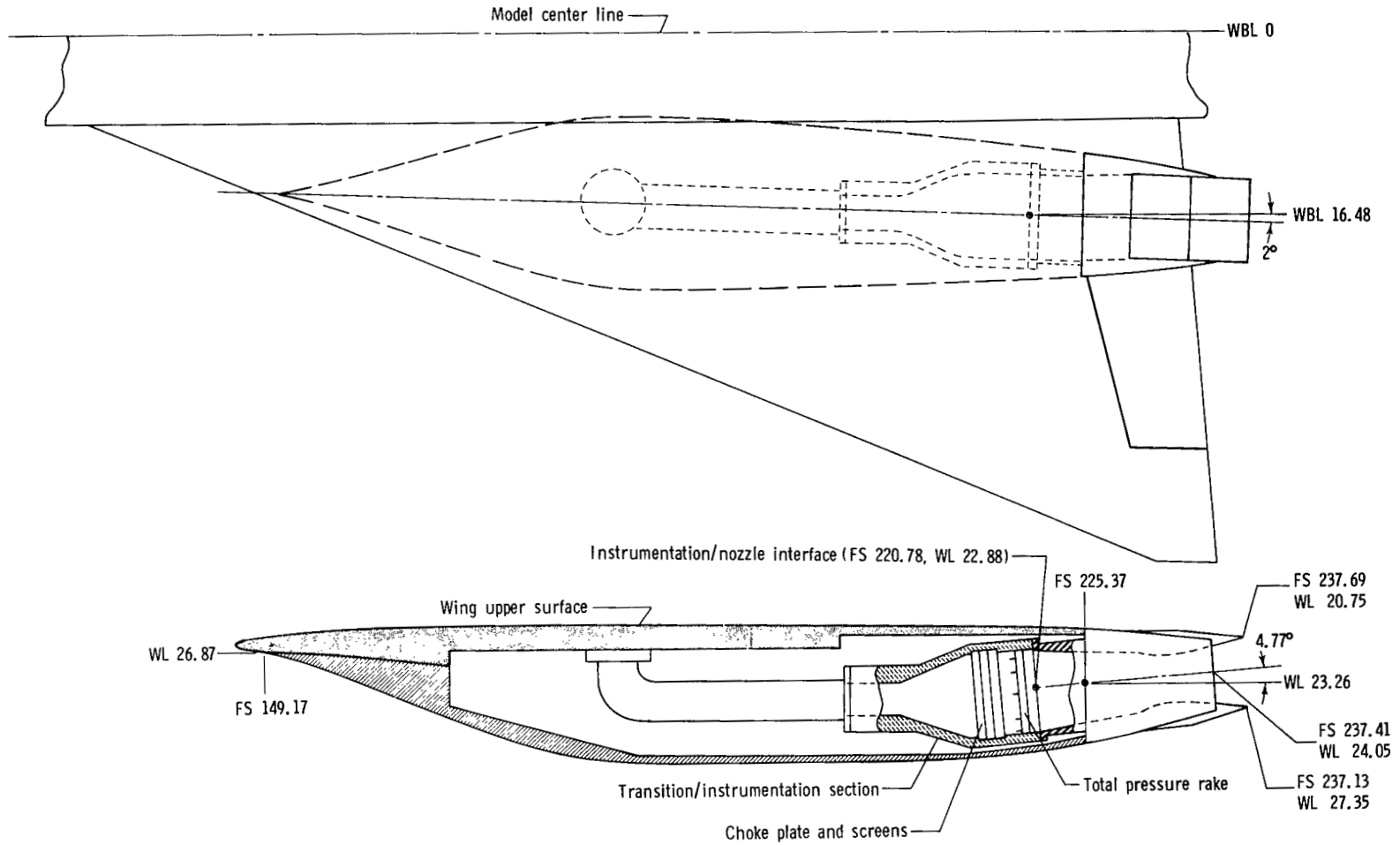
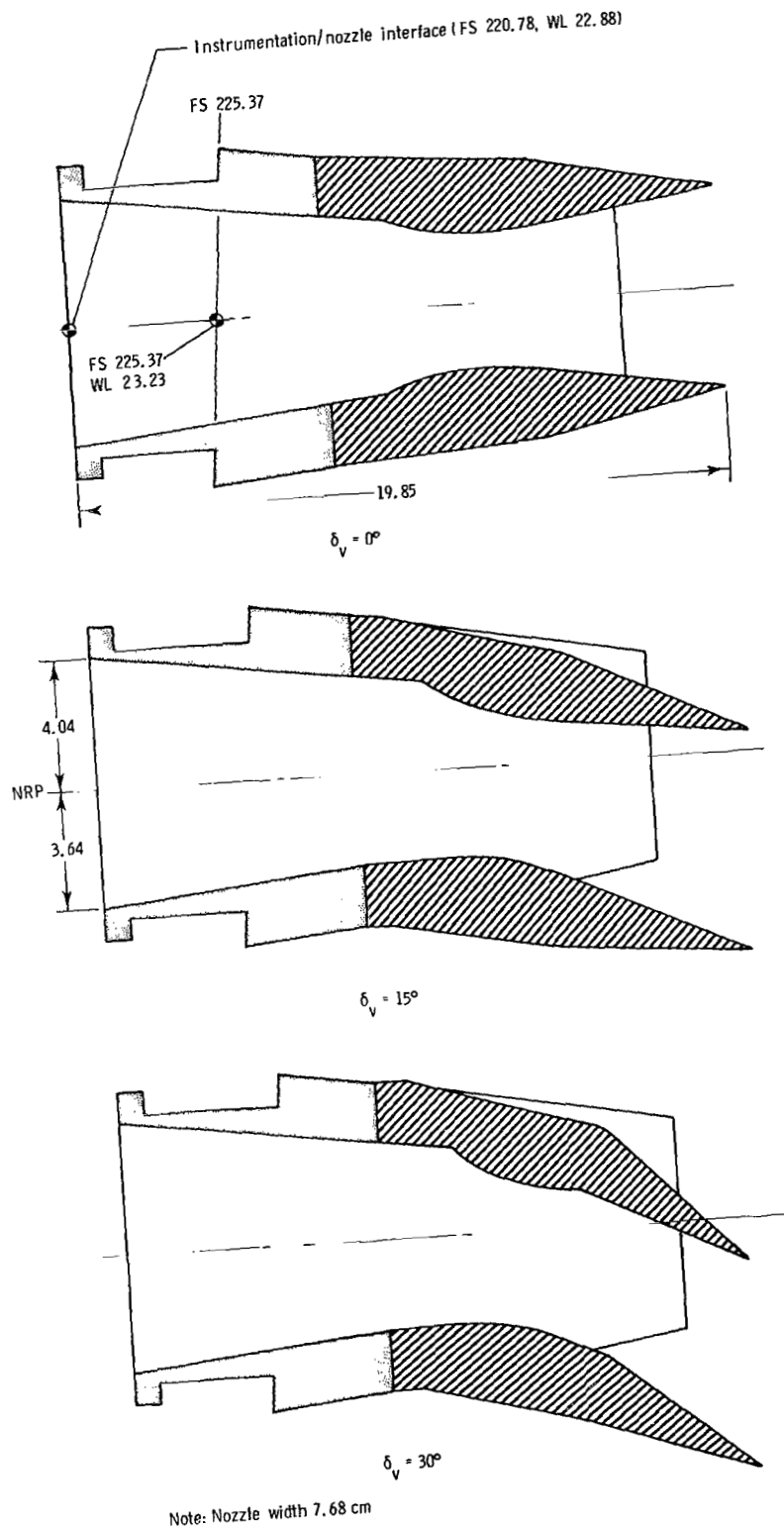


Figure 6.- Sketch showing planform geometry of canard. All dimensions are in centimeters unless otherwise noted.



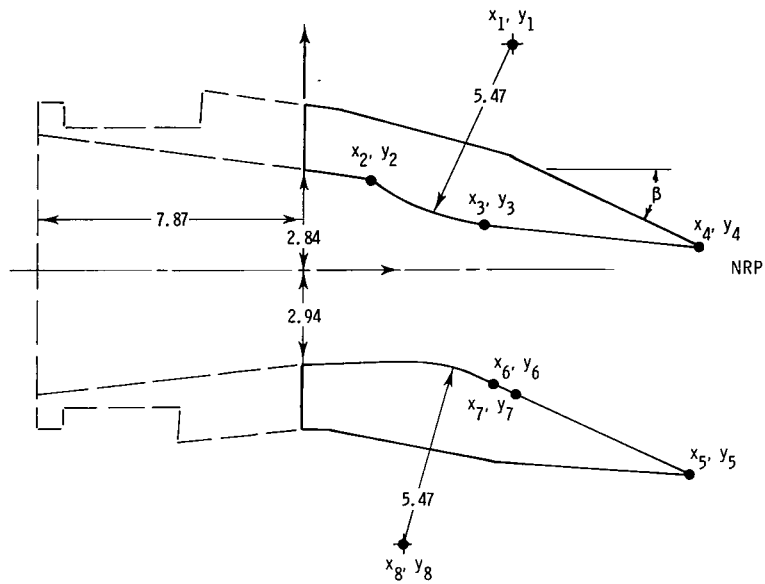
Note: Center line of instrumentation section 4.17° with respect to water line plane

Figure 7.- Nacelle/nozzle installation. All dimensions are in centimeters unless otherwise noted.



(a) Nozzle configurations.

Figure 8.- Details of 2-D C-D nozzle configurations. All dimensions are in centimeters unless otherwise noted.



	$\delta_v, \text{deg}$		
	0	15	30
$x_1$	4.60	6.21	5.84
$y_1$	7.53	6.74	6.57
$x_2$	2.03	2.03	2.03
$y_2$	2.70	2.70	2.70
$x_3$	5.40	5.08	5.86
$y_3$	2.12	1.29	1.03
$x_4$	11.98	11.68	10.79
$y_4$	3.13	0.59	-1.32
$x_5$	11.98	11.45	10.78
$y_5$	-3.13	-6.20	-7.72
$x_6$	5.40	5.94	6.36
$y_6$	-2.12	-3.42	-3.96
$x_7$	5.40	5.50	5.48
$y_7$	-2.12	-3.20	-3.44
$x_8$	4.60	8.07	2.70
$y_8$	-7.53	-8.10	-8.16
$\beta, \text{deg}$	12.13°	27.16°	46.77°

(b) Nozzle details.

Figure 8.- Concluded.

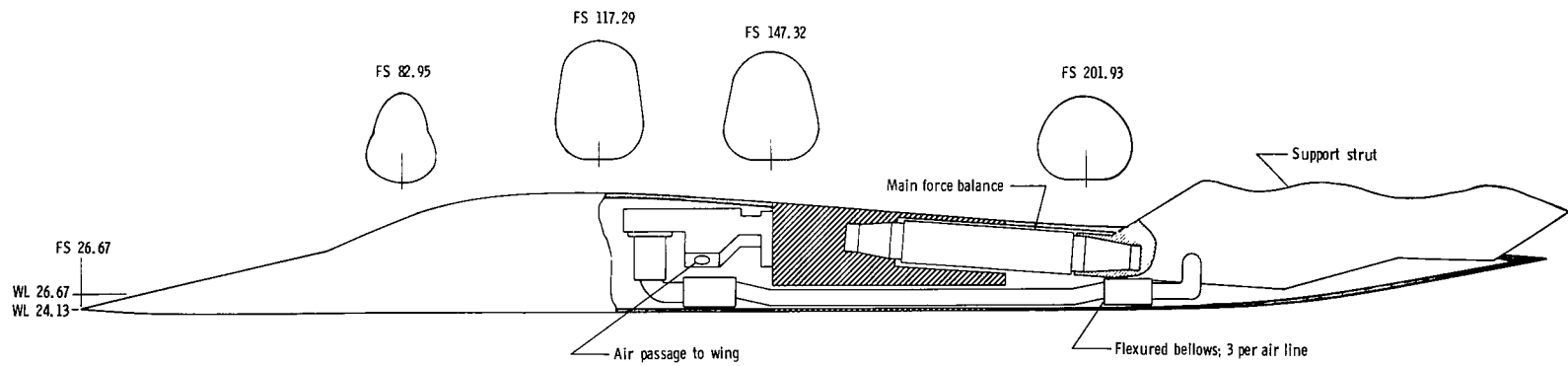


Figure 9.- Sketch showing body arrangement and internal flow hardware. All dimensions are in centimeters unless otherwise noted.

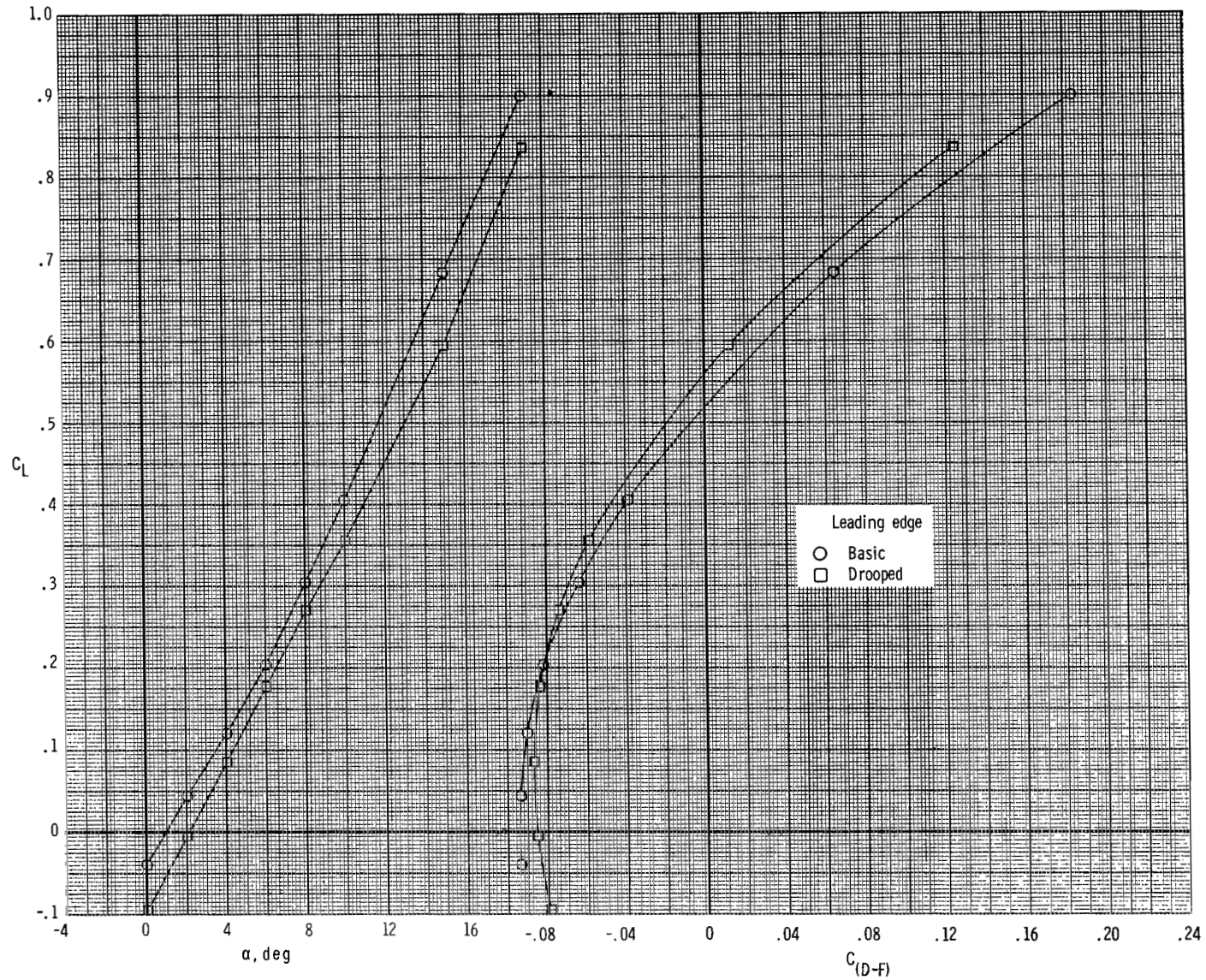
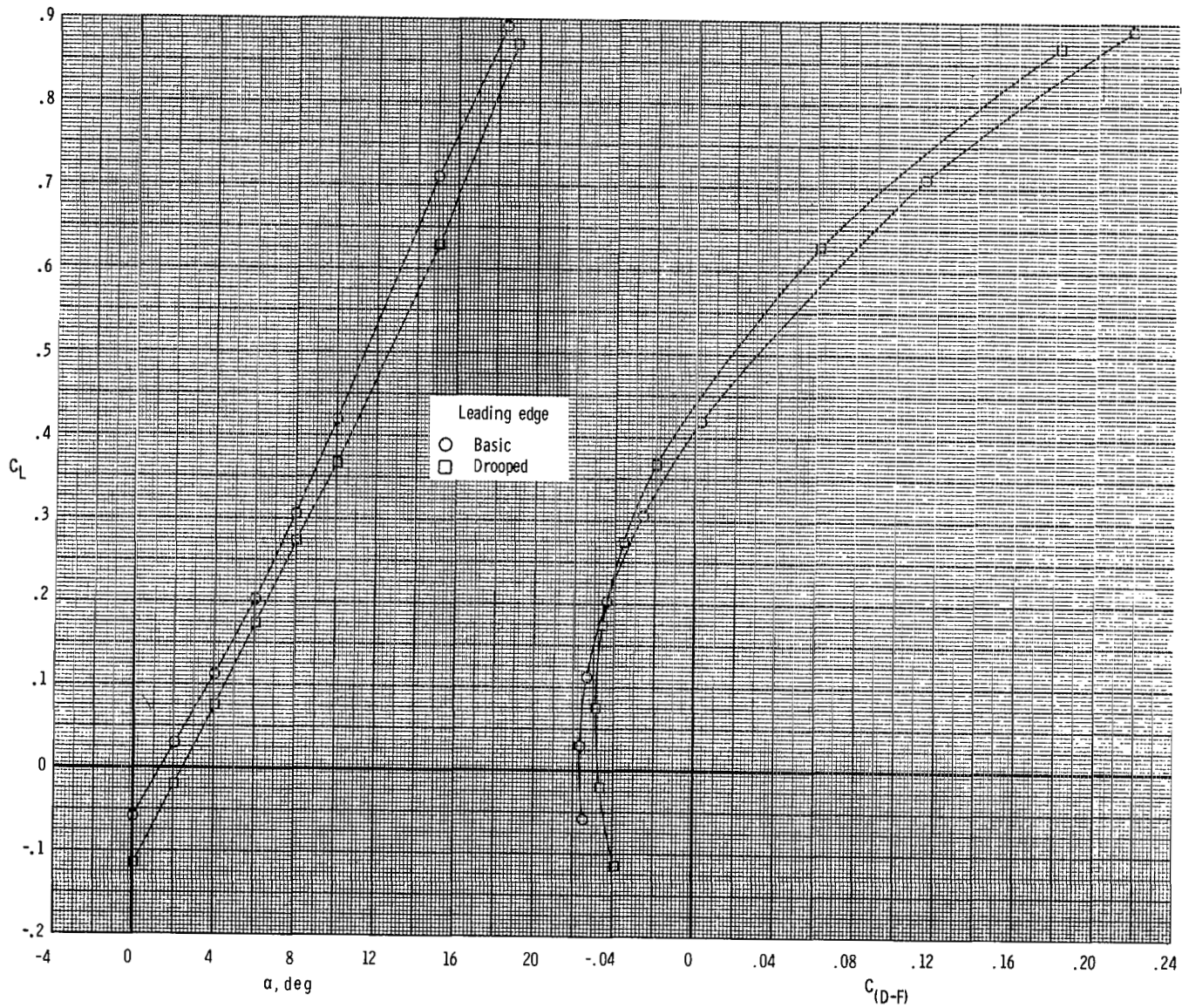
(a)  $M = 0.60$ ,  $NPR = 3.0$ .

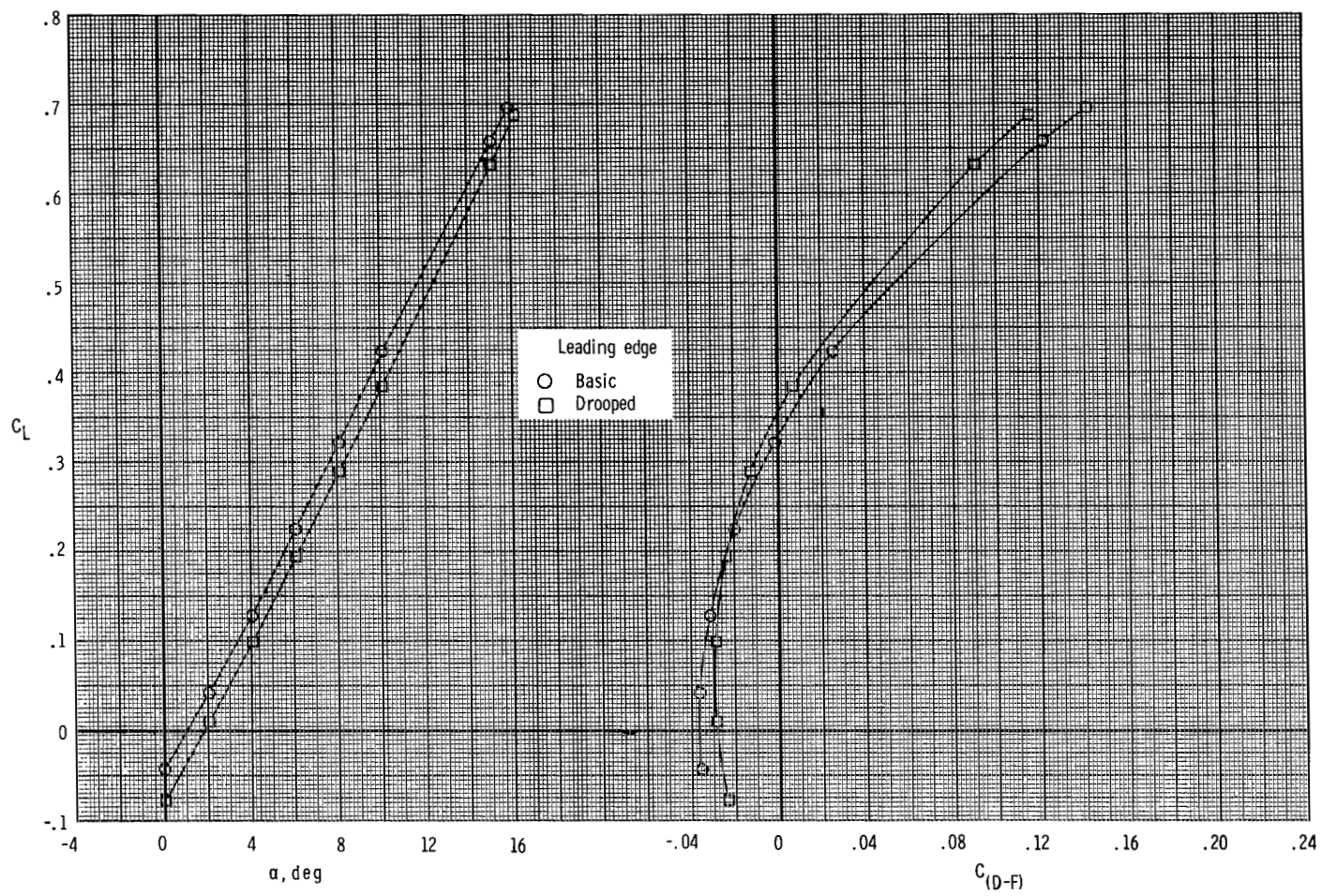
Figure 10.- Effect of drooped leading edge on total aerodynamic characteristics.

$$\delta_v = 15^\circ; \quad \delta_{te} = 0^\circ; \quad \delta_c = 0^\circ.$$



(b)  $M = 0.87$ ,  $NPR = 3.9$ .

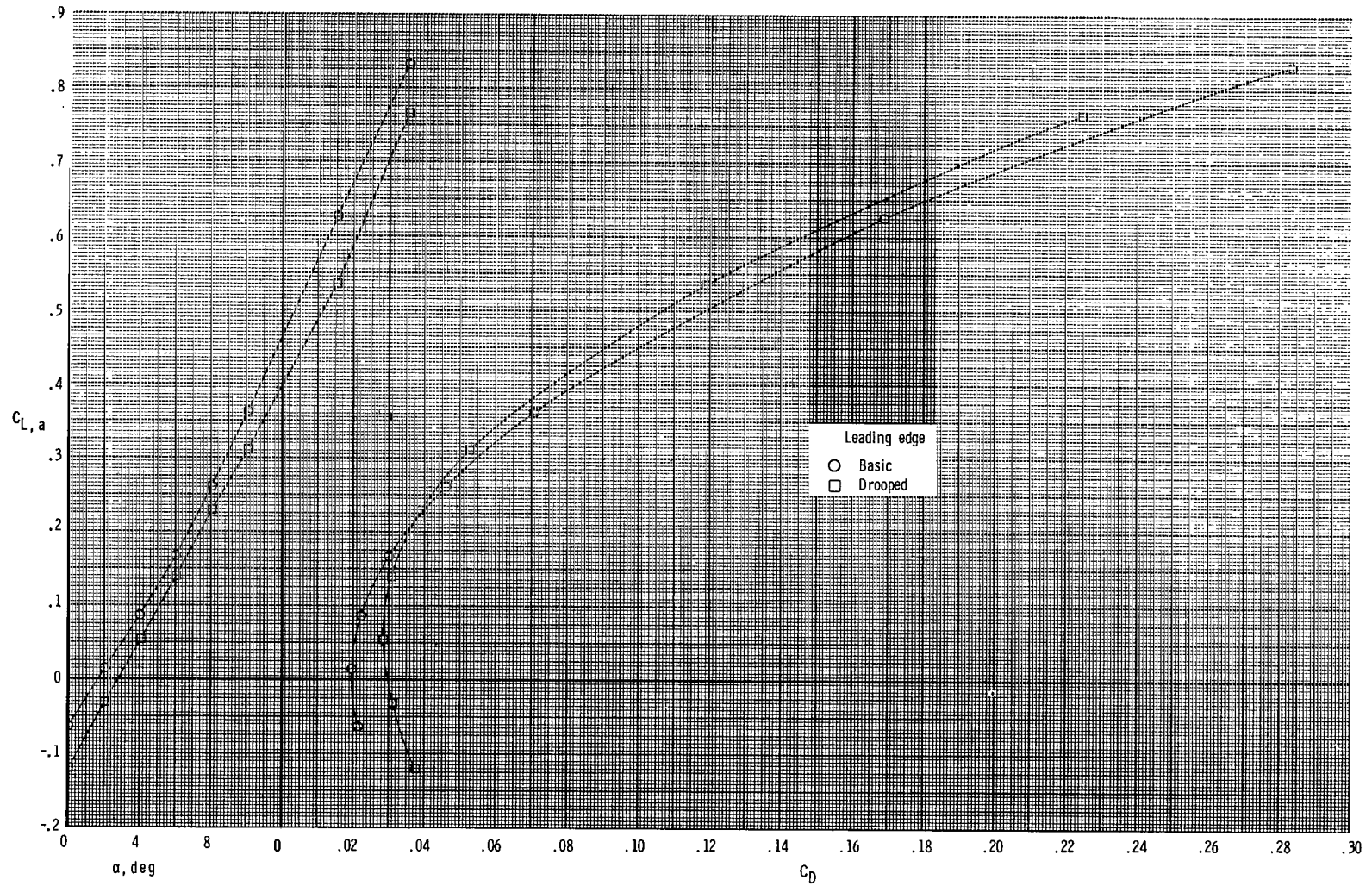
Figure 10.- Continued.



(c)  $M = 1.20$ ,  $NPR = 6.6$ .

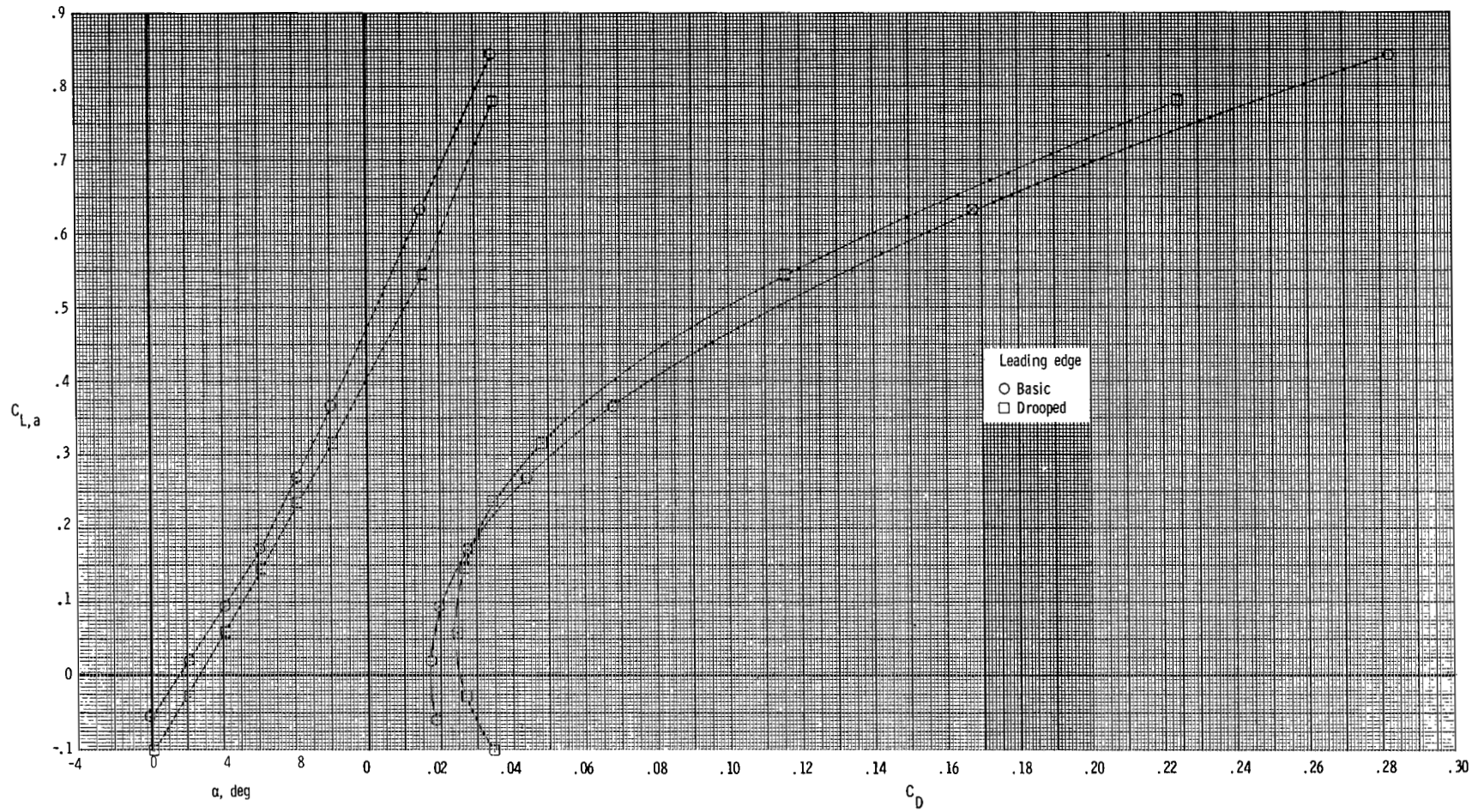
Figure 10.- Concluded.





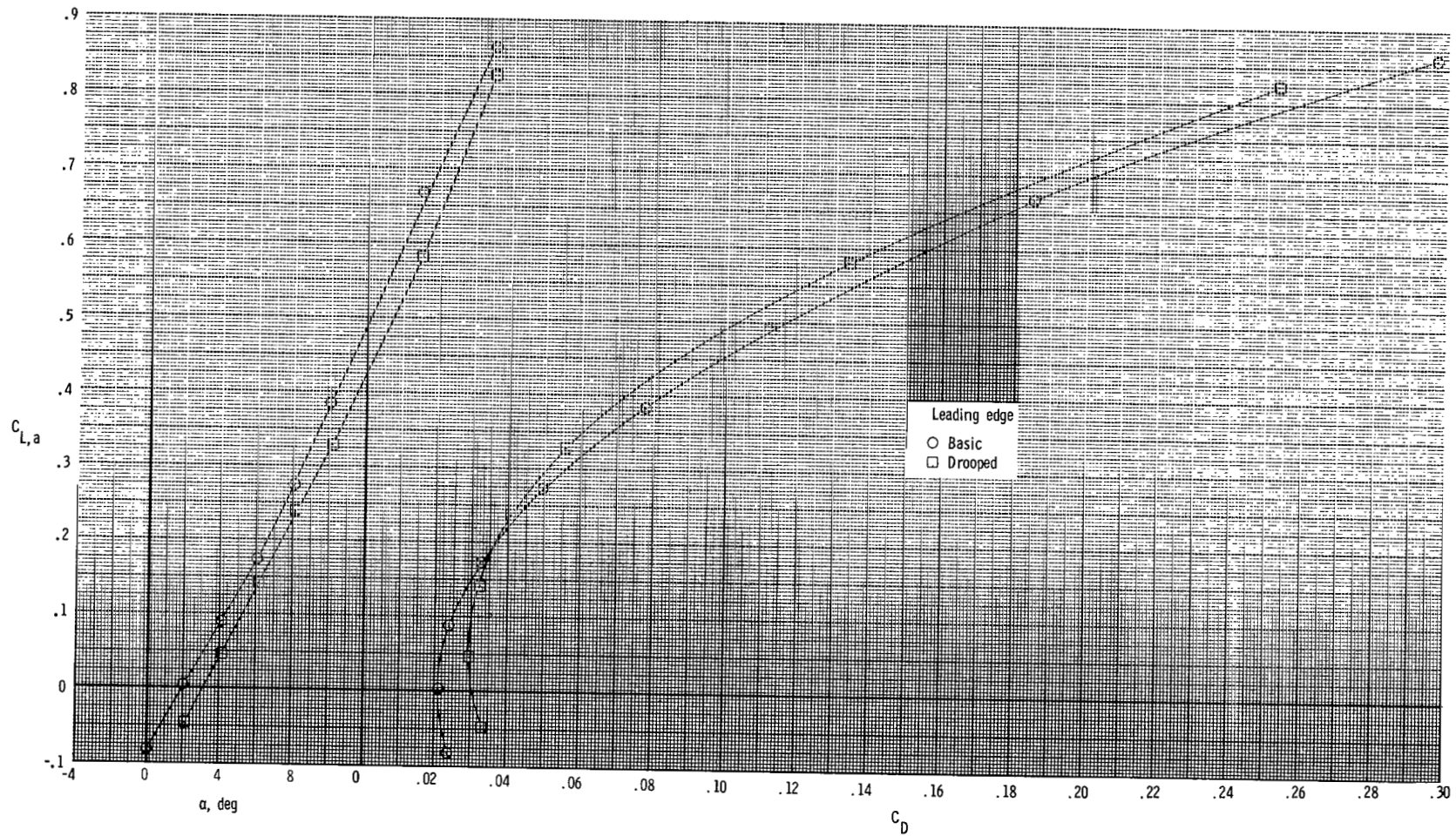
(a)  $M = 0.60$ ,  $NPR = 1.0$ .

Figure 11.- Effect of drooped leading edge on thrust-removed aerodynamic characteristics.  $\delta_v = 15^\circ$ ;  $\delta_{te} = 0^\circ$ ;  $\delta_c = 0^\circ$ .



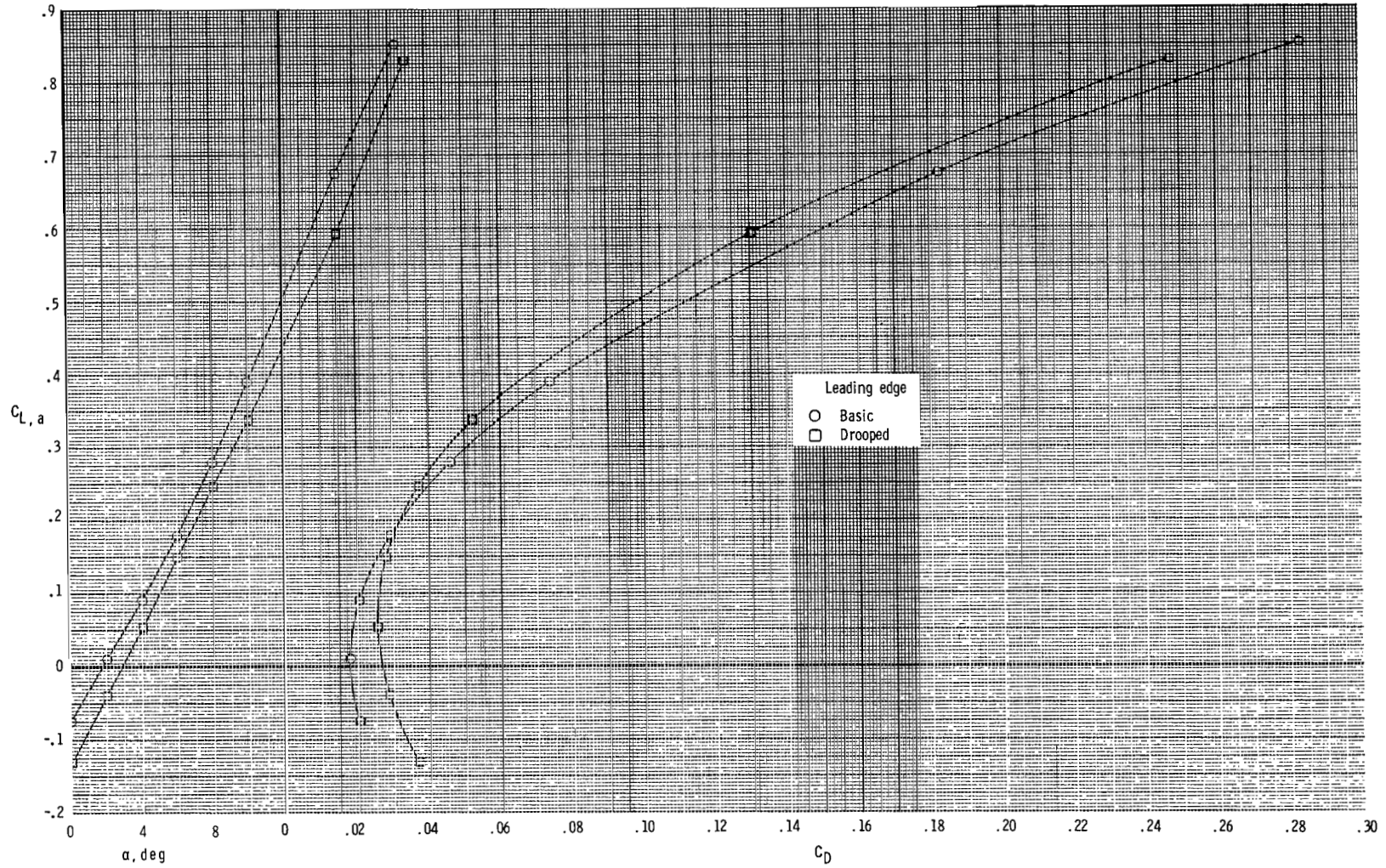
(b)  $M = 0.60$ ,  $NPR = 3.0$ .

Figure 11.- Continued.



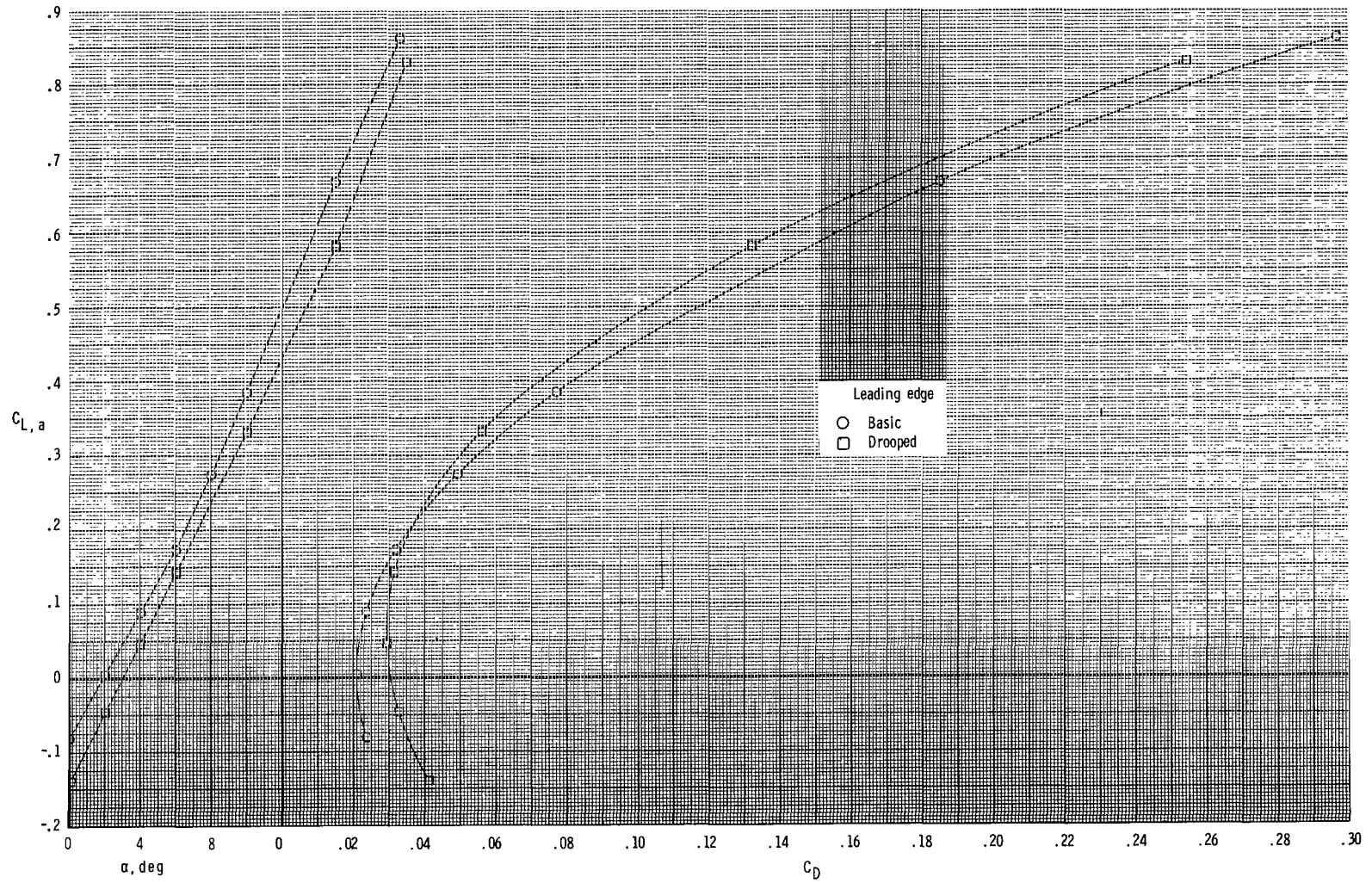
(c)  $M = 0.87$ ,  $NPR = 1.0$ .

Figure 11.- Continued.



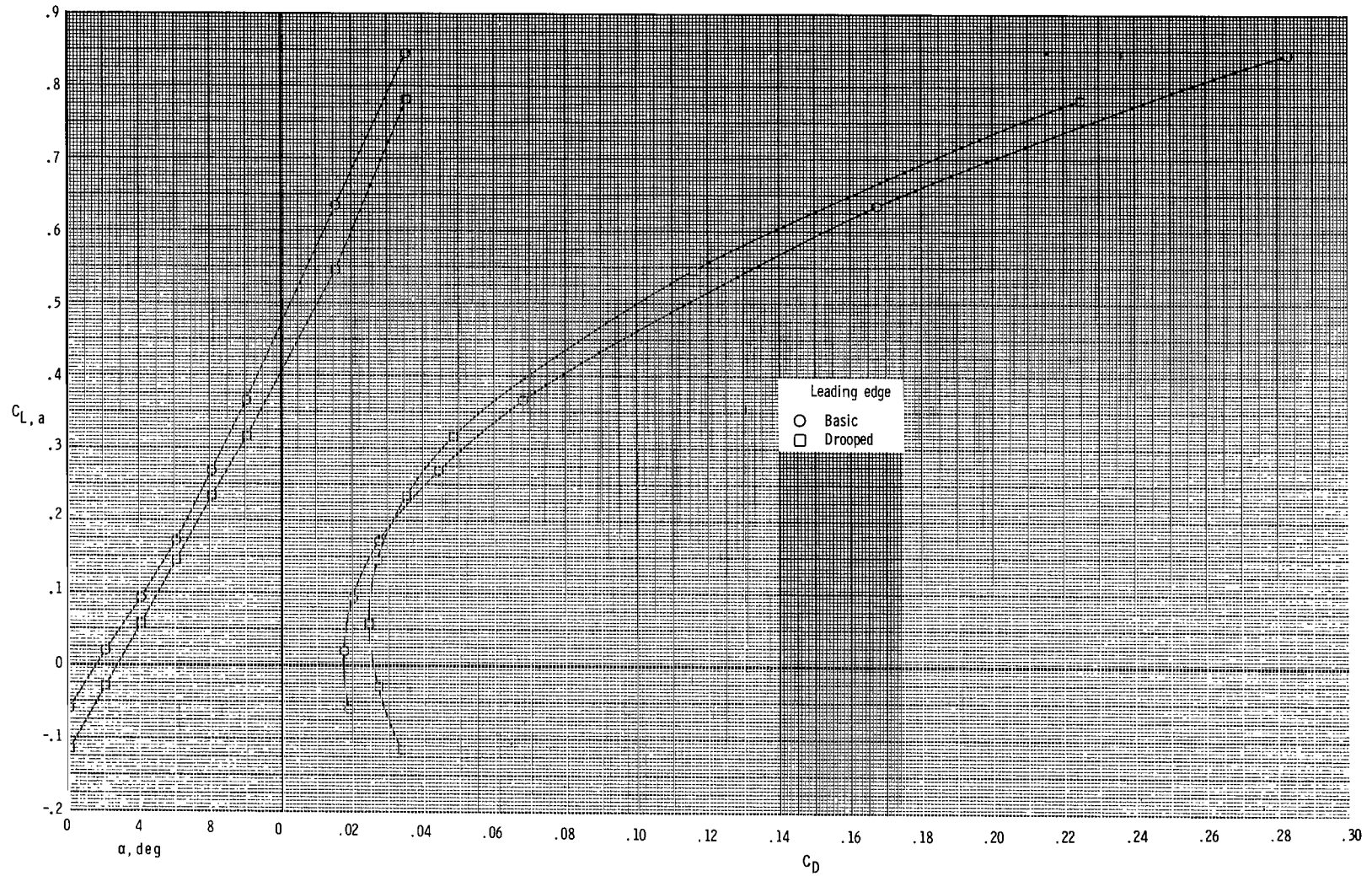
(d)  $M = 0.87$ ,  $NPR = 3.9$ .

Figure 11.- Continued.



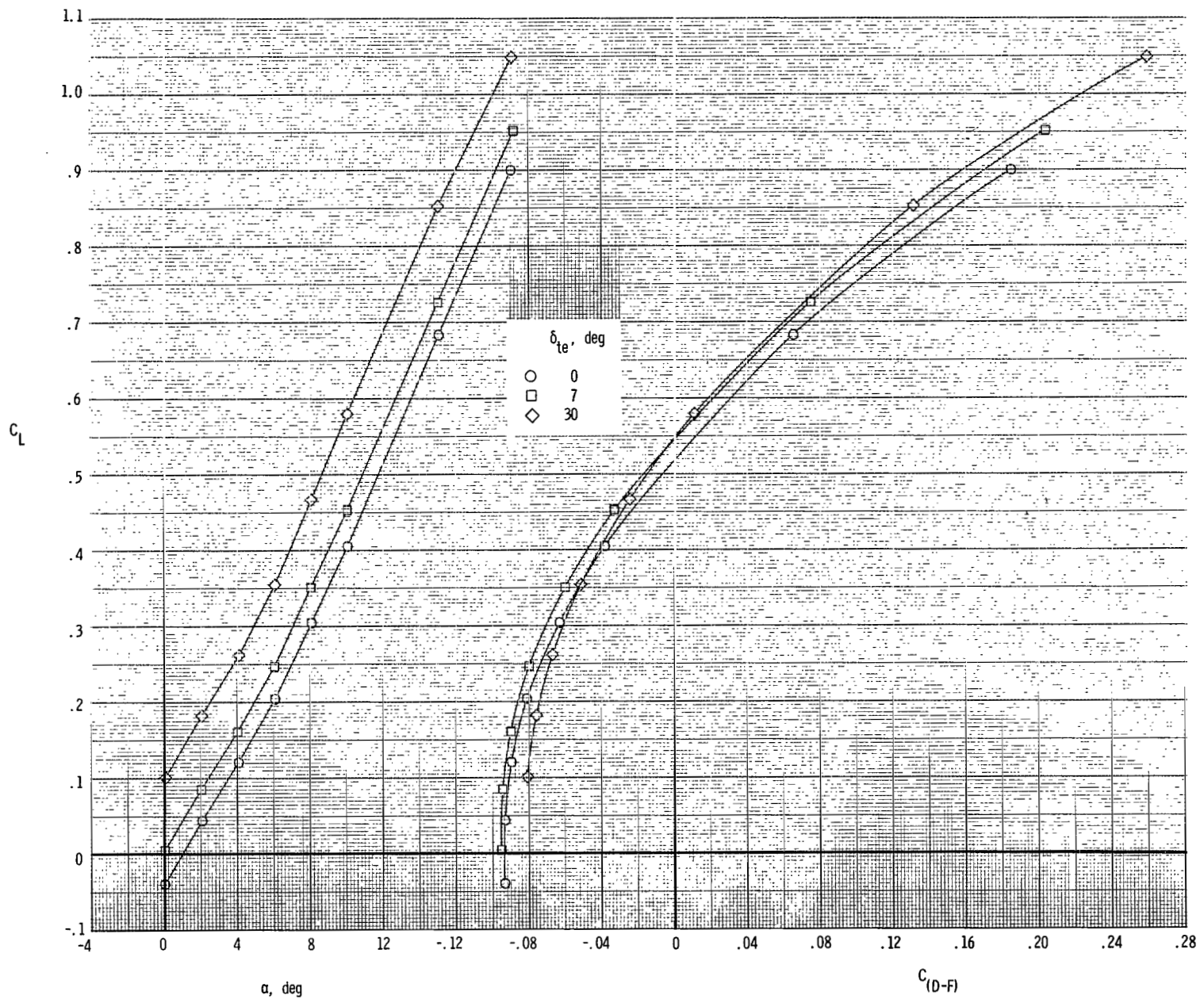
(e)  $M = 1.20$ ,  $NPR = 1.0$ .

Figure 11.- Continued.



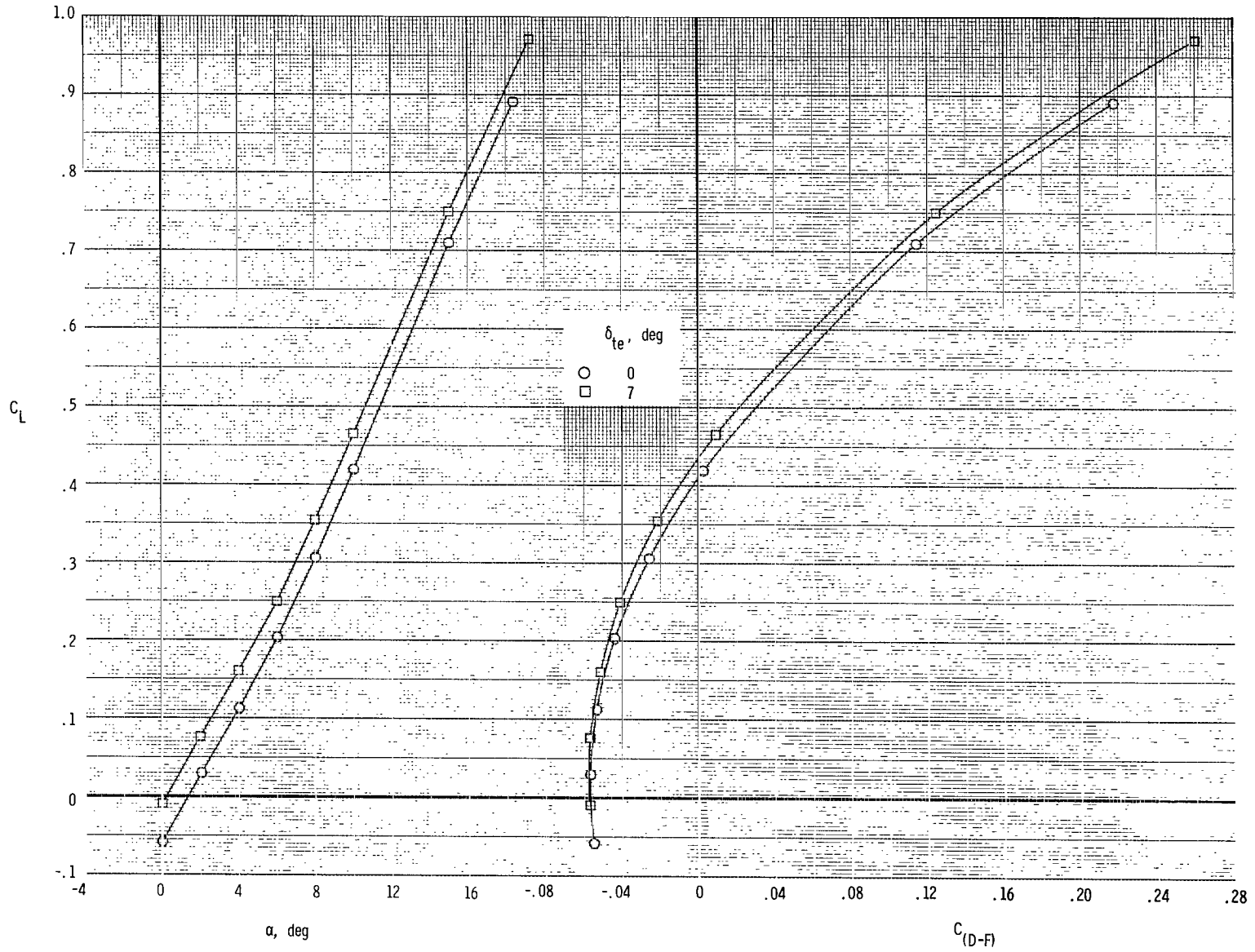
(f)  $M = 1.20$ ,  $NPR = 6.6$ .

Figure 11.- Concluded.



(a)  $M = 0.60$ ,  $NPR = 3.0$ .

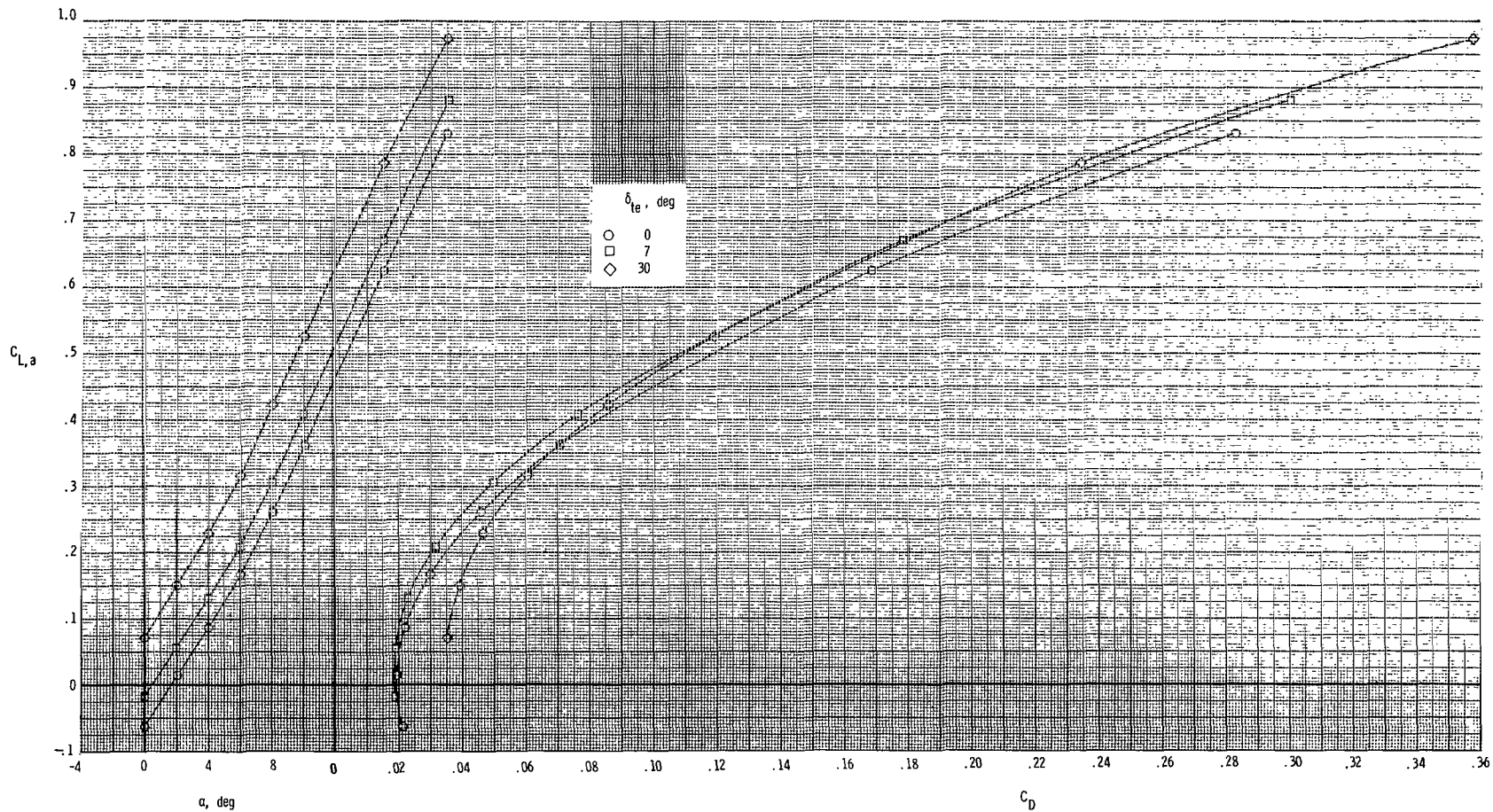
Figure 12.- Effect of trailing-edge flap deflection on total aerodynamic characteristics.  
 $\delta_v = 15^\circ$ ; basic LE;  $\delta_c = 0^\circ$ .



(b)  $M = 0.87$ ,  $NPR = 3.9$ .

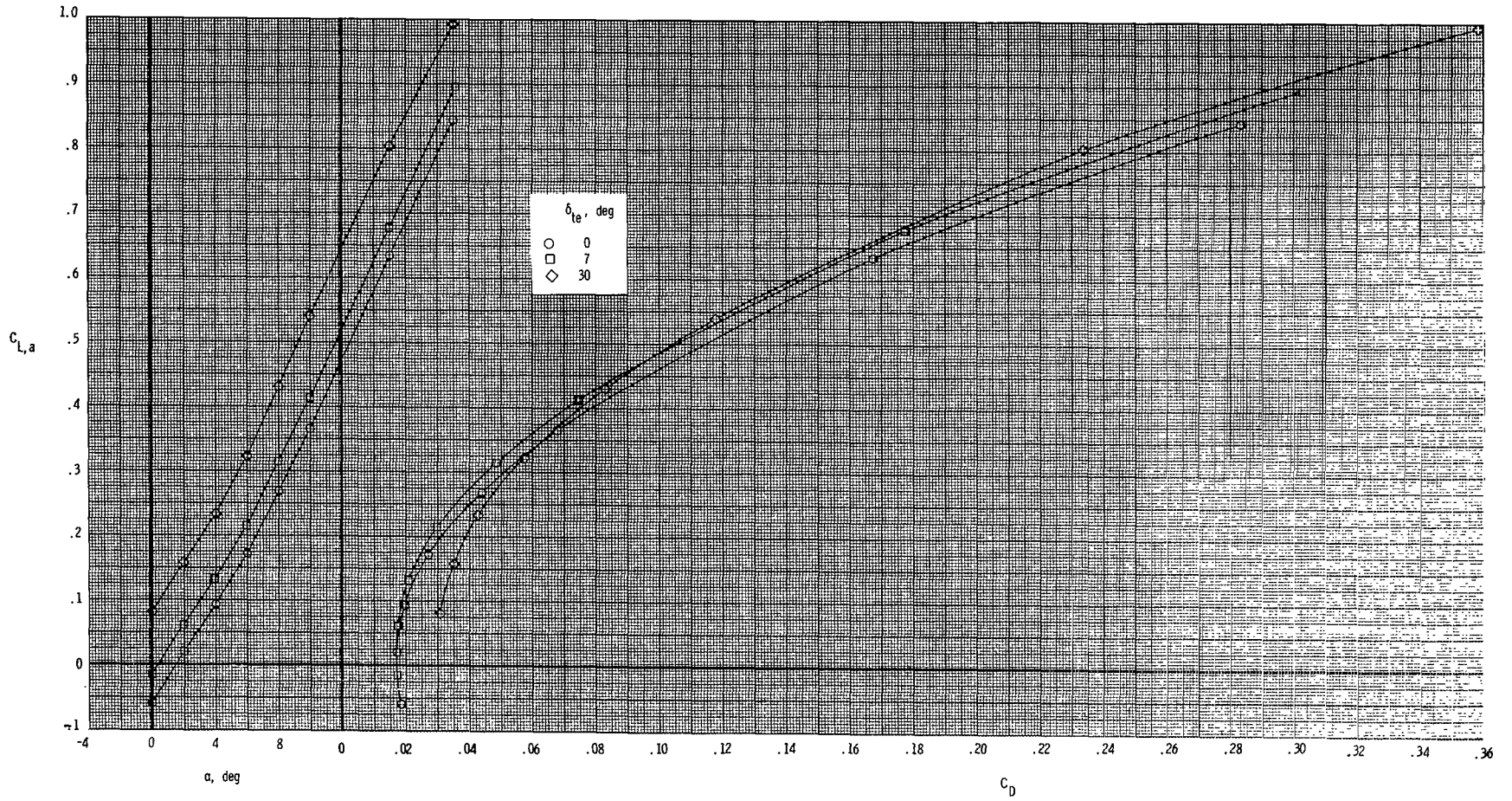
Figure 12.- Concluded.





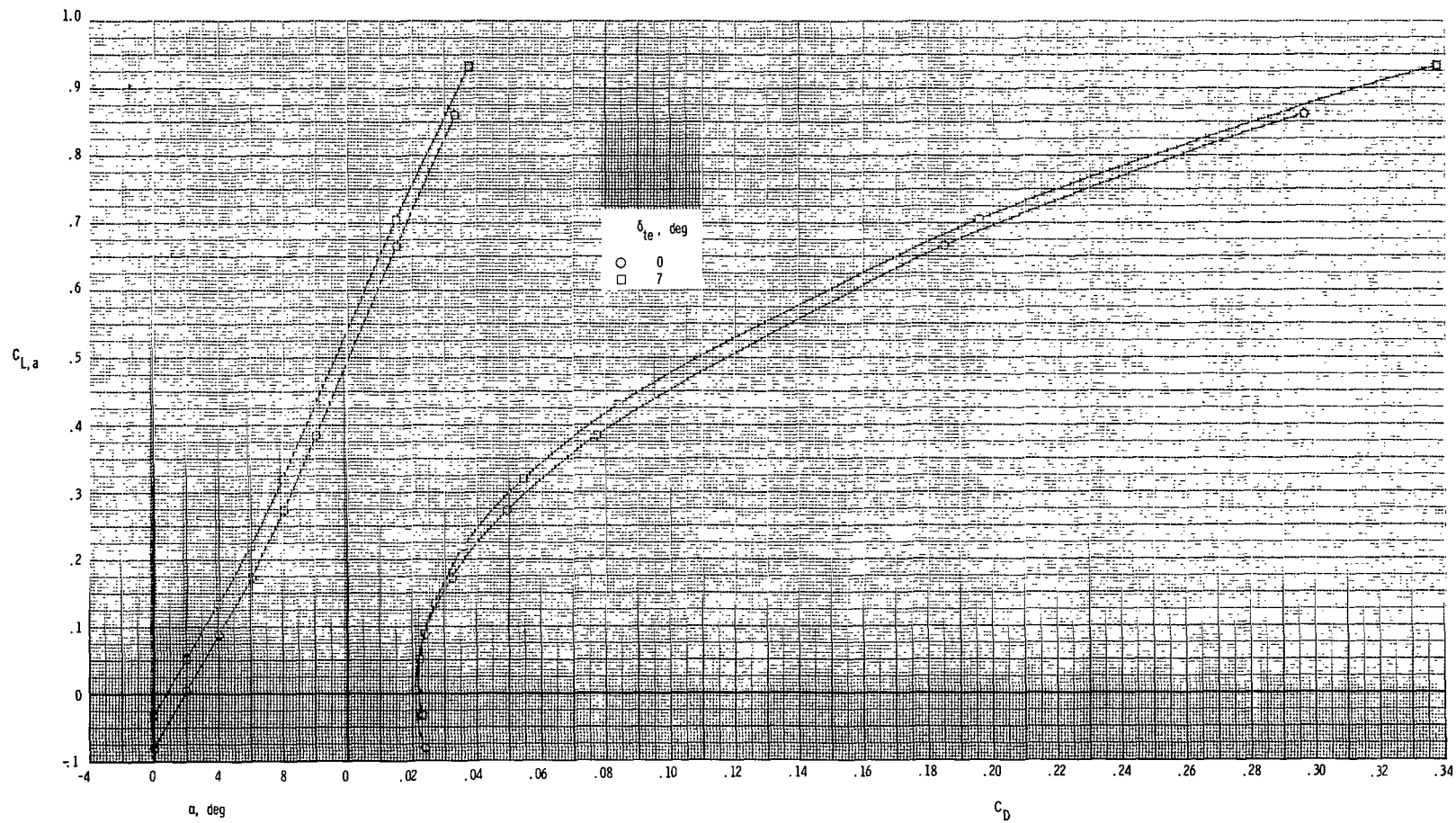
(a)  $M = 0.60$ ,  $NPR = 1.0$ .

Figure 13.- Effect of trailing-edge flap deflection on thrust-removed aerodynamic characteristics.  $\delta_v = 15^\circ$ ; basic LE;  $\delta_c = 0^\circ$ .



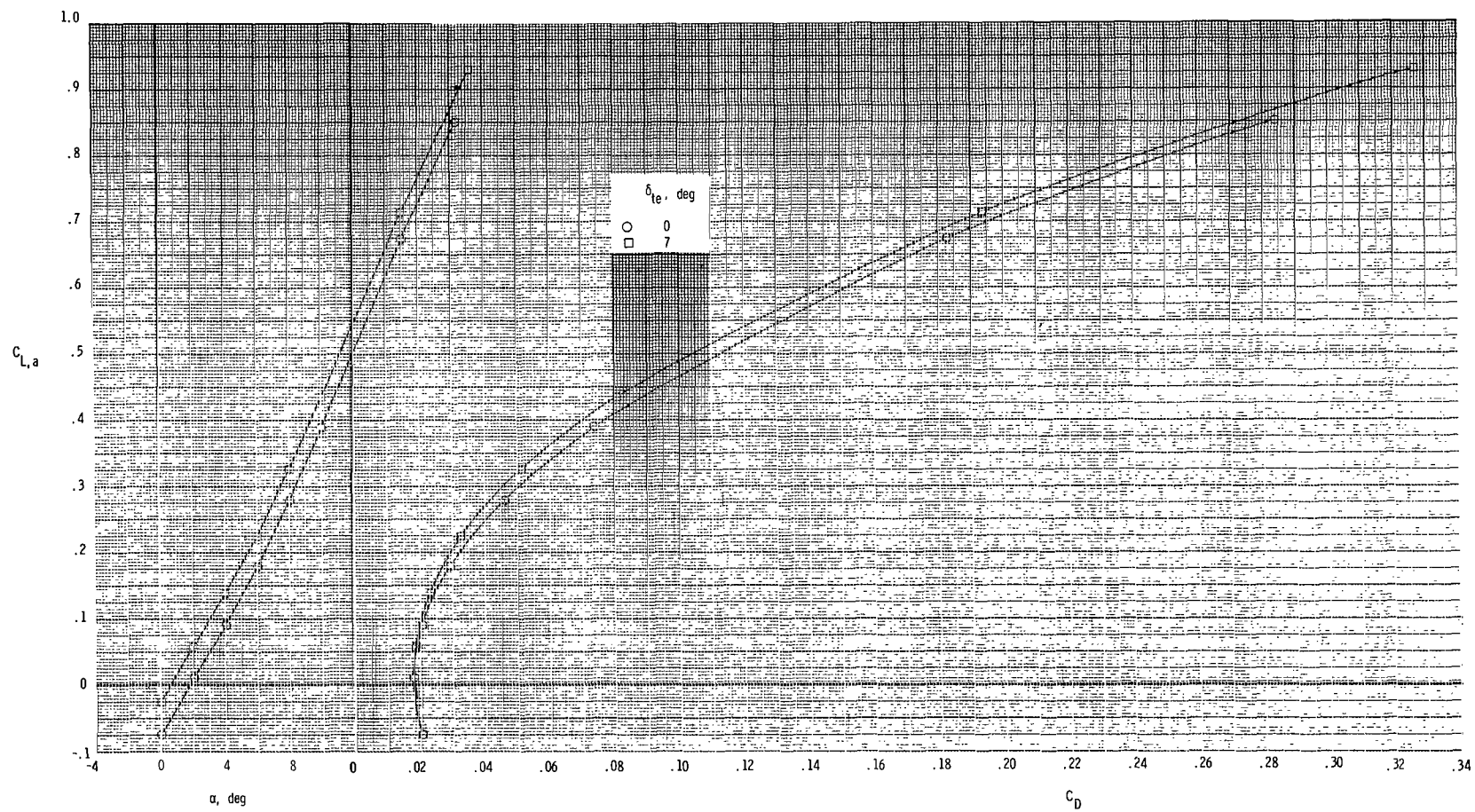
(b)  $M = 0.60, NPR = 3.0.$

Figure 13.- Continued.



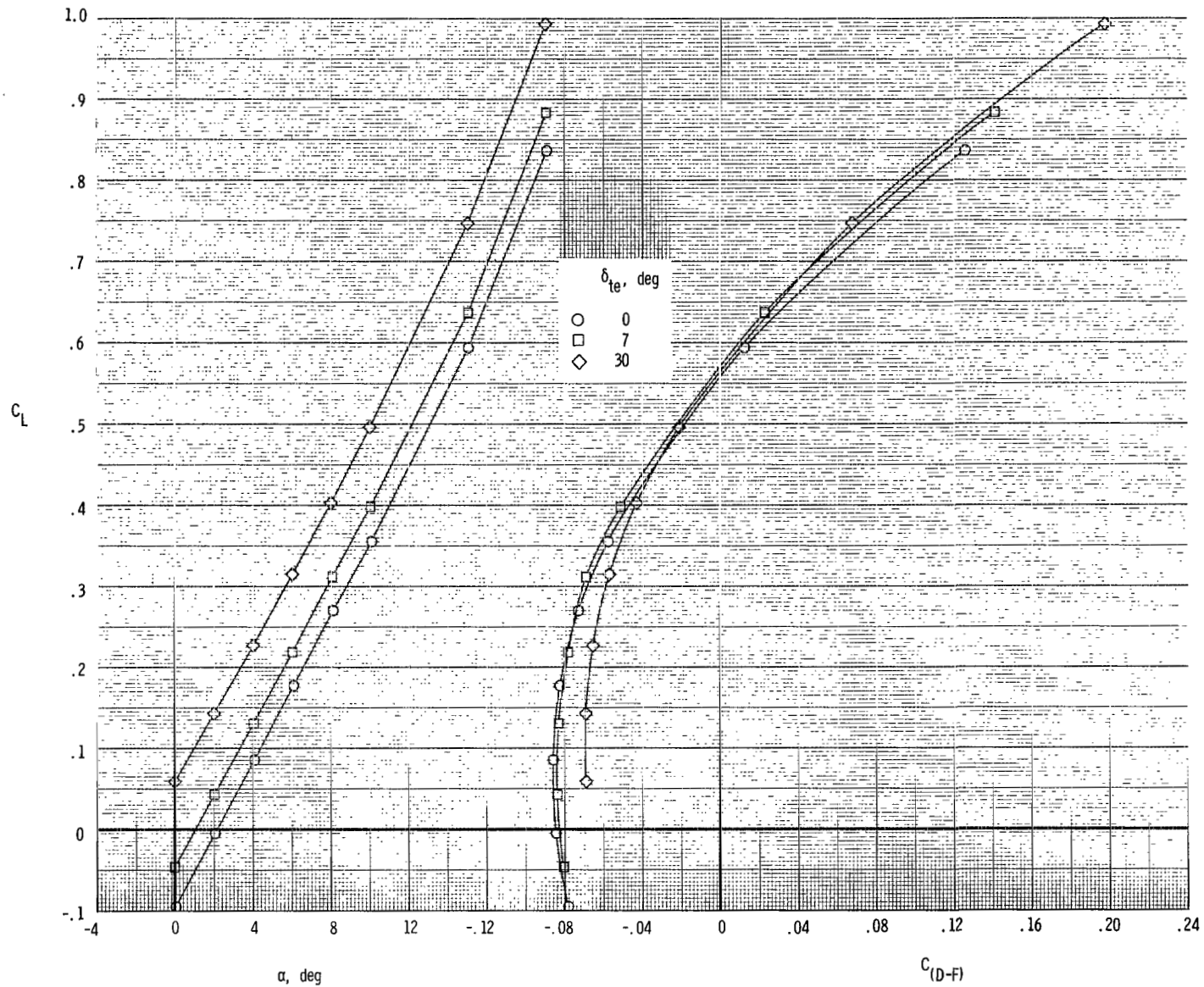
(c)  $M = 0.87$ ,  $NPR = 1.0$ .

Figure 13.- Continued.



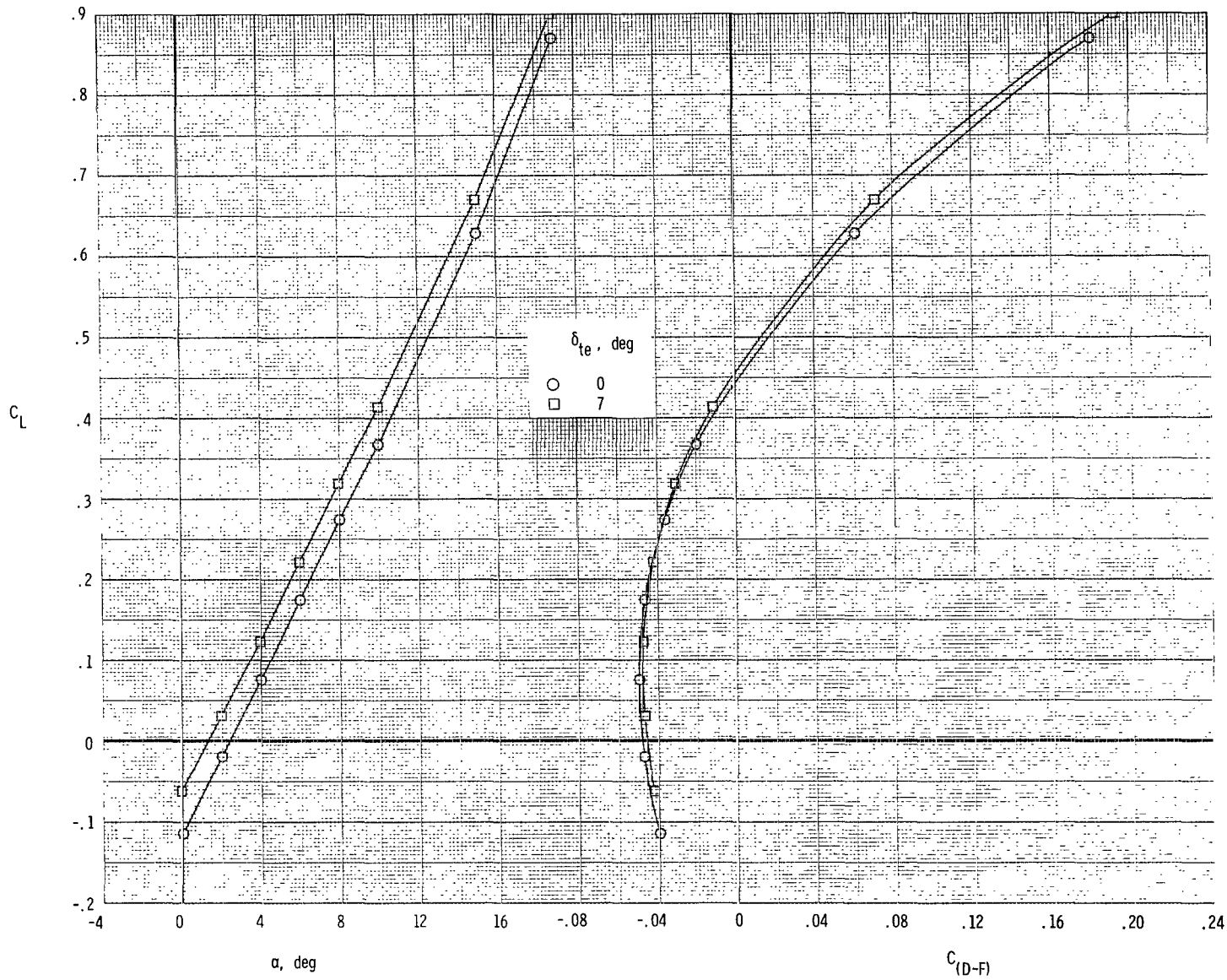
(d)  $M = 0.87$ ,  $NPR = 3.9$ .

Figure 13.- Concluded.



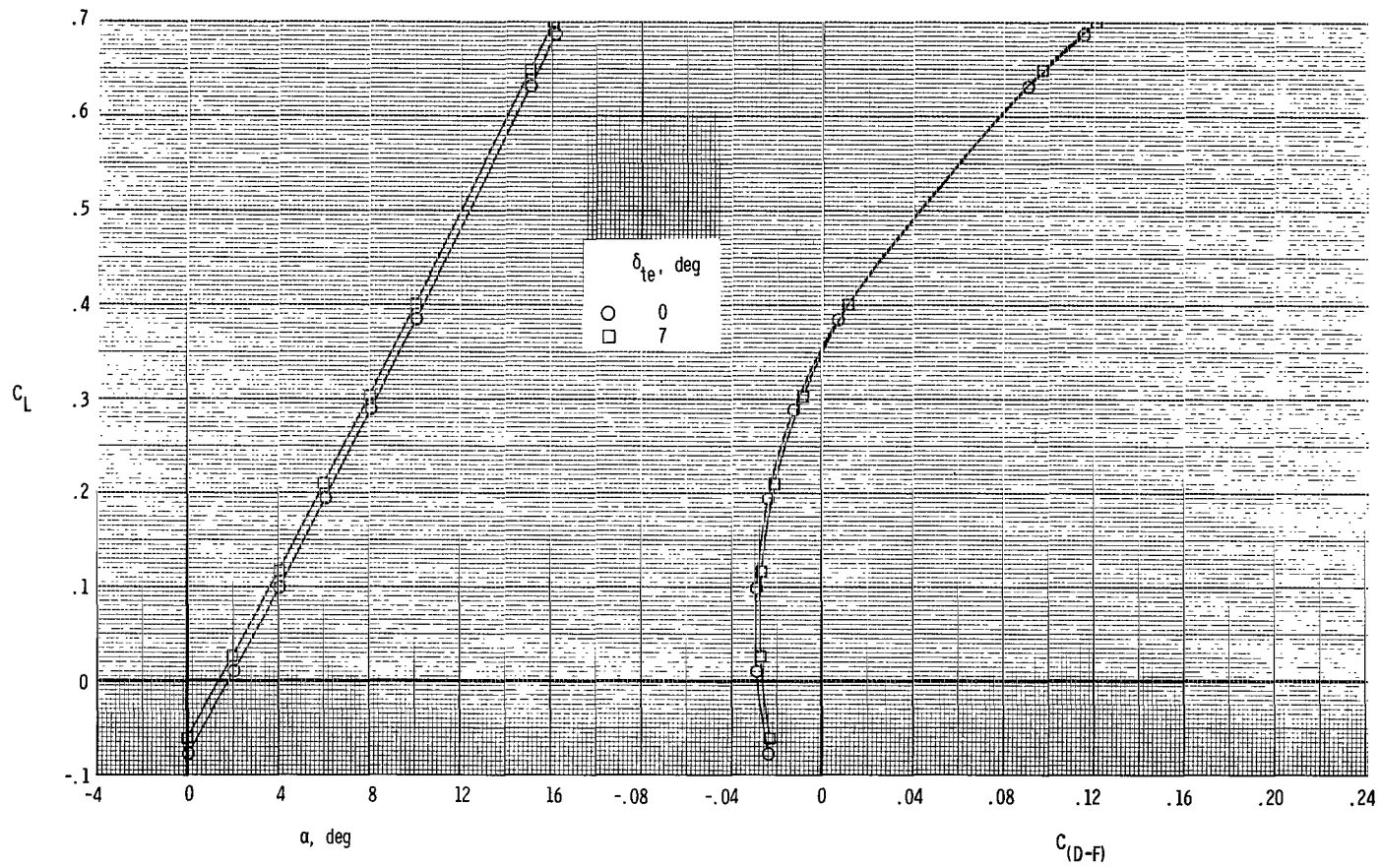
(a)  $M = 0.60$ ,  $NPR = 3.0$ .

Figure 14.- Effect of trailing-edge flap deflection on total aerodynamic characteristics.  $\delta_v = 15^\circ$ ; drooped LE;  $\delta_c = 0^\circ$ .



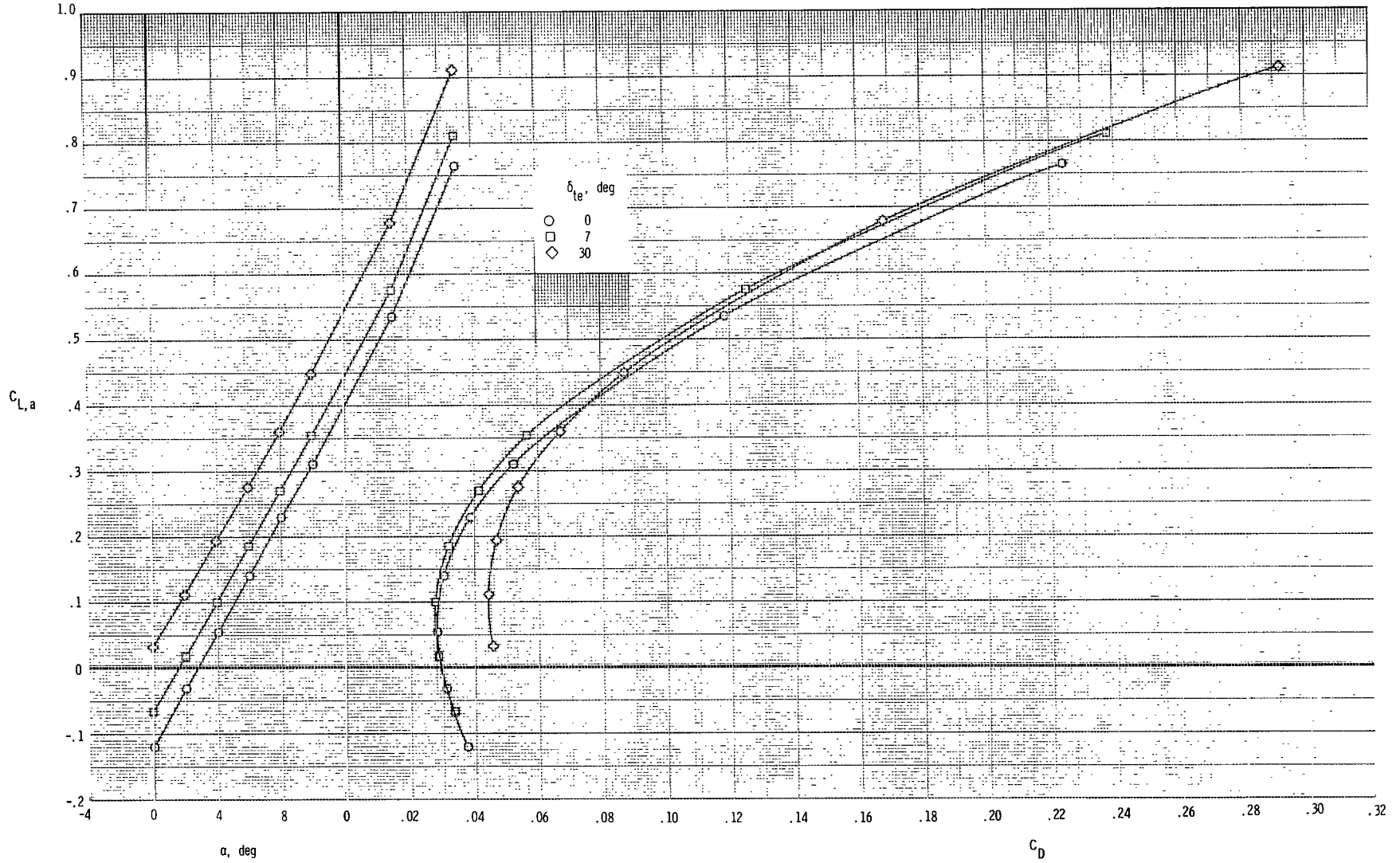
(b)  $M = 0.87$ ,  $NPR = 3.9$ .

Figure 14.- Continued.



(c)  $M = 1.20$ ,  $NPR = 6.6$ .

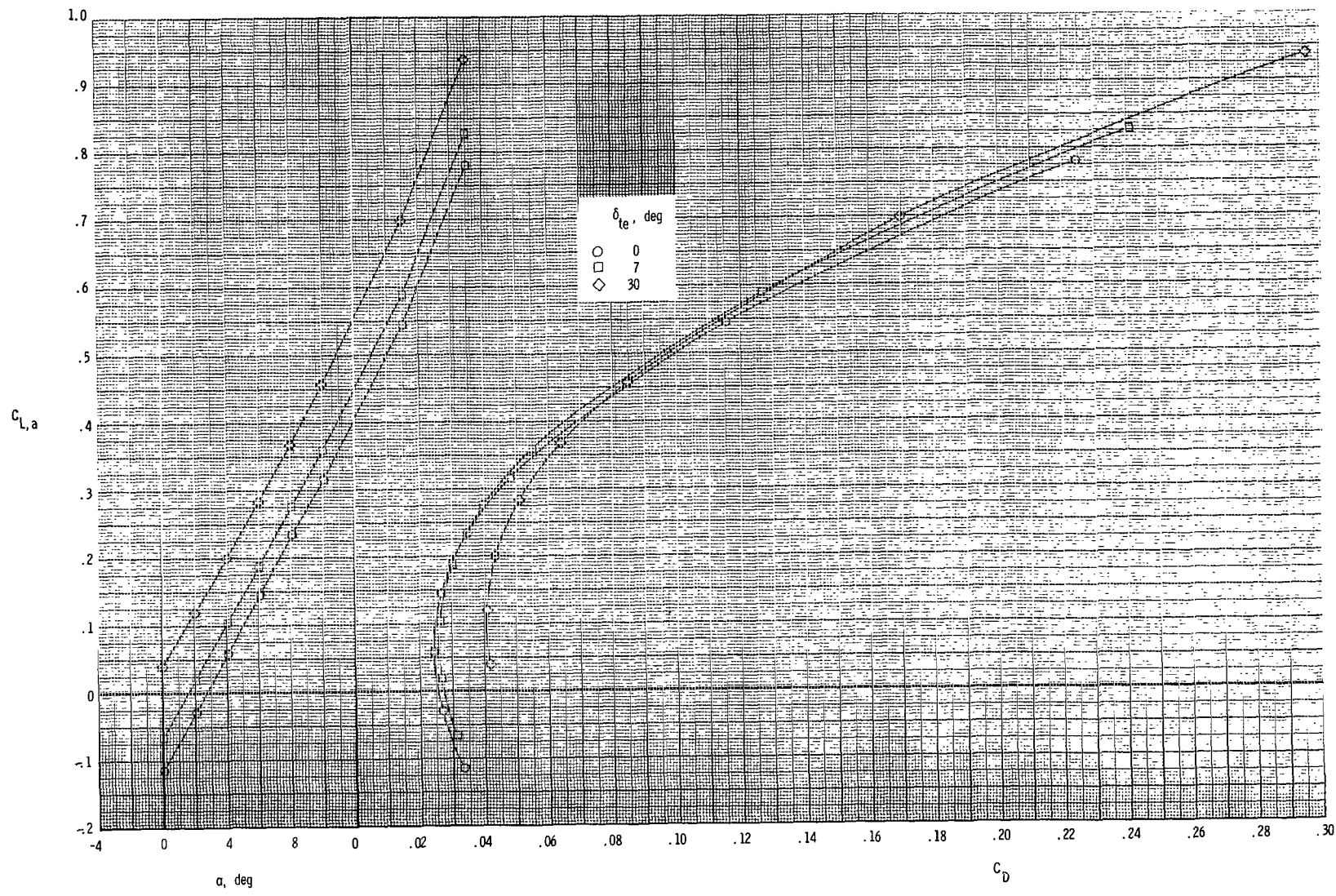
Figure 14.- Concluded.



(a)  $M = 0.60$ ,  $NPR = 1.0$ .

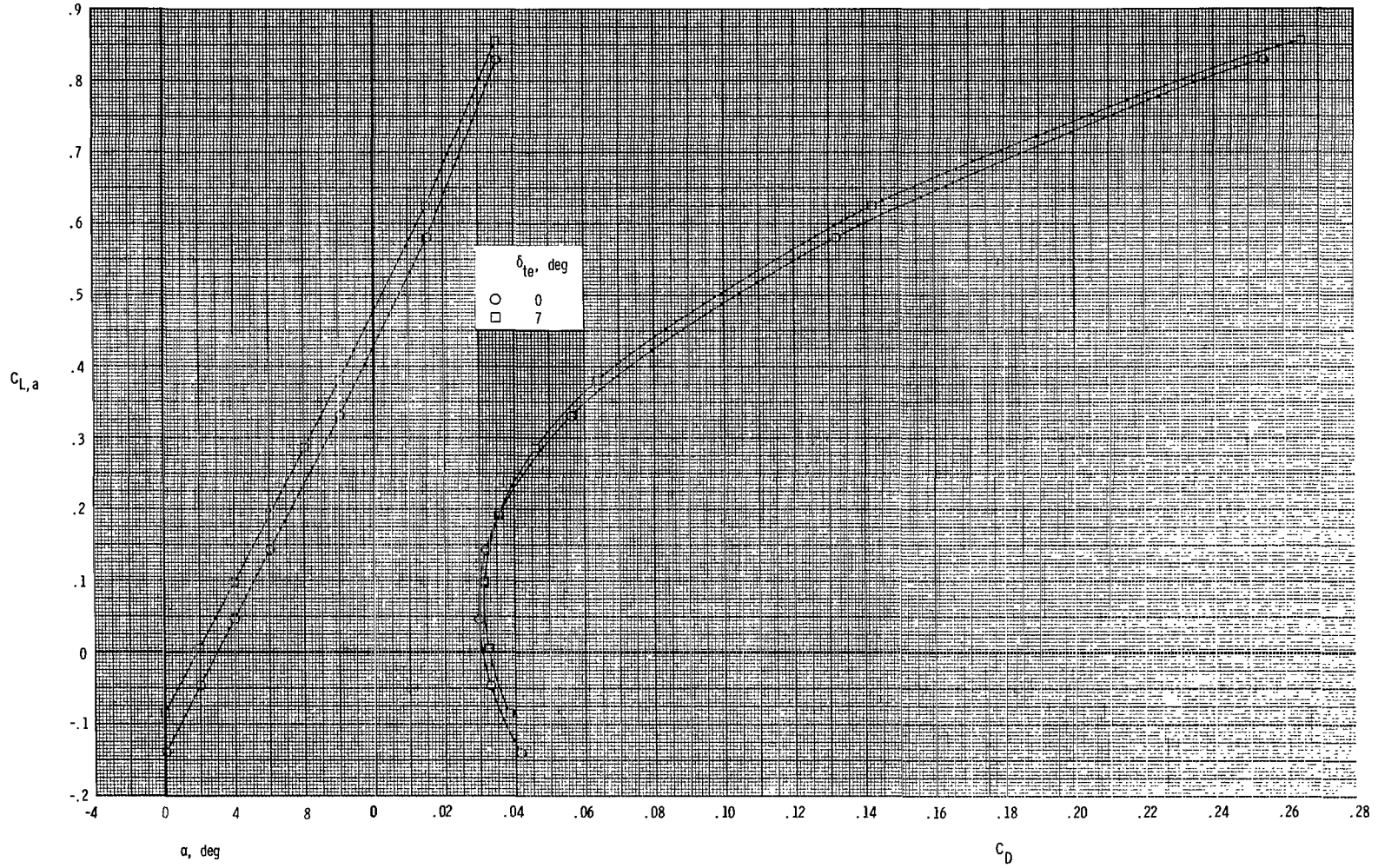
Figure 15.- Effect of trailing-edge flap deflection on thrust-removed aerodynamic characteristics.  $\delta_v = 15^\circ$ ; drooped LE;  $\delta_c = 0^\circ$ .





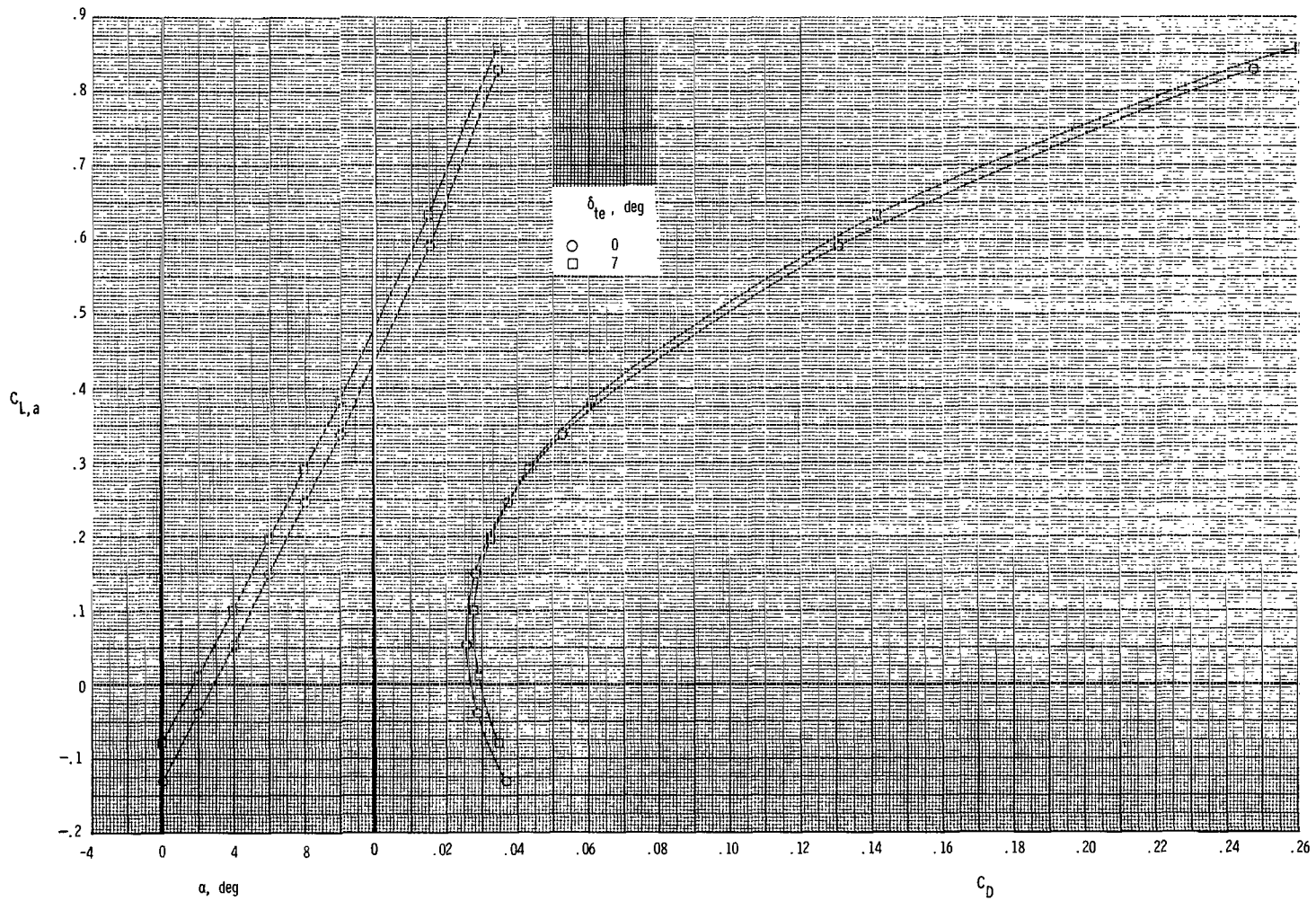
(b)  $M = 0.60$ ,  $NPR = 3.0$ .

Figure 15.- Continued.



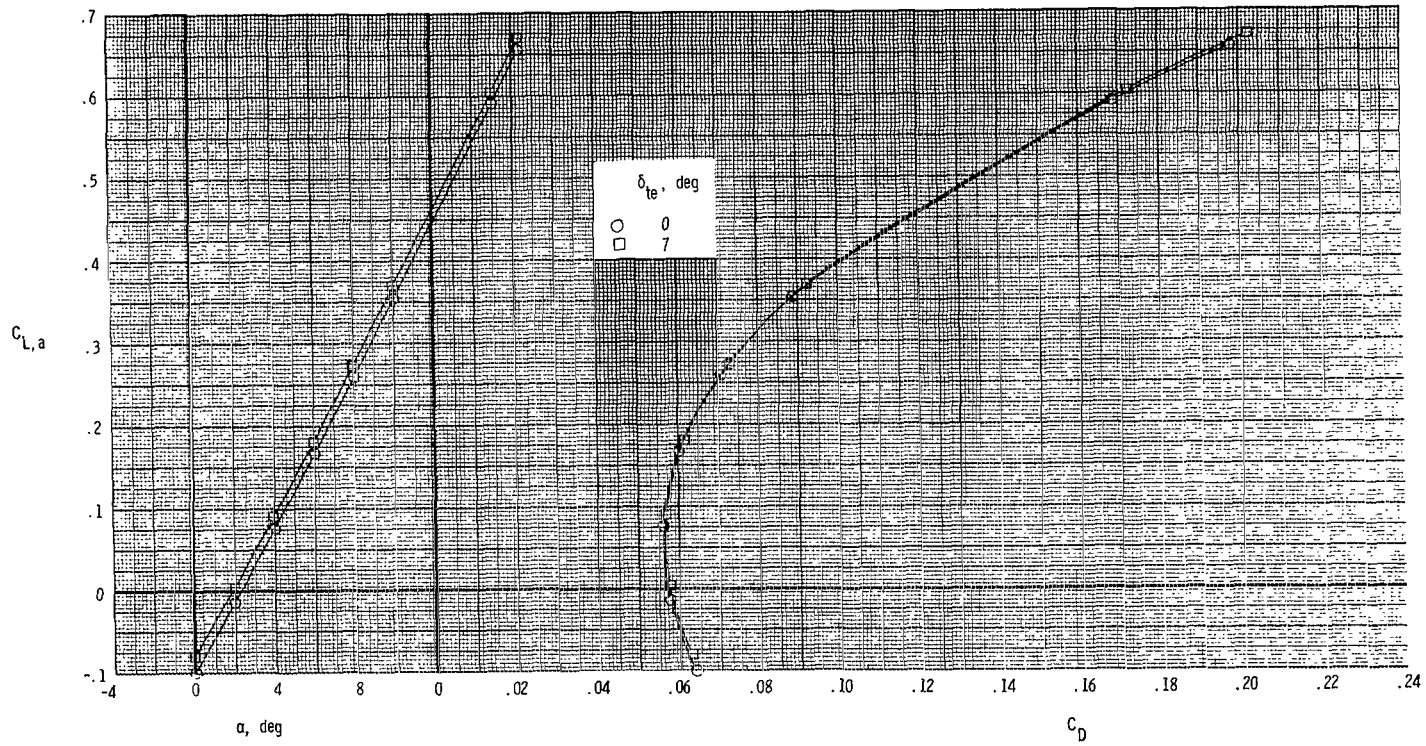
(c)  $M = 0.87, NPR = 1.0.$

Figure 15.- Continued.



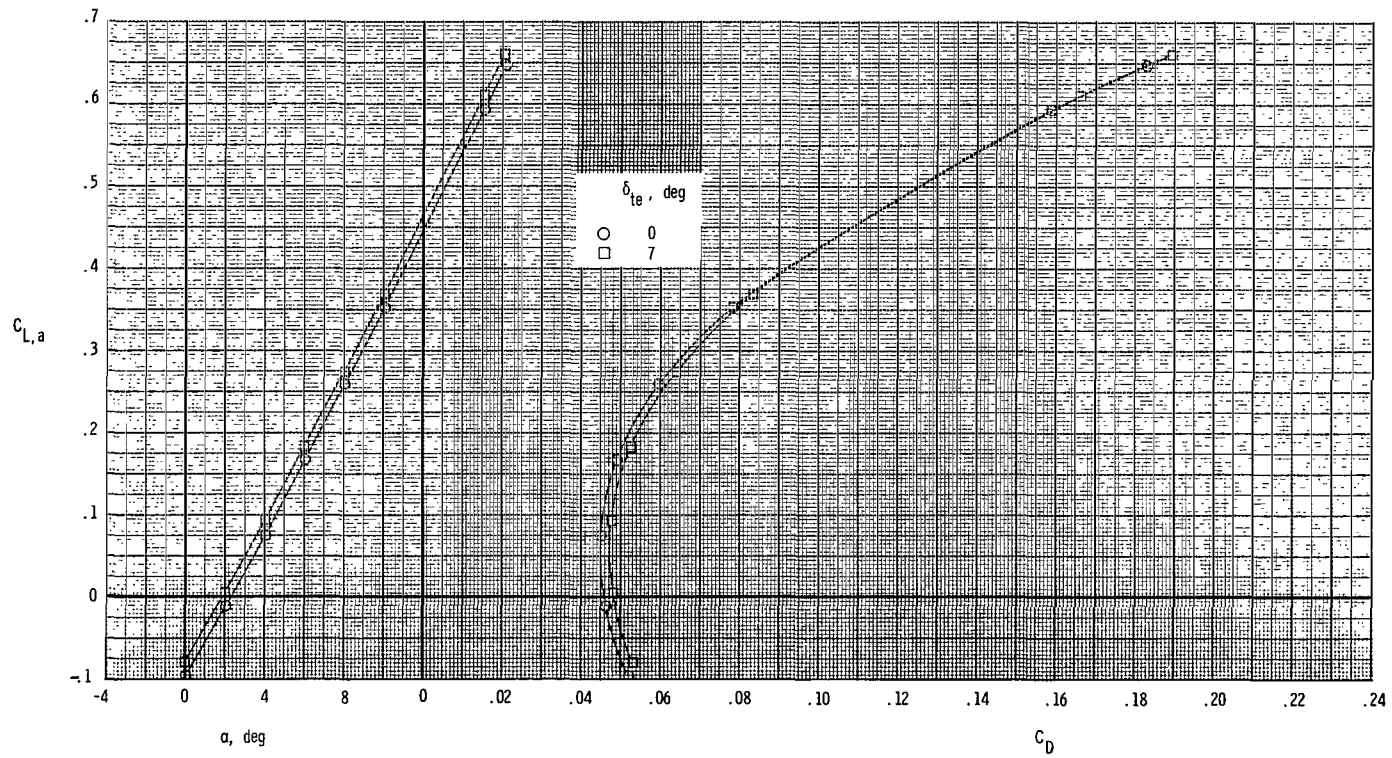
(d)  $M = 0.87$ ,  $NPR = 3.9$ .

Figure 15.- Continued.



(e)  $M = 1.20$ ,  $NPR = 1.0$ .

Figure 15.- Continued.



(f)  $M = 1.20$ ,  $NPR = 6.6$ .

Figure 15.- Concluded.

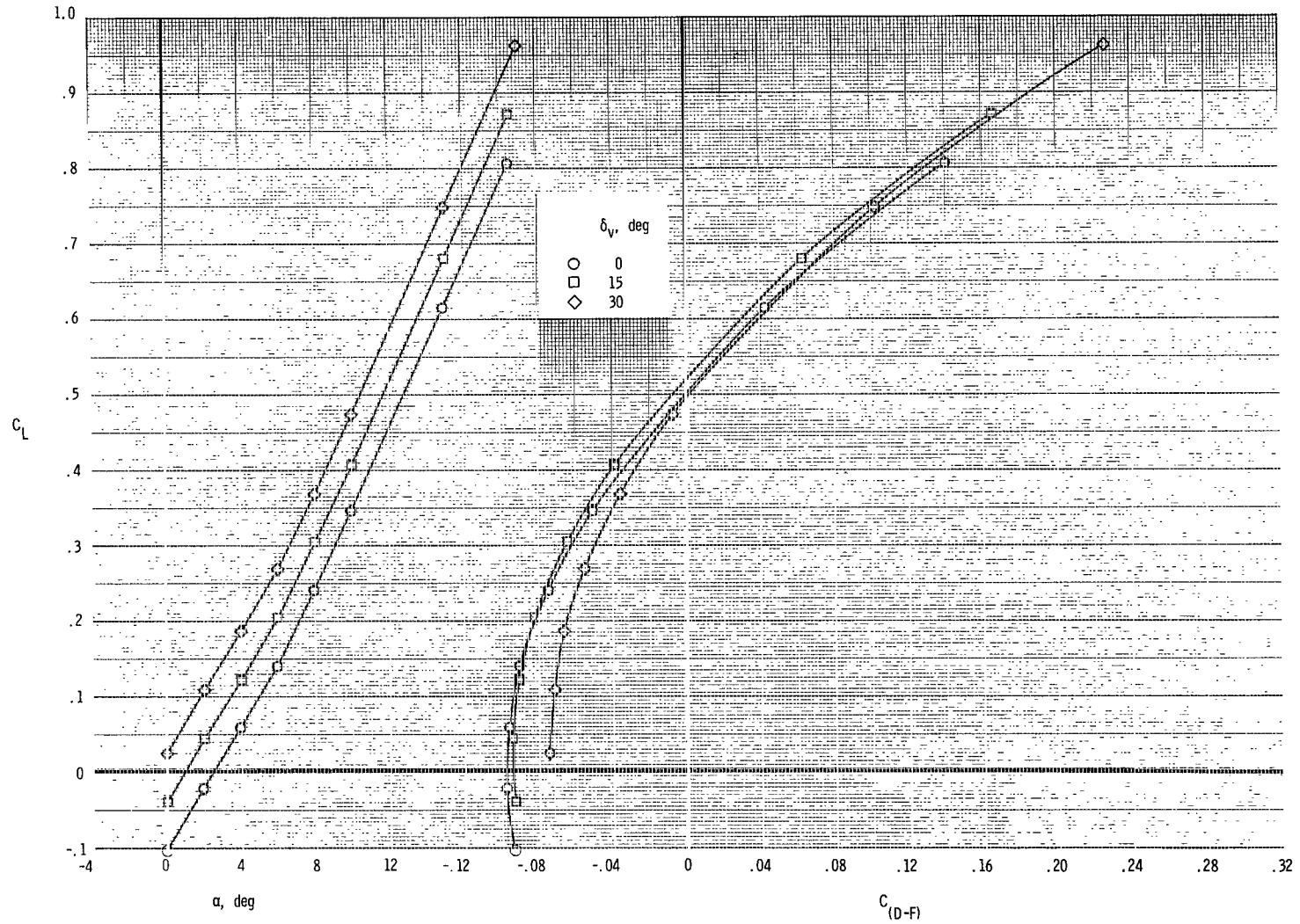
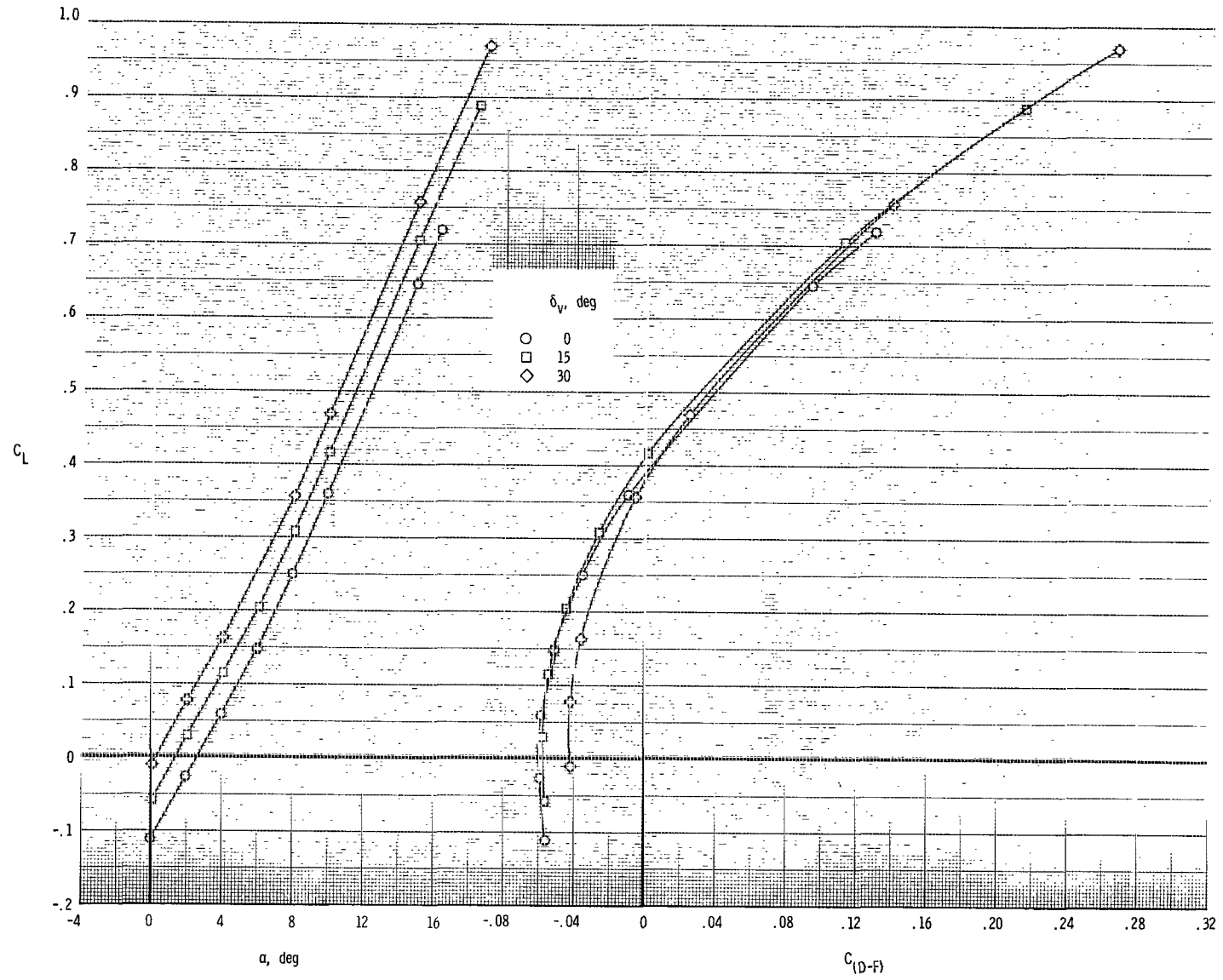
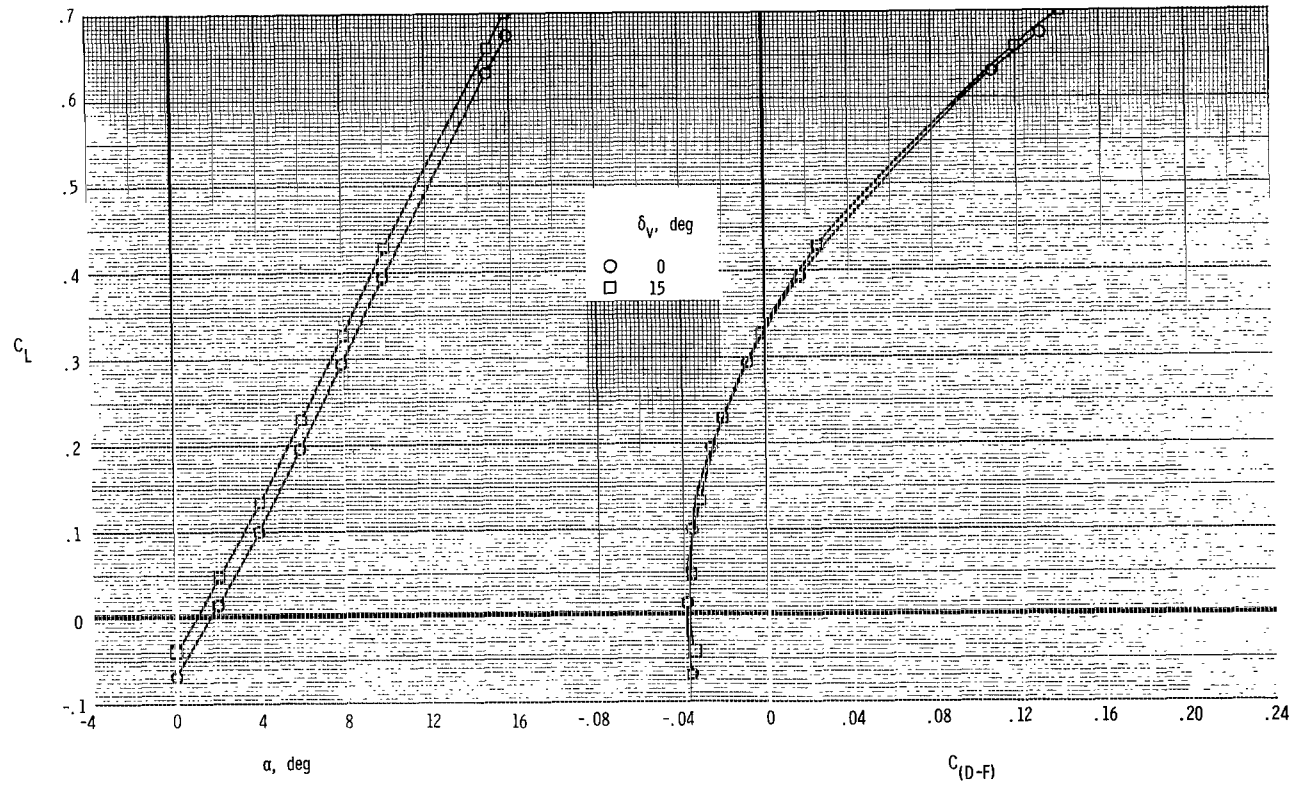
(a)  $M = 0.60$ ,  $NPR = 3.0$ .

Figure 16.- Effect of vector angle on total aerodynamic characteristics. Basic LE;  
 $\delta_{te} = 0^\circ$ ;  $\delta_c = 0^\circ$ .



(b)  $M = 0.87$ ,  $NPR = 3.9$ .

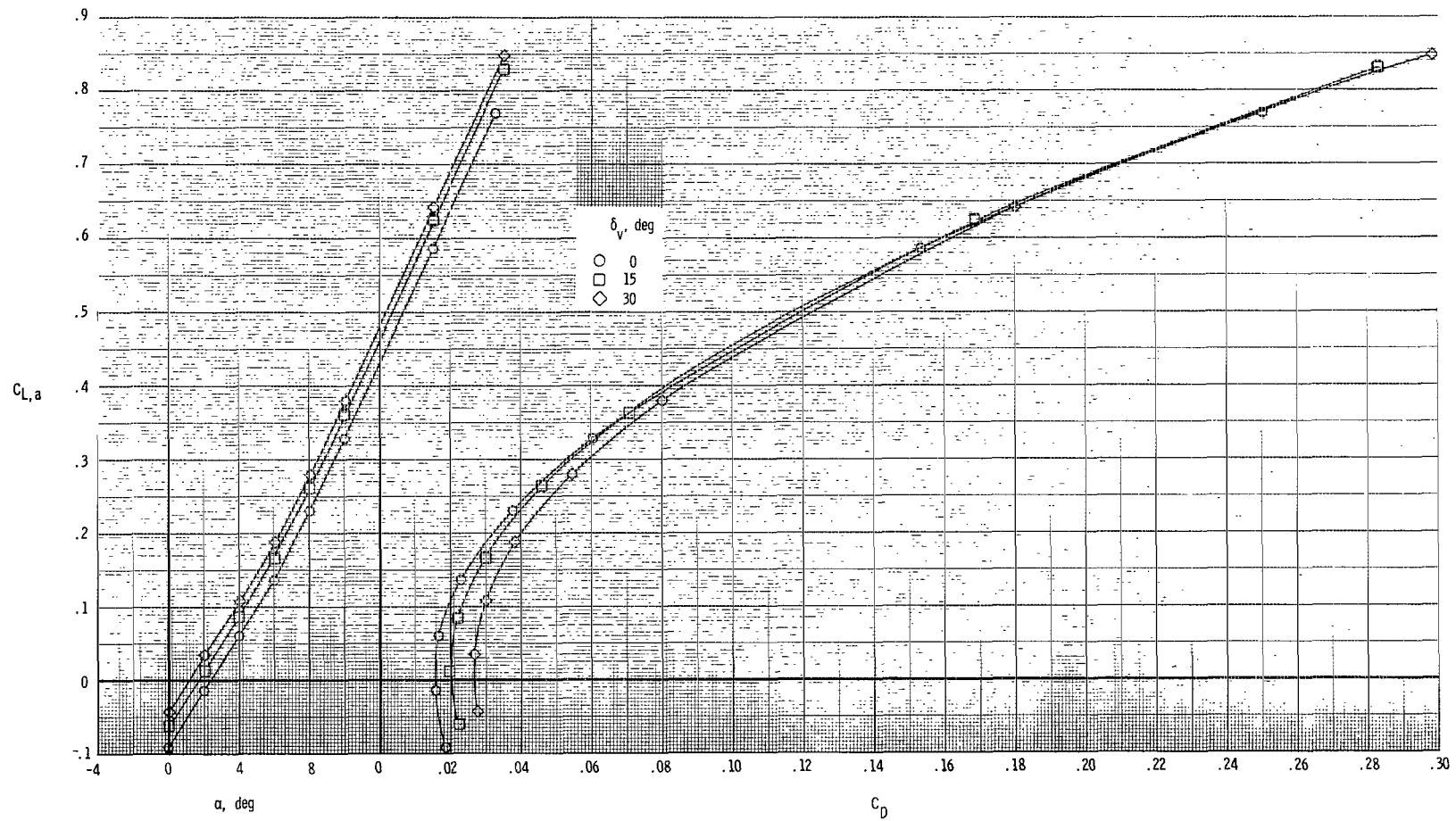
Figure 16.- Continued.



(c)  $M = 1.20$ ,  $NPR = 6.6$ .

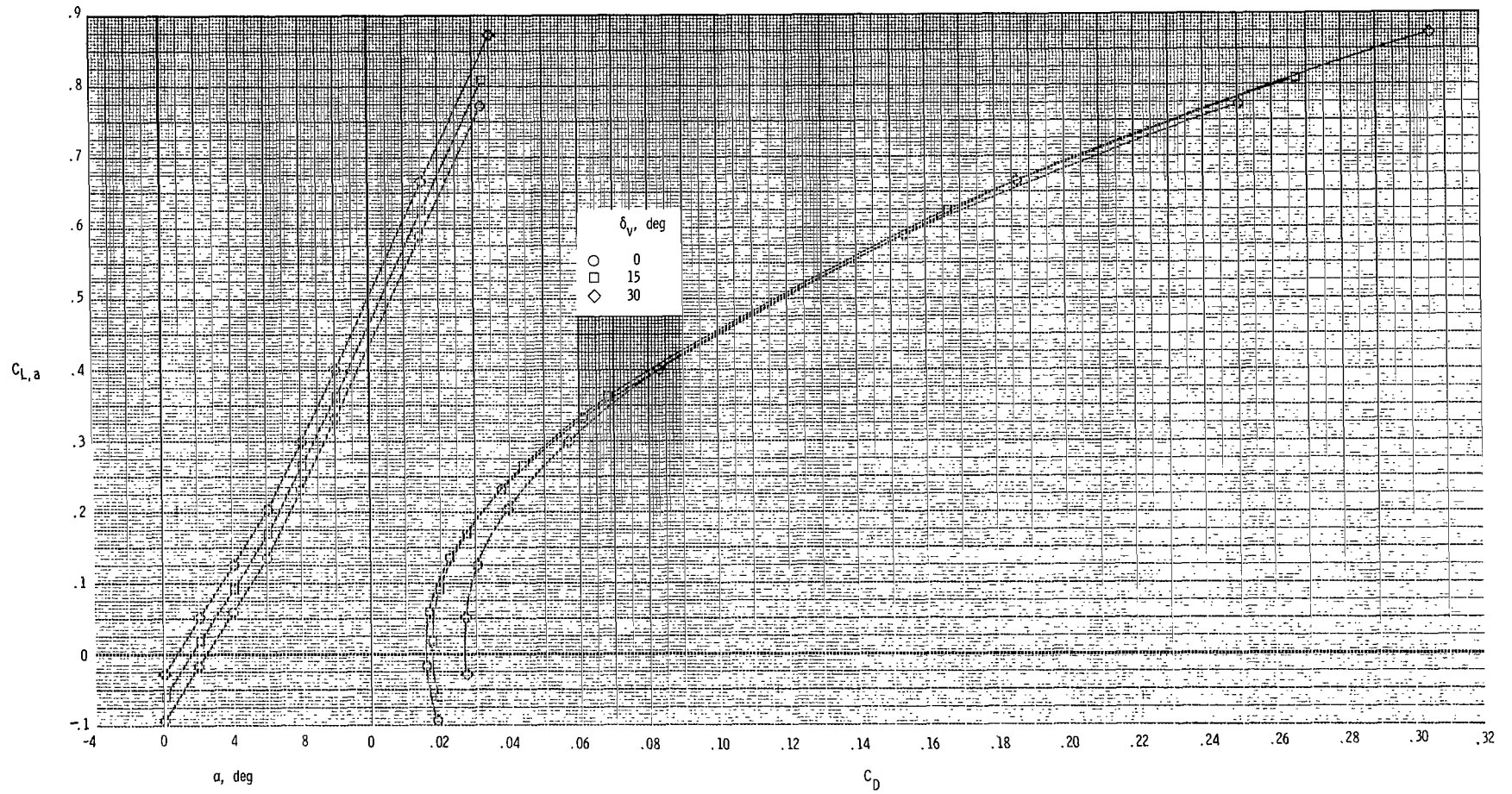
Figure 16.- Concluded.





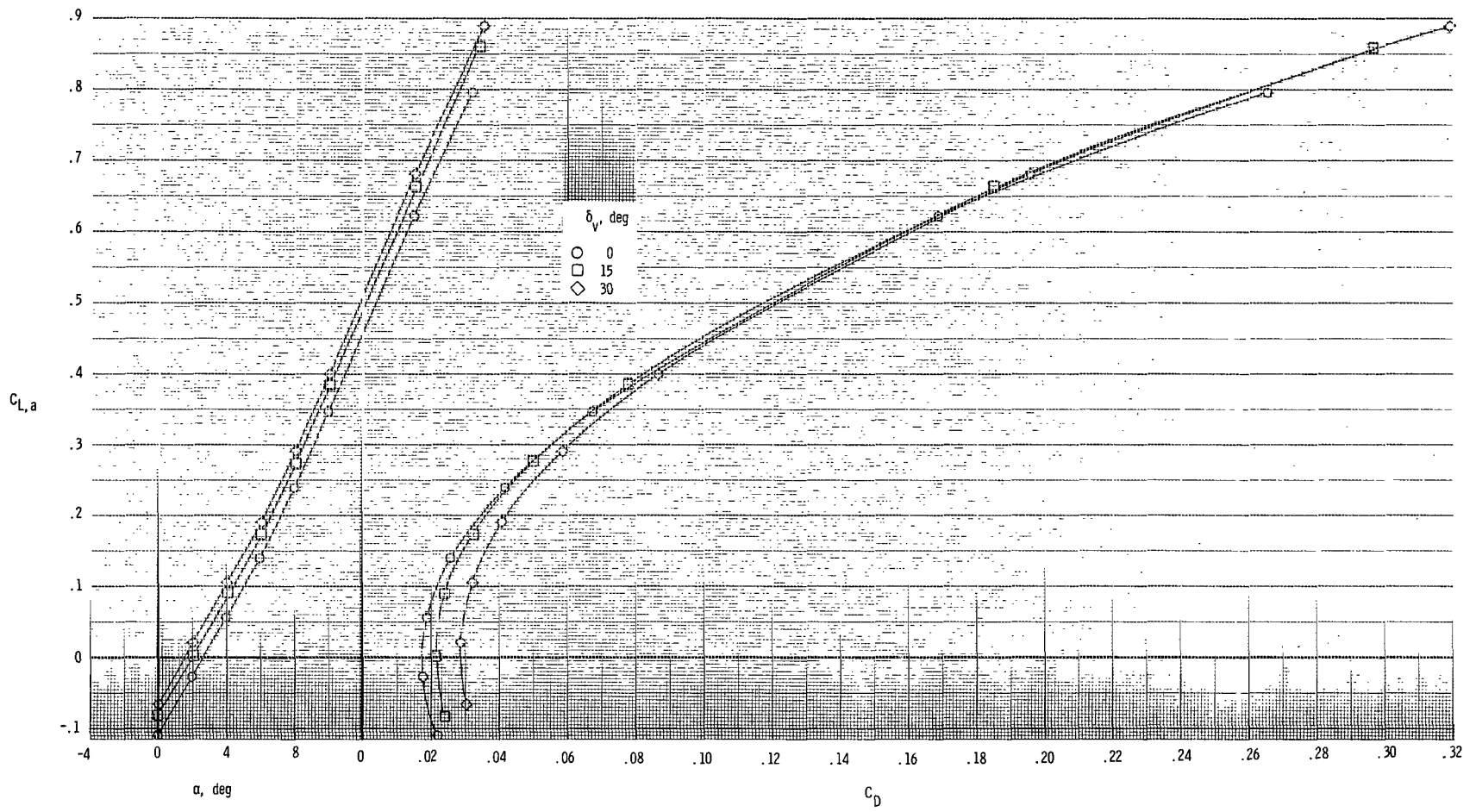
(a)  $M = 0.60$ ,  $NPR = 1.0$ .

Figure 17.- Effect of vector angle on thrust-removed aerodynamic characteristics.  
Basic LE;  $\delta_{te} = 0^\circ$ ;  $\delta_c = 0^\circ$ .



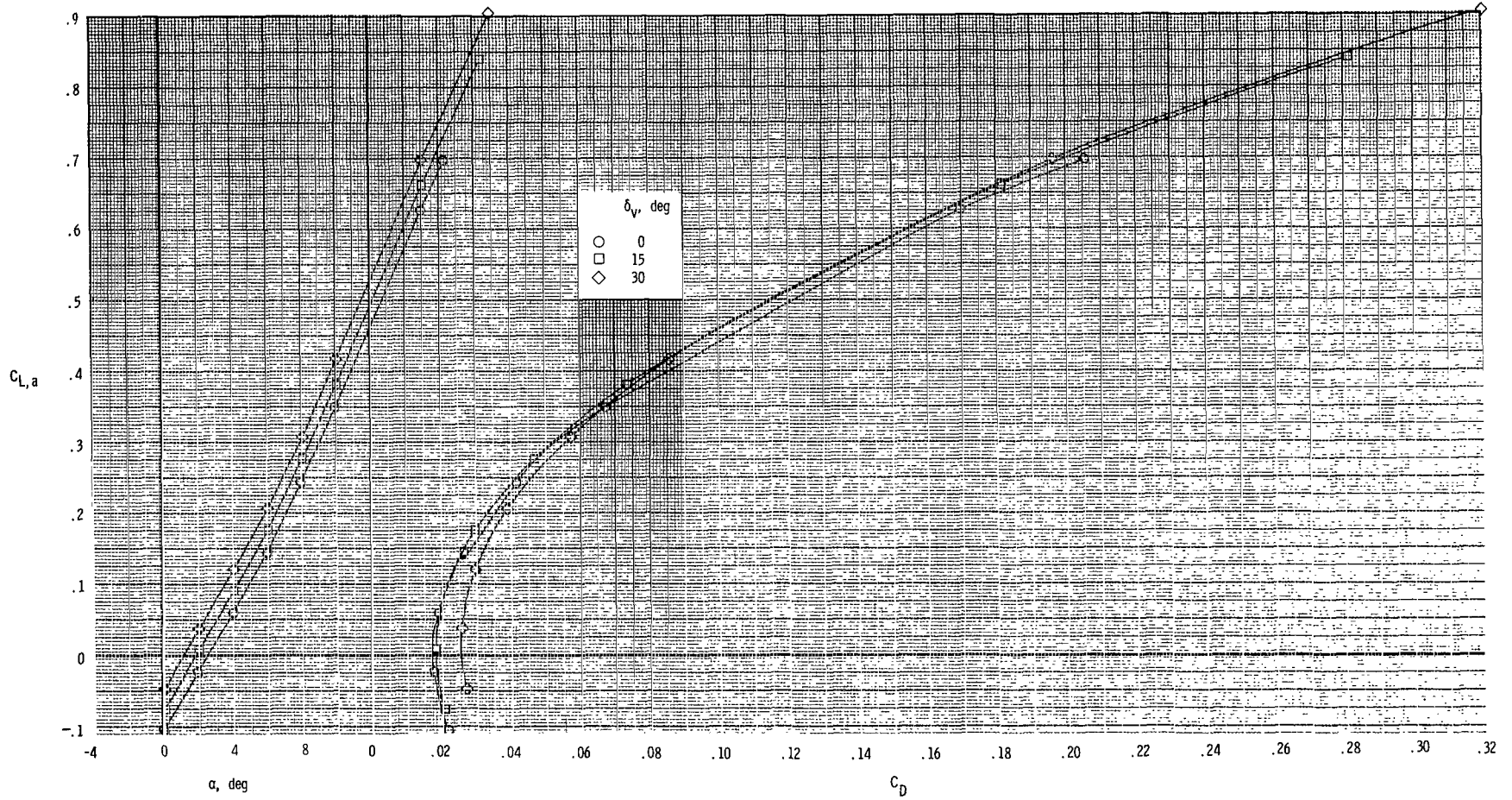
(b)  $M = 0.60$ ,  $NPR = 3.0$ .

Figure 17.- Continued.



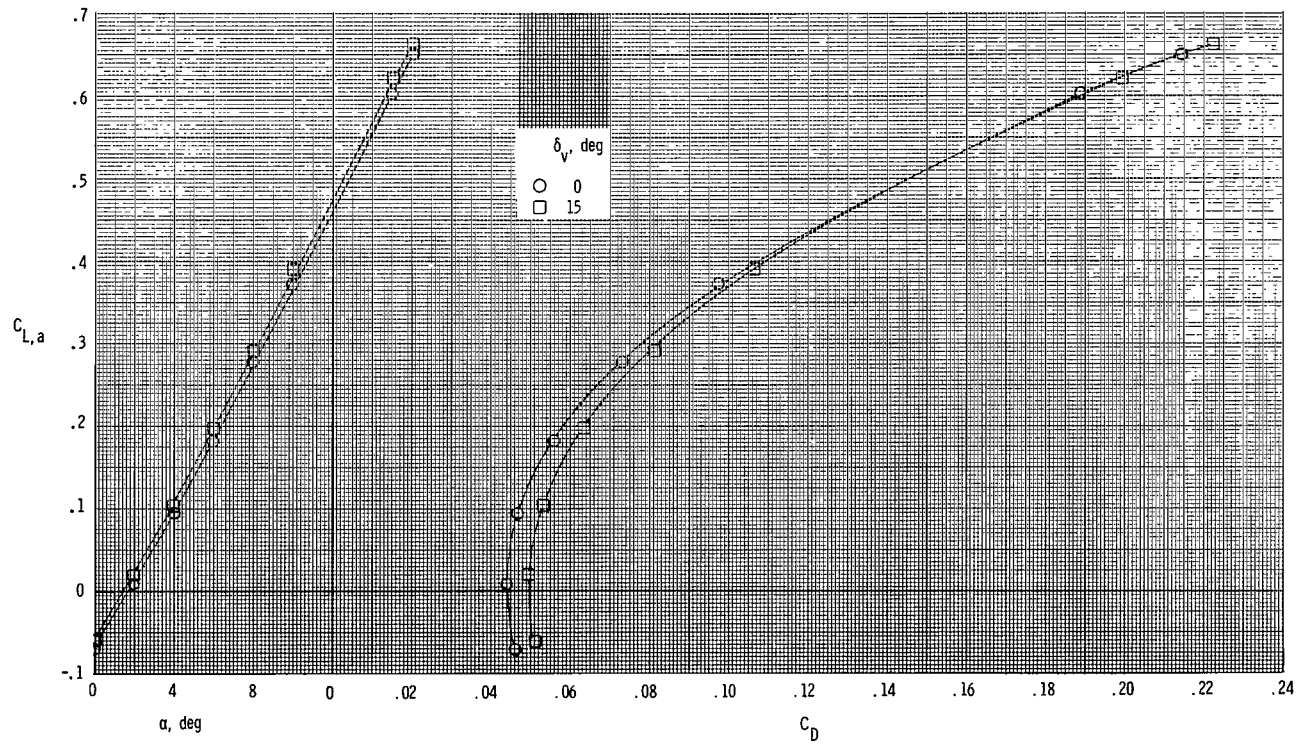
(c)  $M = 0.87, \text{ NPR} = 1.0.$

Figure 17.- Continued.



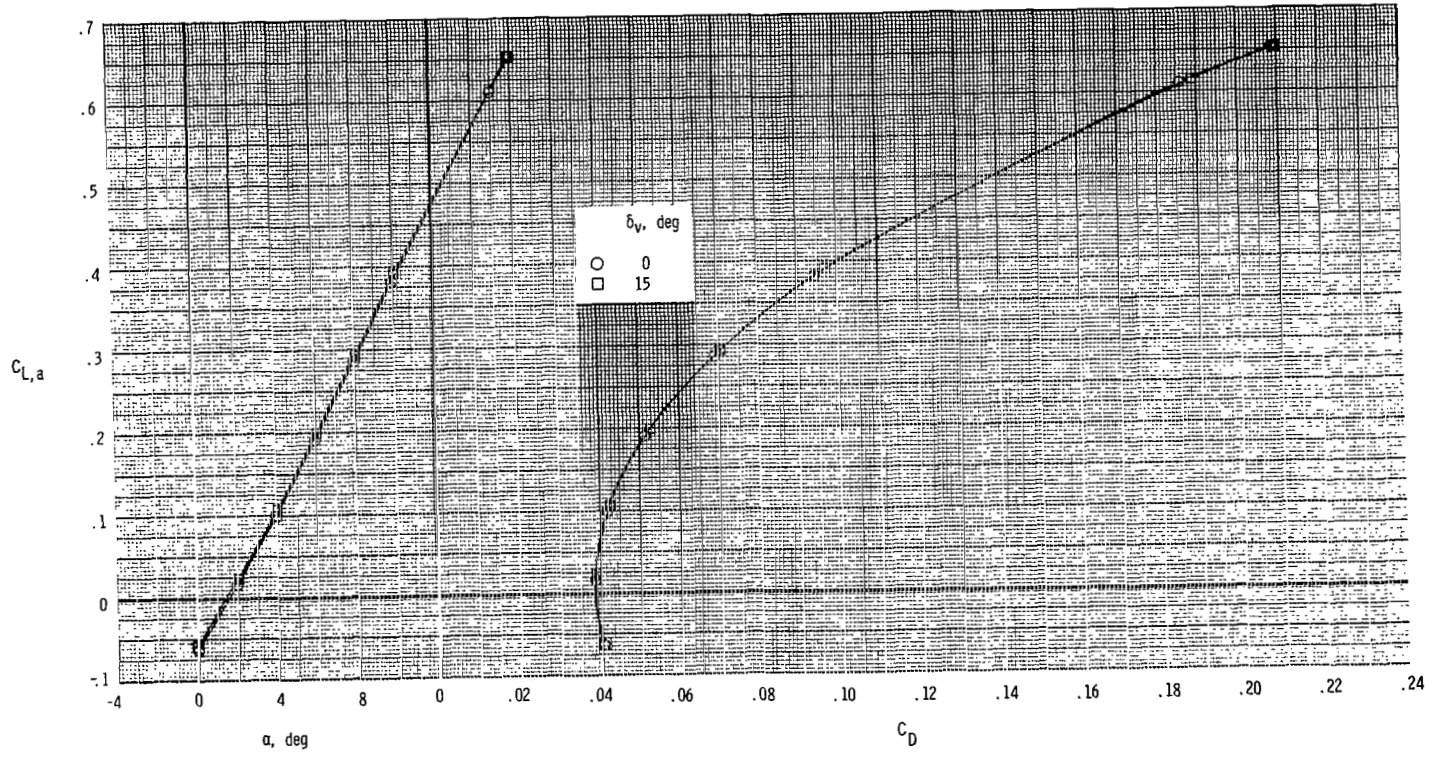
(d)  $M = 0.87$ ,  $NPR = 3.9$ .

Figure 17.- Continued.



(e)  $M = 1.20$ ,  $NPR = 1.0$ .

Figure 17.- Continued.



(f)  $M = 1.20$ ,  $NPR = 6.6$ .

Figure 17.- Concluded.

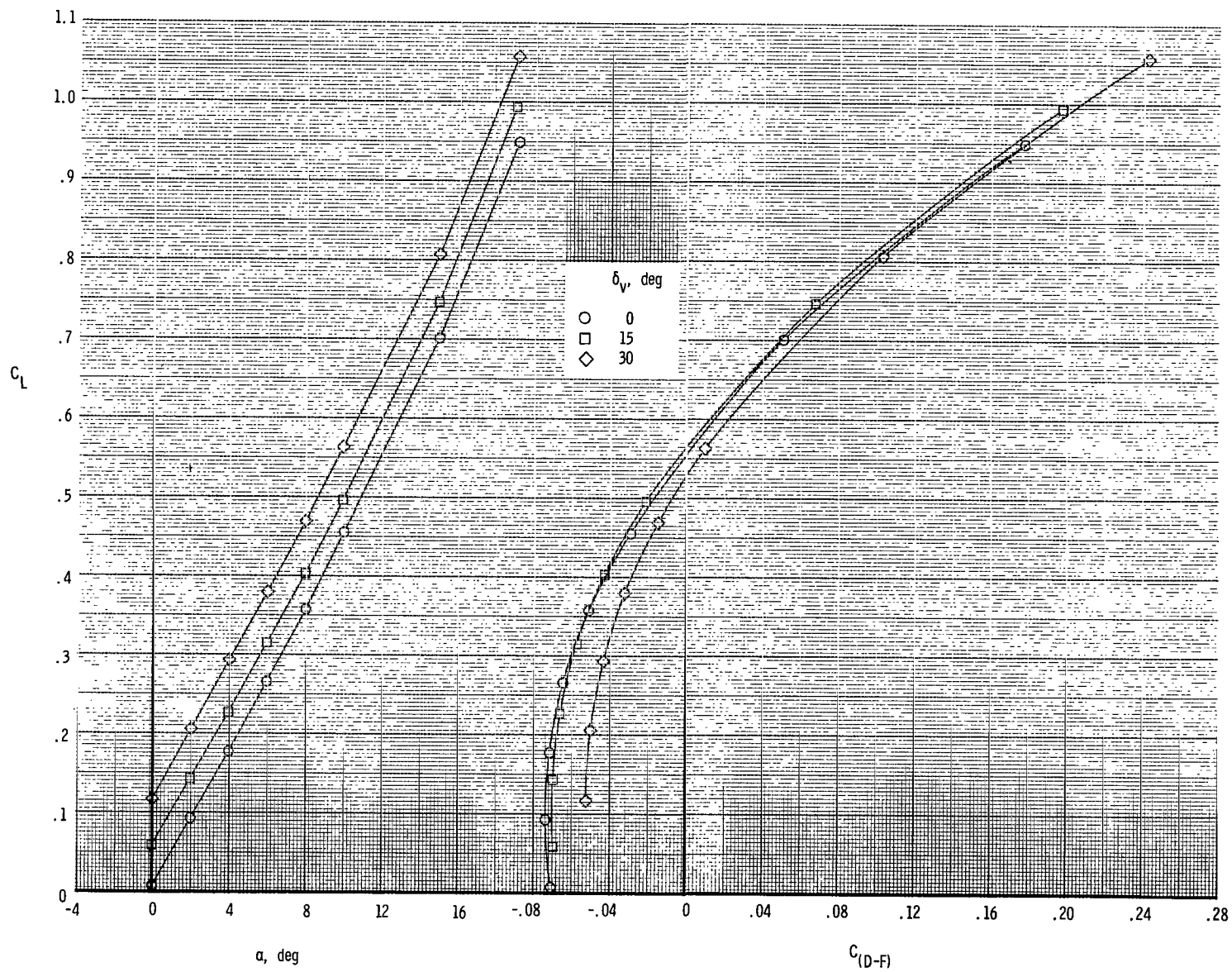
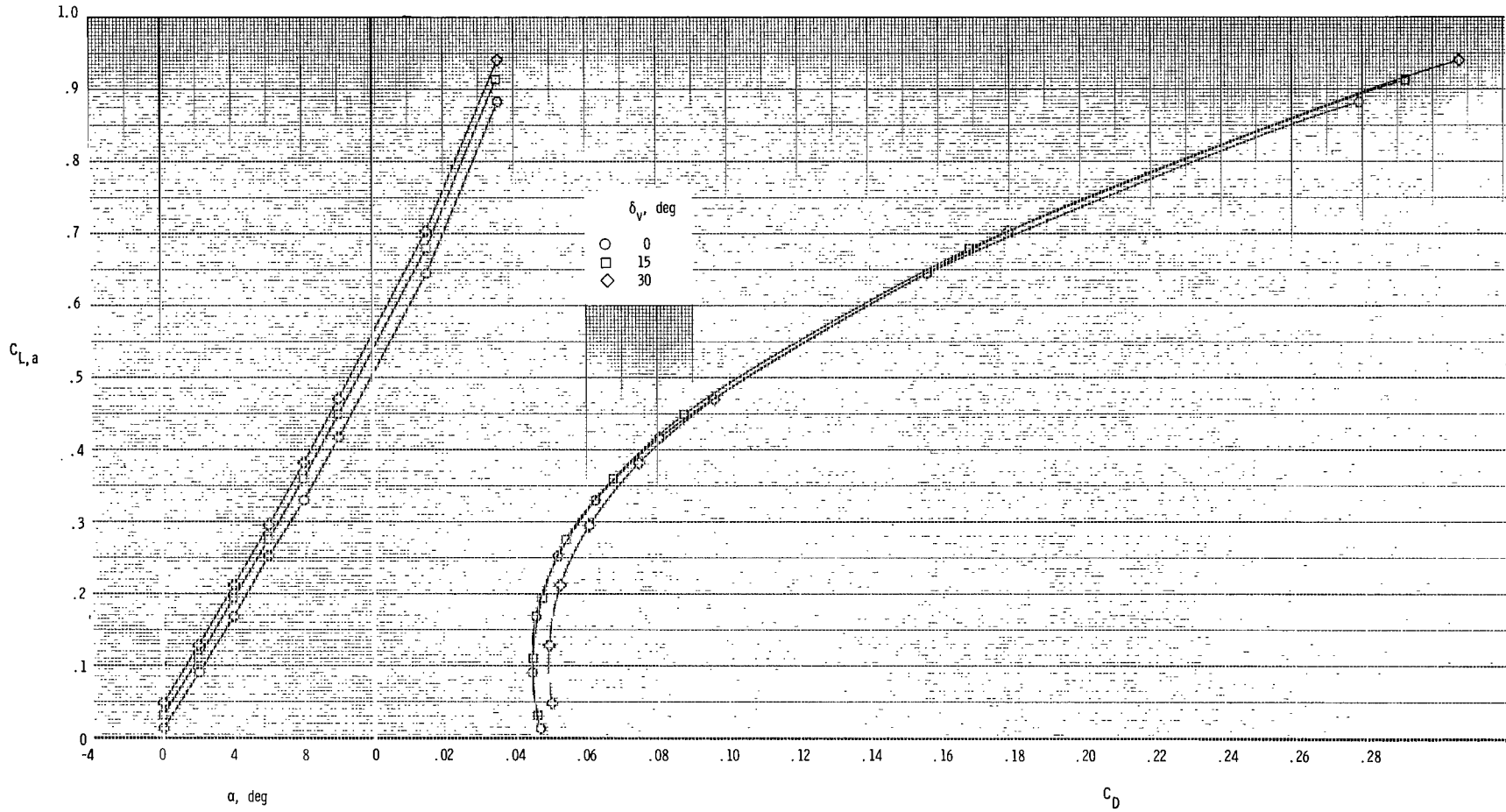


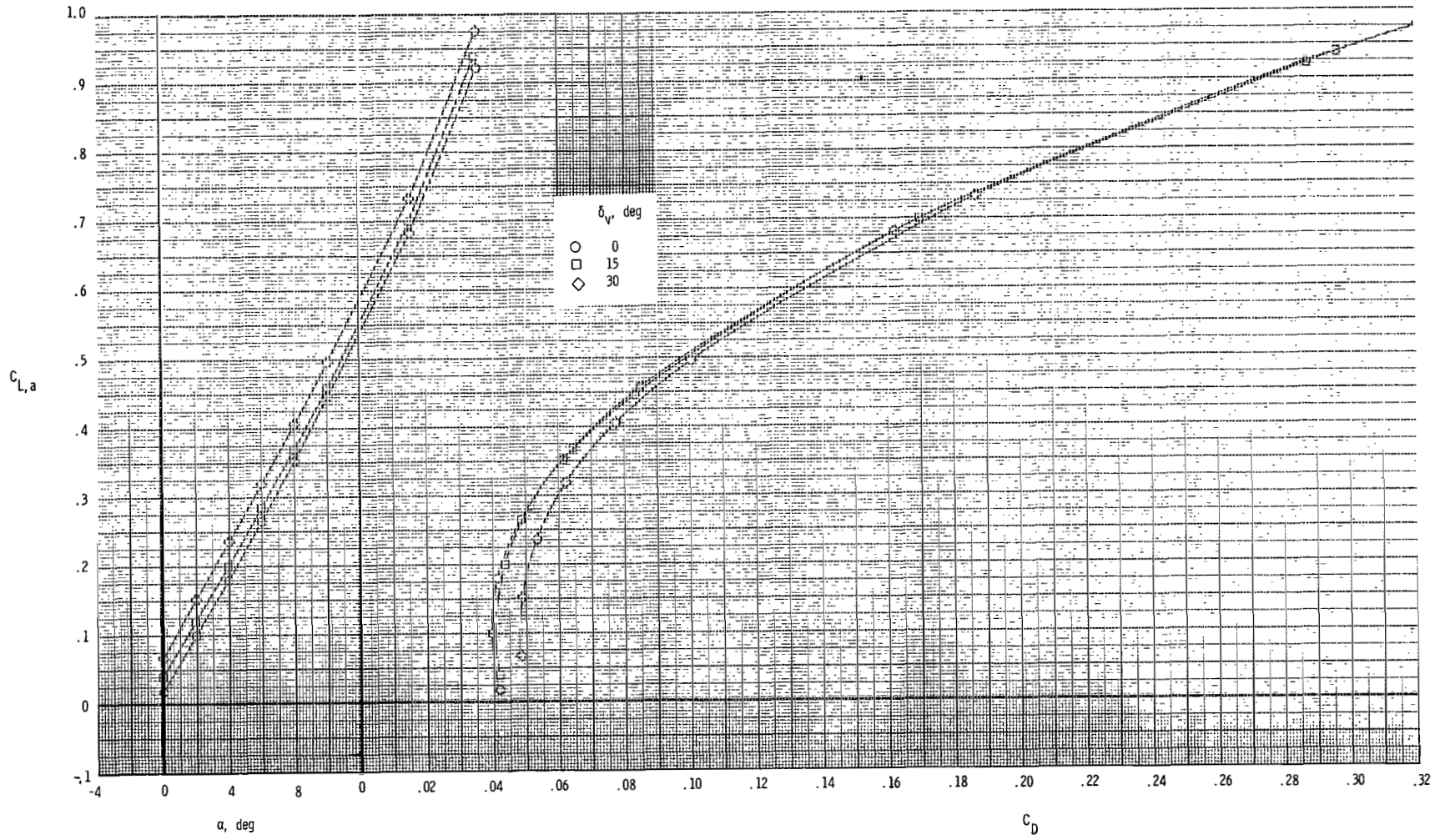
Figure 18.- Effect of vectoring on total aerodynamic characteristics. Drooped LE;  
 $\delta_{te} = 30^\circ$ ;  $\delta_c = 0^\circ$ ;  $M = 0.60$ ;  $NPR = 3.0$ .



(a) NPR = 1.0.

Figure 19.- Effect of vectoring on thrust-removed aerodynamic characteristics.  
Drooped LE;  $\delta_{te} = 30^\circ$ ;  $\delta_c = 0^\circ$ ;  $M = 0.60$ .





(b) NPR = 3.0.

Figure 19.- Concluded.

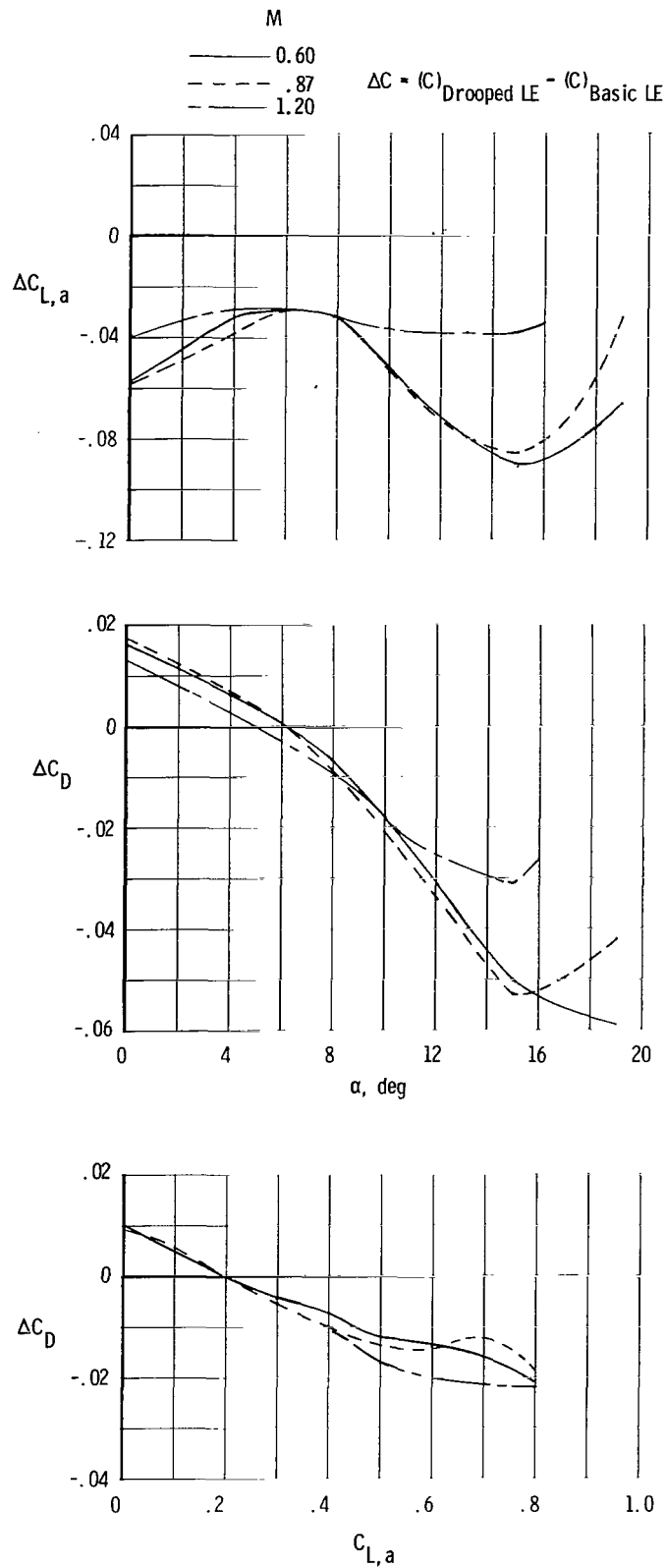
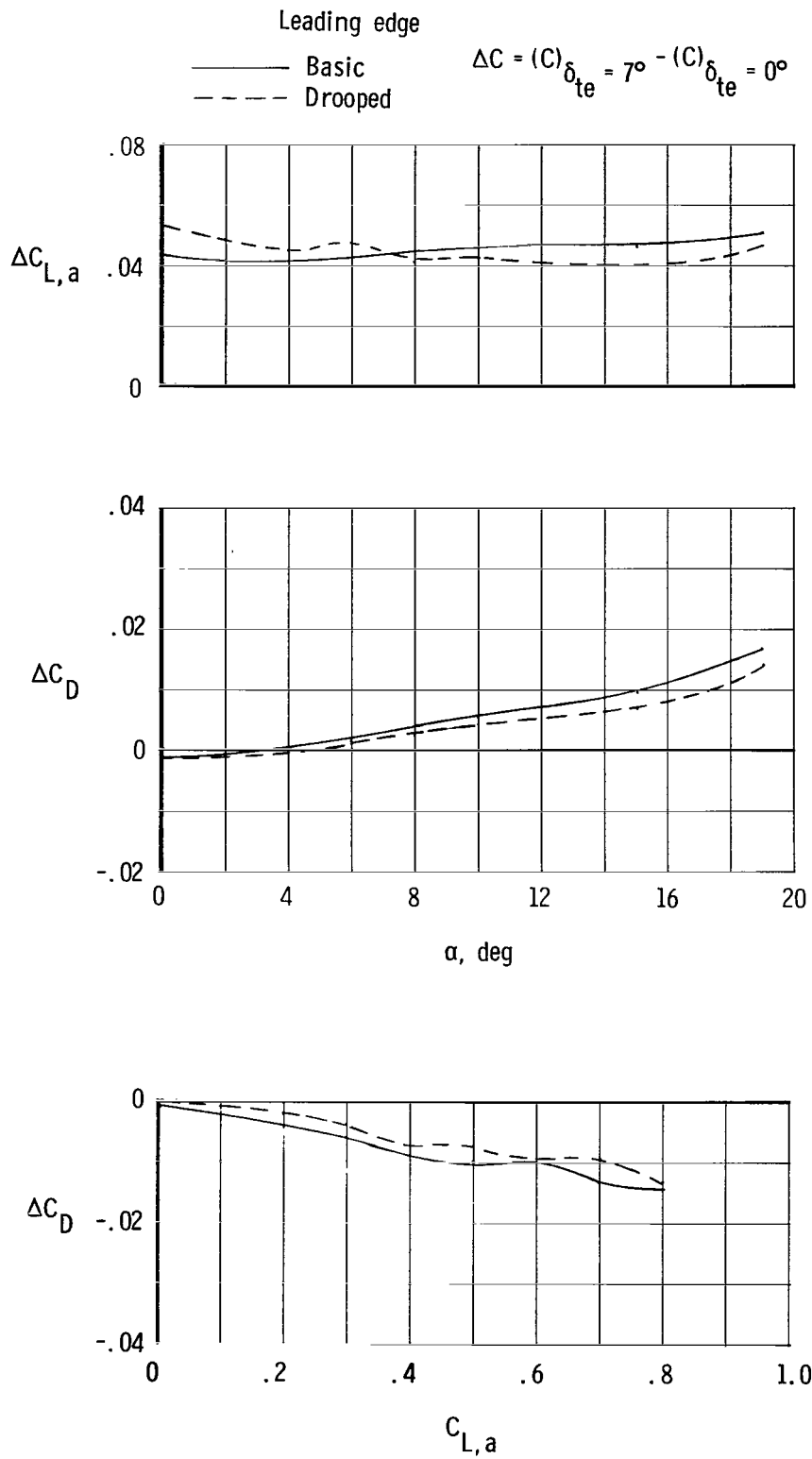
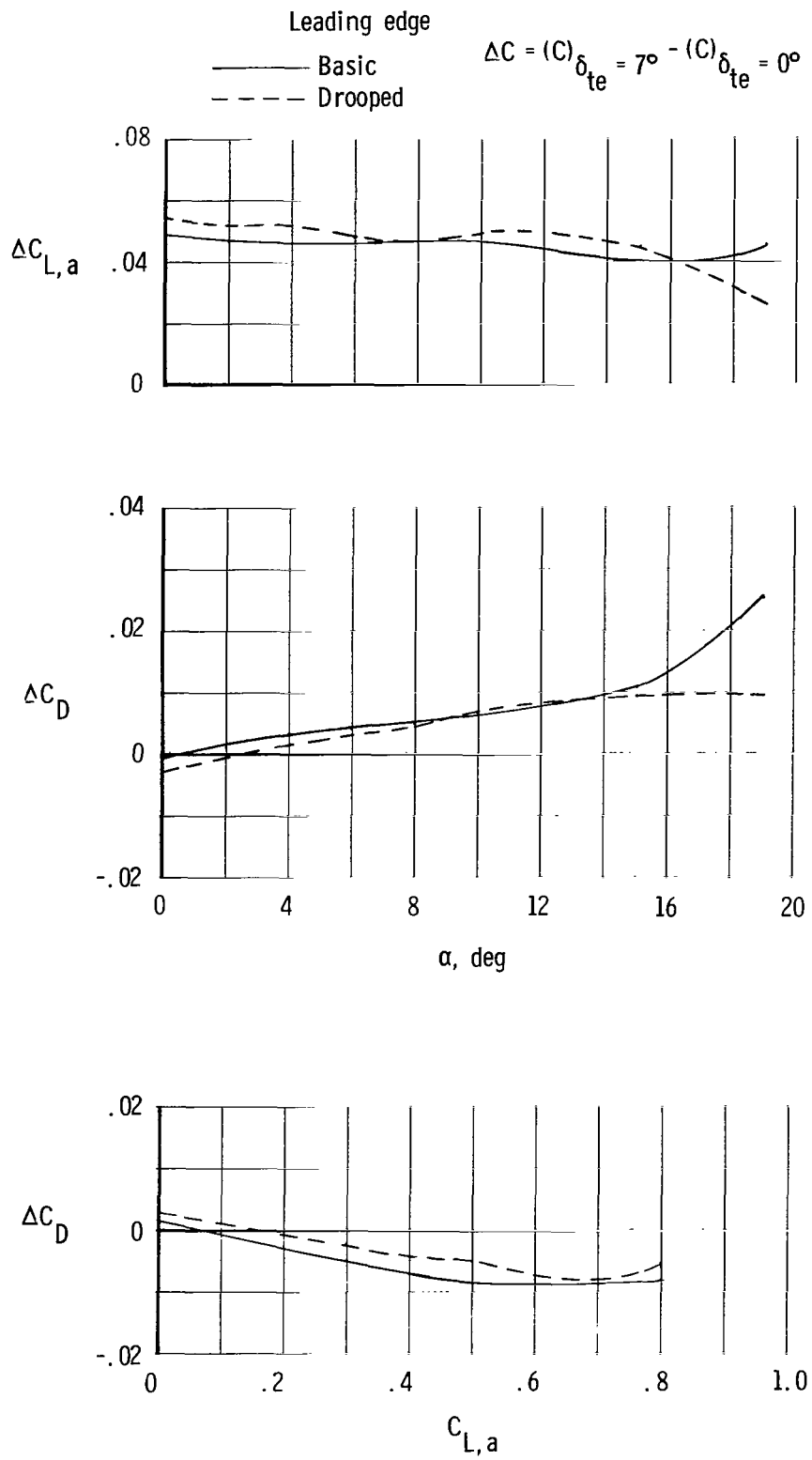


Figure 20.- Incremental lift and drag coefficients due to drooped leading edge.  $\delta_{te} = 0^\circ$ ; NPR = 1.0.



(a)  $\delta_{te} = 7^\circ$ ,  $M = 0.60$ .

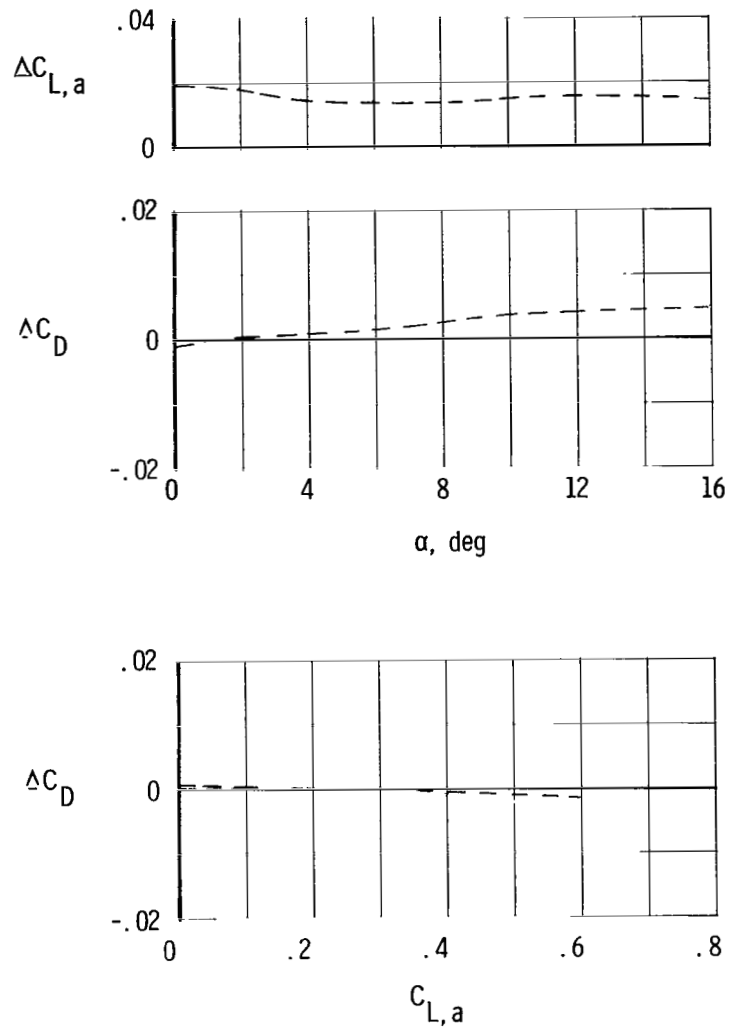
Figure 21.- Incremental lift and drag coefficients due to trailing-edge flap deflection. NPR = 1.0.



(b)  $\delta_{te} = 7^\circ$ ,  $M = 0.87$ .

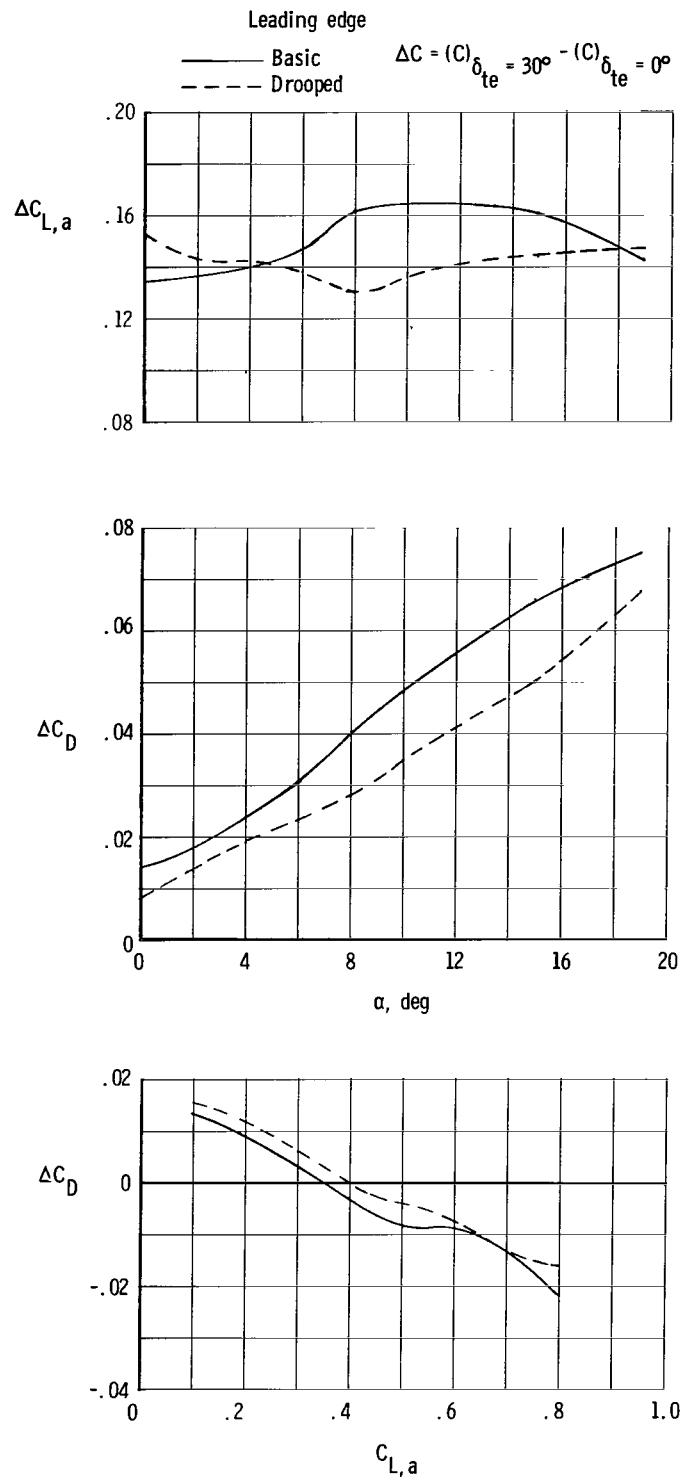
Figure 21.- Continued.

$$\Delta C = (C)_{\delta_{te} = 7^\circ} - (C)_{\delta_{te} = 0^\circ}$$



(c)  $\delta_{te} = 7^\circ$ , drooped LE,  $M = 1.20$ .

Figure 21.- Continued.



(d)  $\delta_{te} = 30^\circ$ ,  $M = 0.60$ .

Figure 21.- Concluded.

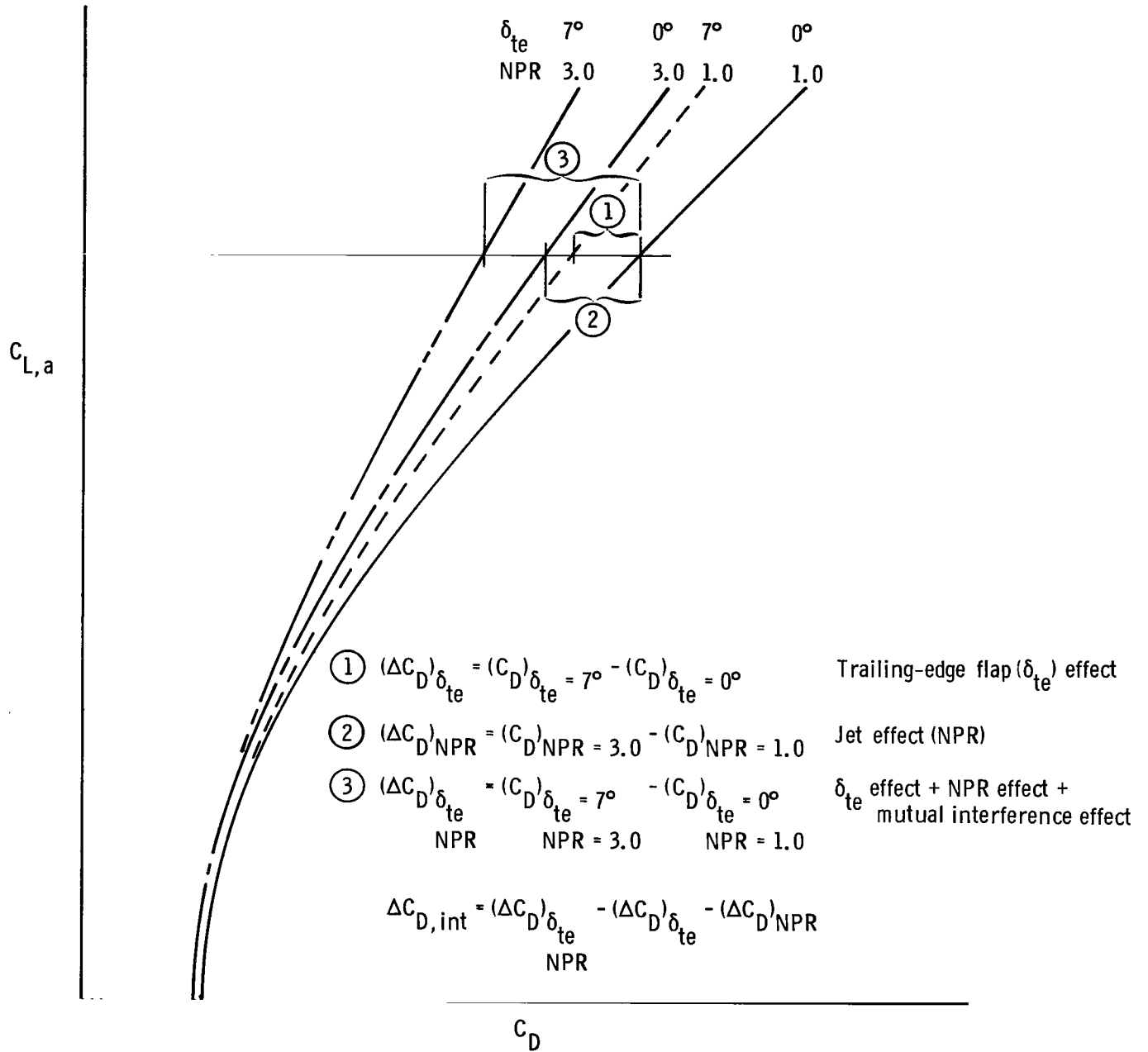


Figure 22.- Sketch indicating various increments used to define incremental interference drag term  $\Delta C_{D,int}$ .  $\delta_v = \text{Constant}$ .

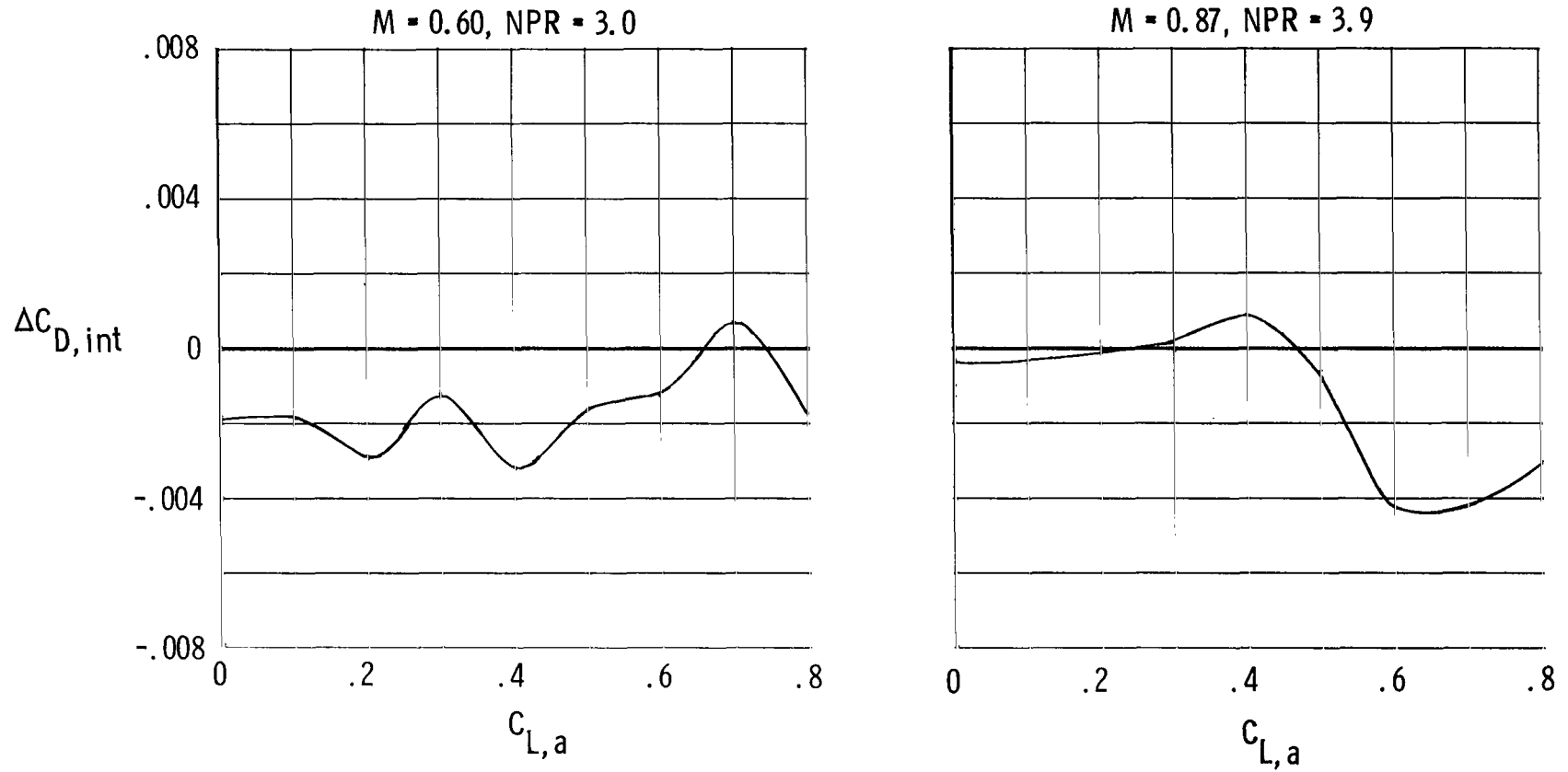
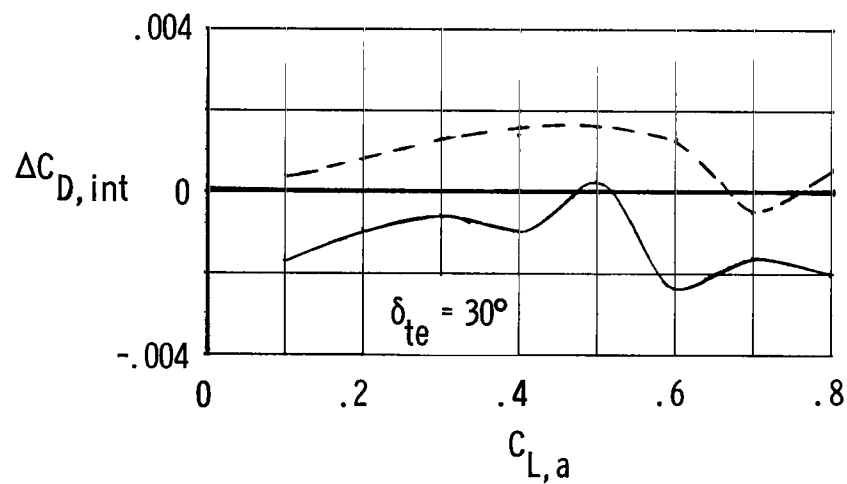
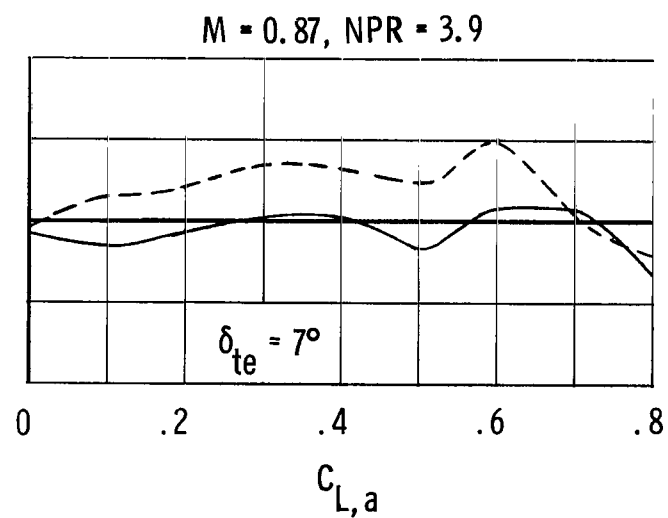
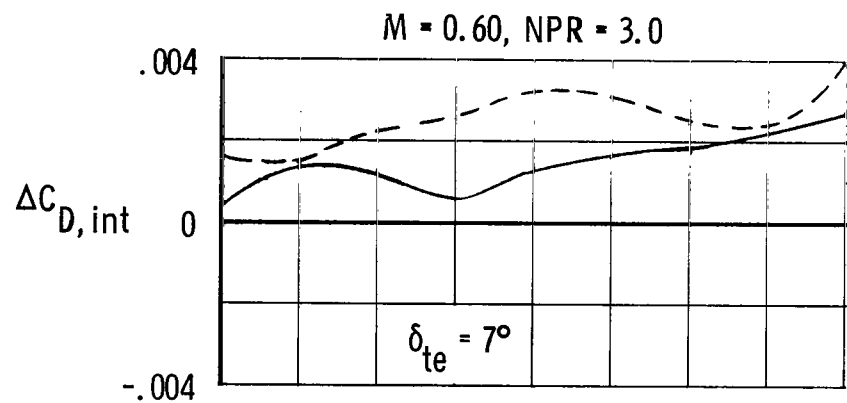


Figure 23.- Effect of leading edge variation on interference drag term  $\Delta C_{D,int}$ .  
 $\delta_{te} = 0^\circ$ ;  $\delta_v = 15^\circ$ ;  $\delta_c = 0^\circ$ .



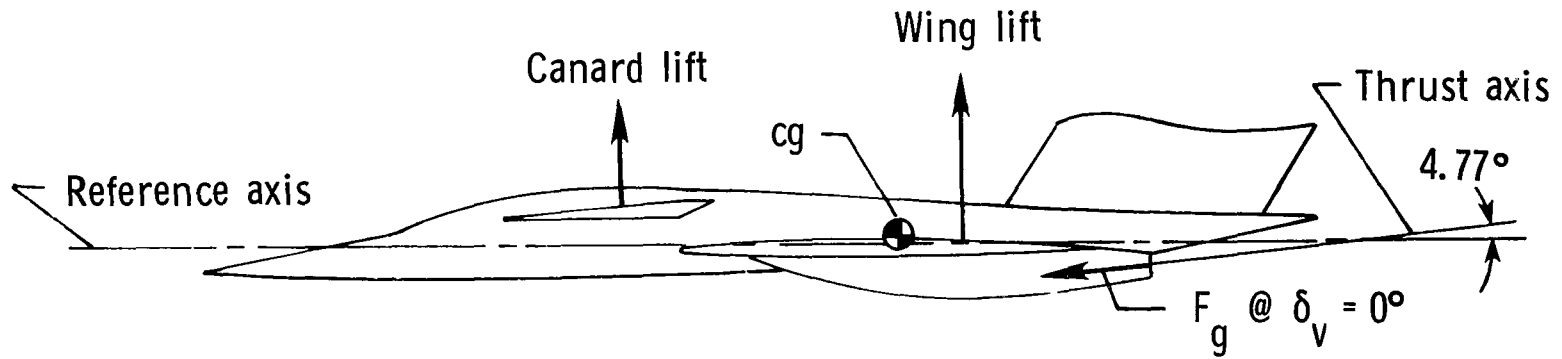


Leading edge

— Basic

- - - Drooped

Figure 24.- Effect of trailing-edge deflection on interference drag term  $\Delta C_{D,int}$ .  
 $\delta_v = 0^\circ; \delta_c = 0^\circ$ .



Force input	Moment direction
$F_g @ \delta_v = 0^\circ$	Nose up
$F_g @ \delta_v > 5^\circ$	Nose down
Drooped LE	Nose up
$\delta_{te}$	Nose down

Figure 25.- Vehicle force diagram.

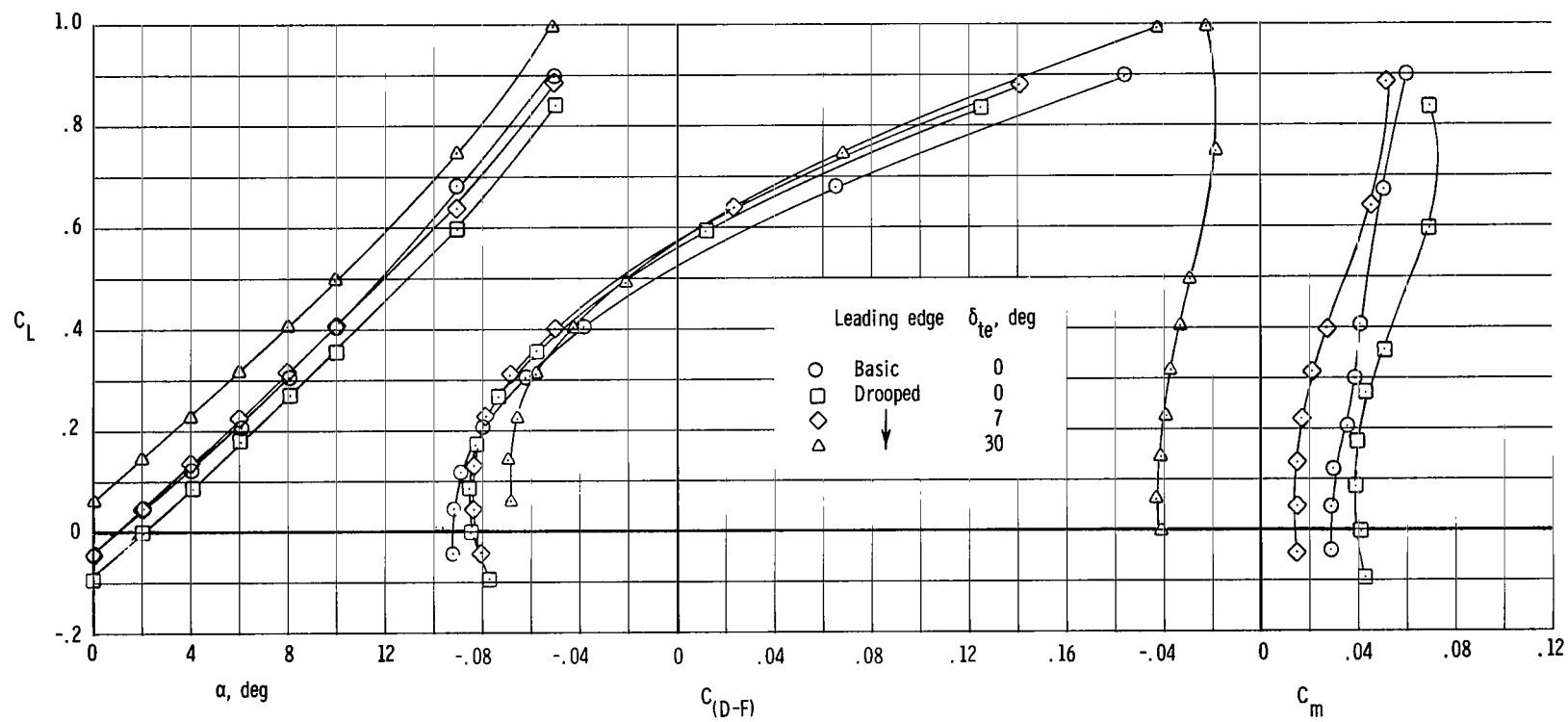
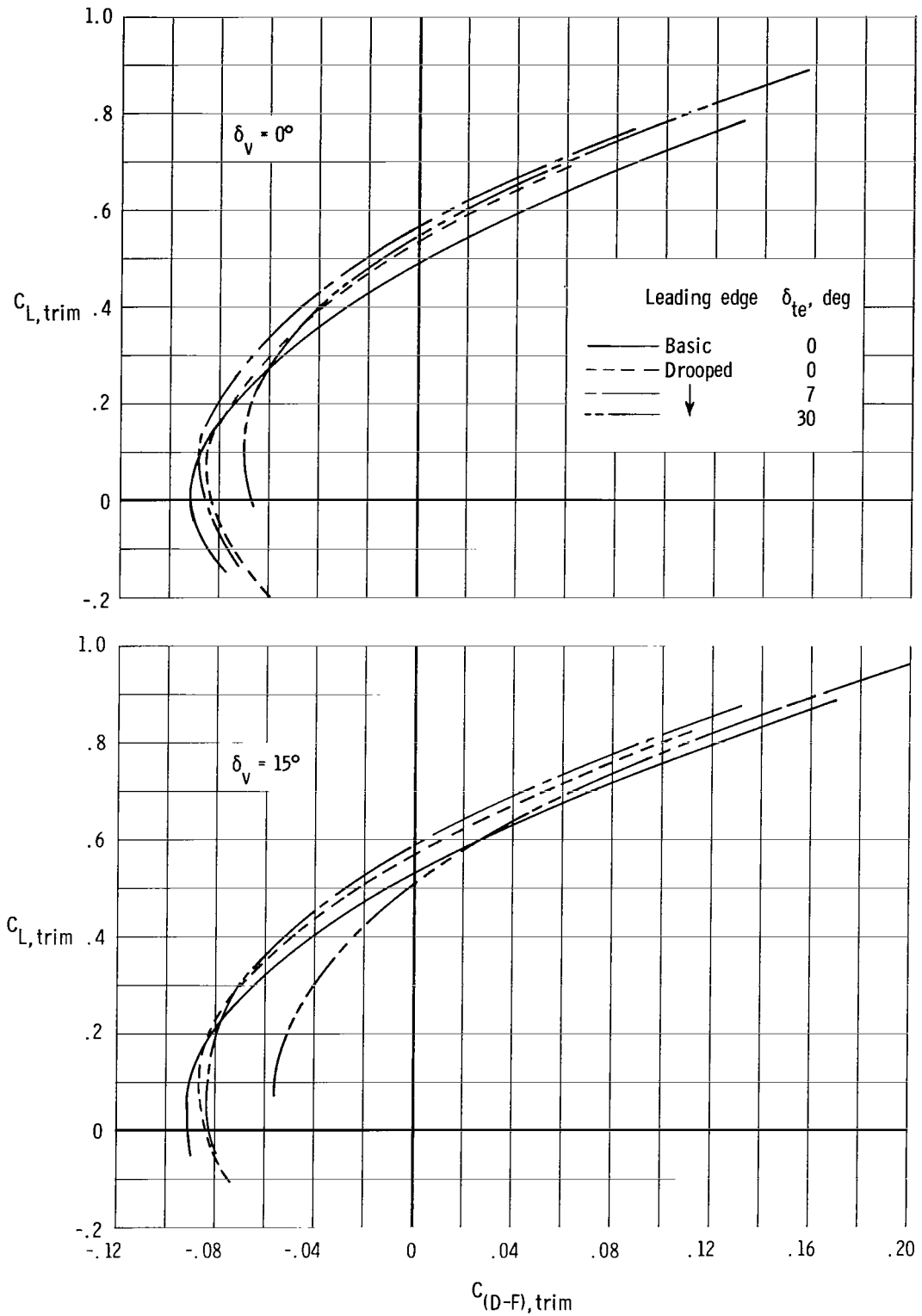
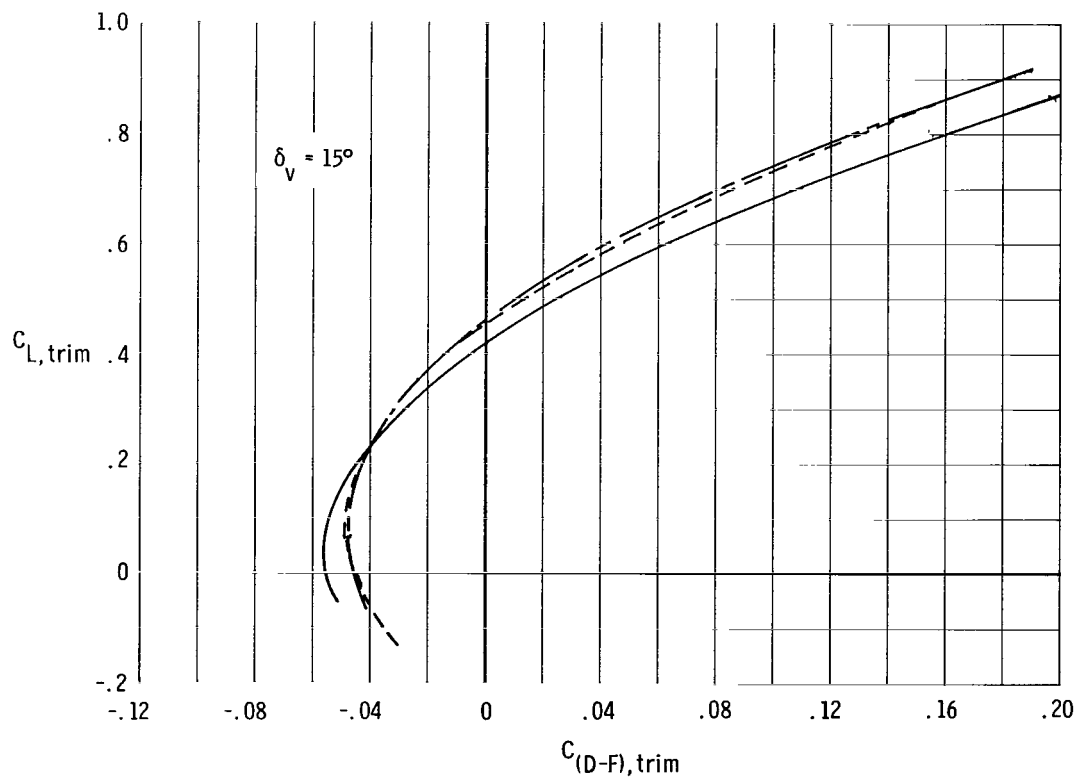
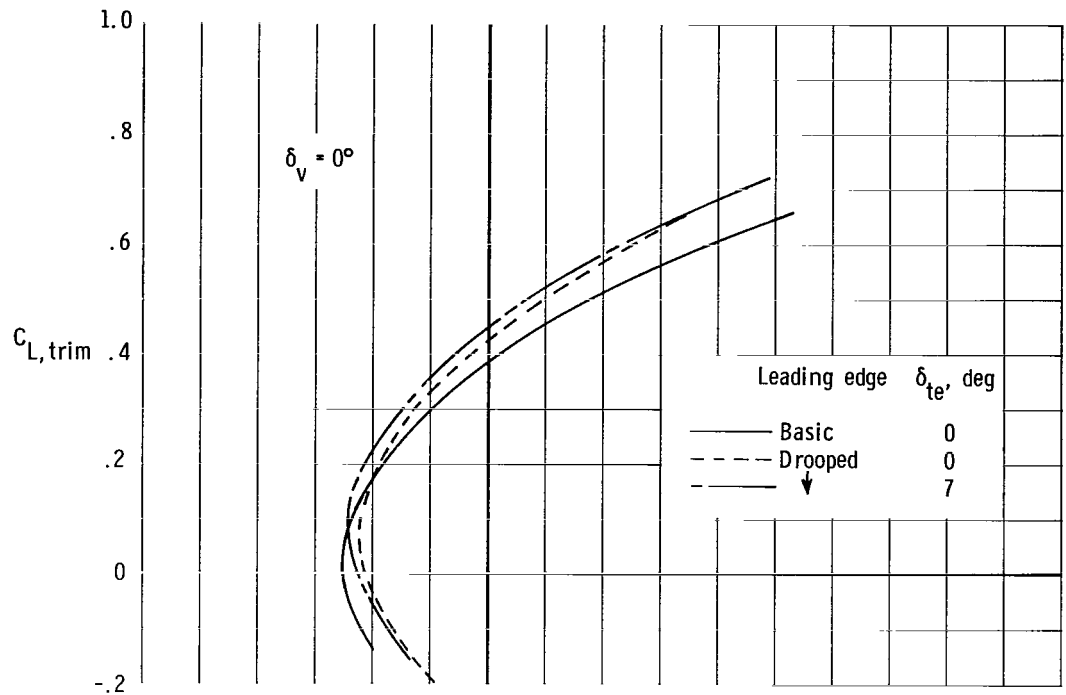


Figure 26.- Typical effect of wing maneuver devices on untrimmed powered longitudinal characteristics.  $\delta_v = 15^\circ$ ;  $\delta_c = 0^\circ$ ;  $M = 0.60$ ;  $NPR = 3.0$ .



(a)  $M = 0.60$ ,  $NPR = 3.0$ .

Figure 27.- Effect of wing maneuver devices on trimmed powered polars.



(b)  $M = 0.87$ ,  $NPR = 3.9$ .

Figure 27.- Concluded.

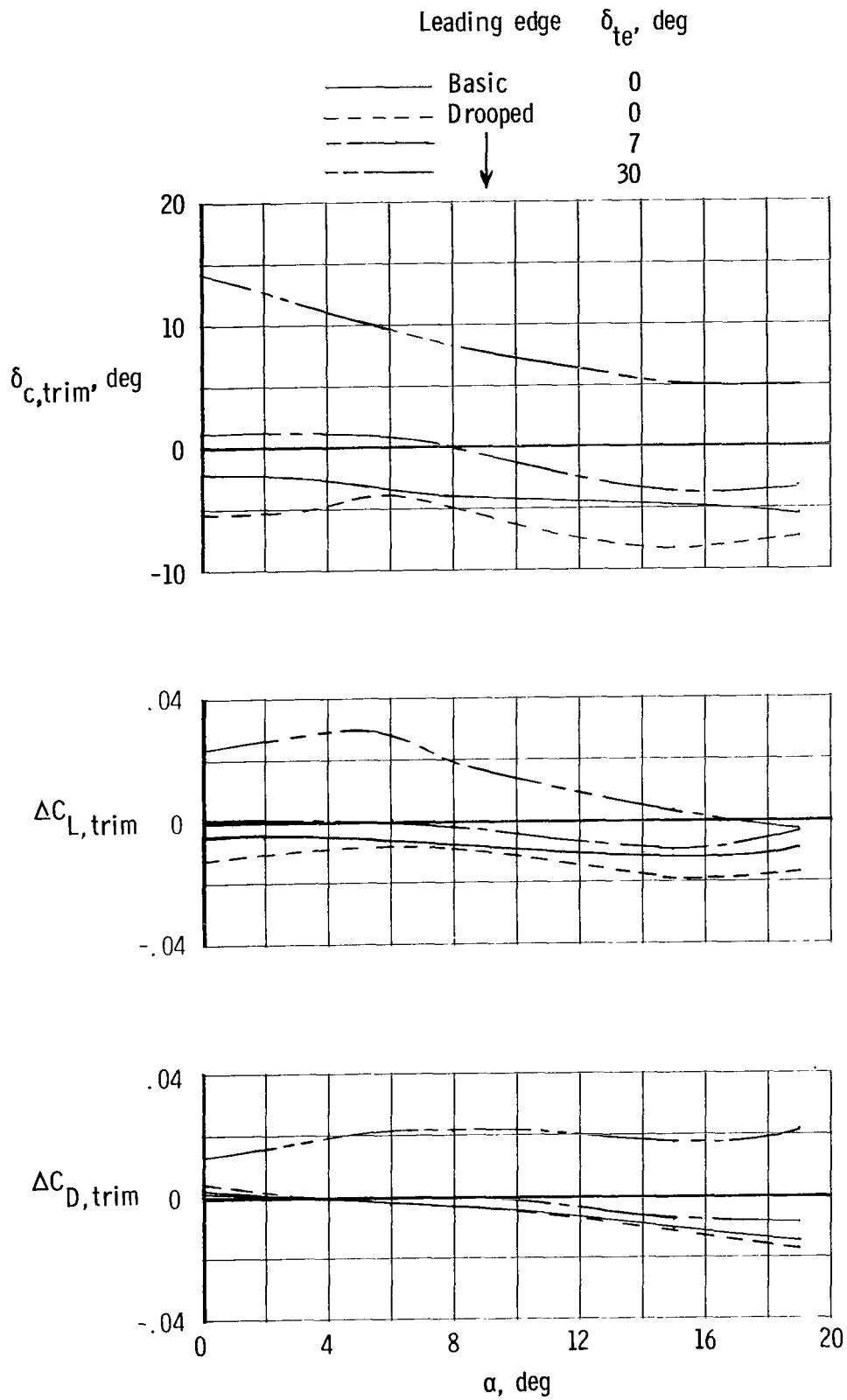


Figure 28.- Canard deflection required for trim and trim drag increments.  
 $\delta_v = 15^\circ$ ;  $M = 0.60$ ;  $NPR = 3.0$ .

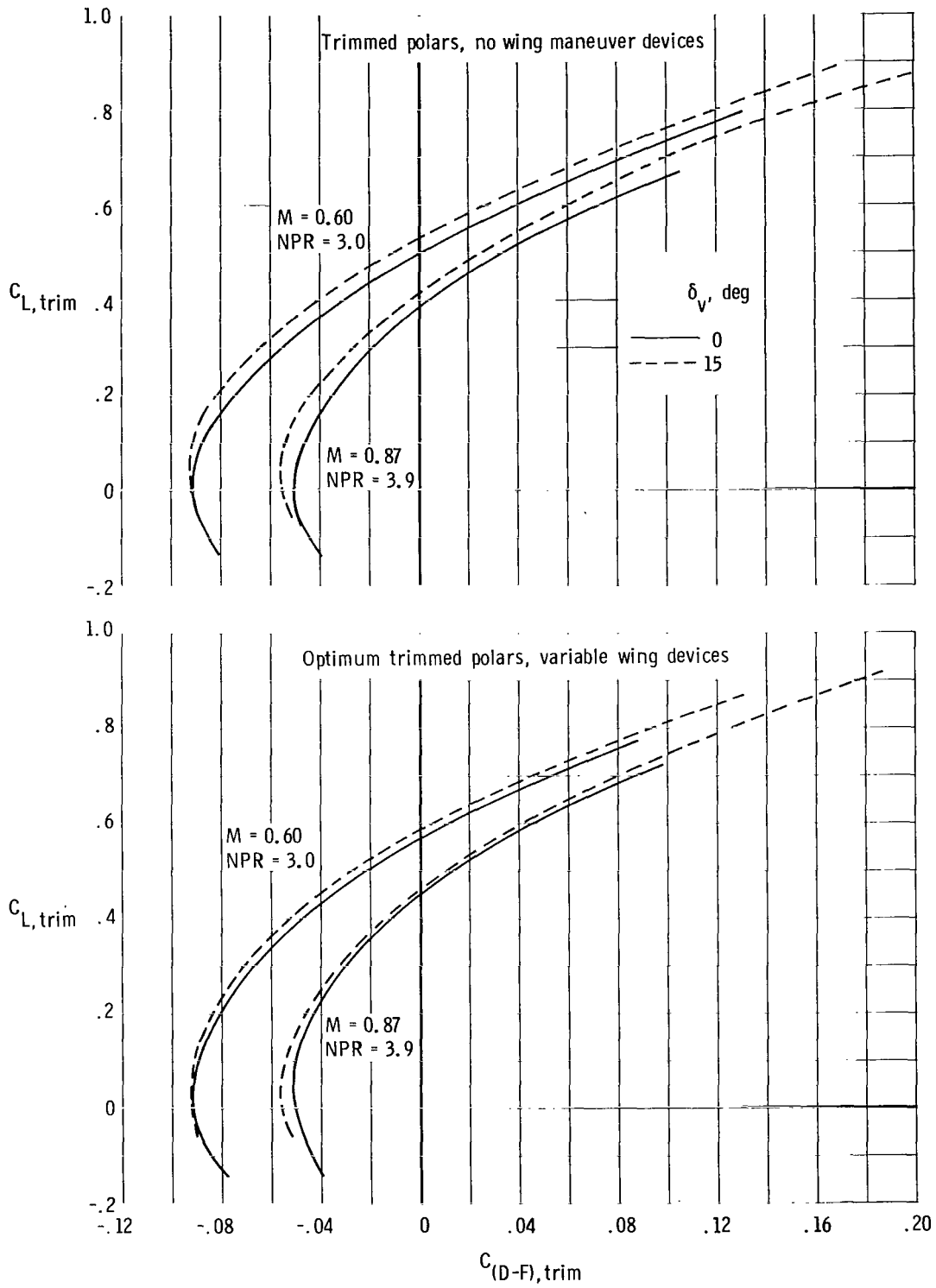


Figure 29.- Trimmed powered and optimum polars.

1. Report No. NASA TP-2119	2. Government Accession No.	3. Recipient's Catalog No.
4. Title and Subtitle EFFECT OF THRUST VECTORING AND WING MANEUVER DEVICES ON TRANSONIC AEROPROPULSIVE CHARACTERISTICS OF A SUPERSONIC FIGHTER AIRCRAFT		5. Report Date February 1983
7. Author(s) Francis J. Capone and David E. Reubush		6. Performing Organization Code 505-43-43-04
9. Performing Organization Name and Address  NASA Langley Research Center Hampton, VA 23665		8. Performing Organization Report No. L-15526
12. Sponsoring Agency Name and Address  National Aeronautics and Space Administration Washington, DC 20546		10. Work Unit No.
15. Supplementary Notes		11. Contract or Grant No.
16. Abstract  The aeropropulsive characteristics of an advanced fighter designed for supersonic cruise have been determined in the Langley 16-Foot Transonic Tunnel. The objectives of this investigation were to evaluate the interactive effects of thrust vectoring and wing maneuver devices on lift and drag and to determine trim characteristics. The wing maneuver devices consisted of a drooped leading edge and a trailing-edge flap. Thrust vectoring was accomplished with two-dimensional (nonaxisymmetric) convergent-divergent nozzles located below the wing in two single-engine podded nacelles. A canard was utilized for trim. Thrust vector angles of 0°, 15°, and 30° were tested in combination with a drooped wing leading edge and with wing trailing-edge flap deflections up to 30°. This investigation was conducted at Mach numbers from 0.60 to 1.20, at angles of attack from 0° to 20°, and at nozzle pressure ratios from about 1 (jet off) to 10. Reynolds number based on mean aerodynamic chord varied from $9.24 \times 10^6$ to $10.56 \times 10^6$ .		13. Type of Report and Period Covered Technical Paper
17. Key Words (Suggested by Author(s))  Fighter aircraft Supersonic cruise Nonaxisymmetric nozzles Trailing-edge flaps		14. Sponsoring Agency Code
19. Security Classif. (of this report) Unclassified		18. Distribution Statement  Unclassified - Unlimited  Subject Category 02
20. Security Classif. (of this page) Unclassified	21. No. of Pages 86	22. Price A05



National Aeronautics and  
Space Administration

Washington, D.C.  
20546

Official Business  
Penalty for Private Use, \$300

THIRD-CLASS BULK RATE

Postage and Fees Paid  
National Aeronautics and  
Space Administration  
NASA-451



7 1 10, A, 330214 S00903DS  
DEPT OF THE AIR FORCE  
AF WEAPONS LABORATORY  
ATTN: TECHNICAL LIBRARY (SUL)  
KIRTLAND AFB TX 75717

S

**NASA**

---

POSTMASTER: If Undeliverable (Section 158  
Postal Manual) Do Not Return